

Aus dem Deutsches Rheuma-Forschungszentrum  
der Medizinischen Fakultät Charité – Universitätsmedizin Berlin

DISSERTATION

Bone marrow maintains isotype switched memory B cells  
in stromal niches.

zur Erlangung des akademischen Grades  
Medical Doctor - Doctor of Philosophy (MD/PhD)

vorgelegt der Medizinischen Fakultät  
Charité – Universitätsmedizin Berlin

von

Richard Kwasi Addo

aus Accra, Ghana

Datum der Promotion: 21st June, 2020

## Table of content

<b>Synopsis</b> .....	<b>I</b>
<b>1 Abstract</b> .....	<b>3</b>
<b>2 Introduction</b> .....	<b>6</b>
2.1 Immunological memory.....	6
2.2 Memory B cells.....	6
2.3 Tissue maintenance of memory lymphocytes.....	6
2.4 BM stromal niches in maintenance of memory lymphocytes.....	7
<b>3 Materials and Methods</b> .....	<b>7</b>
3.1 Mice.....	7
3.2 Immunizations and infections.....	7
3.3 Cyclophosphamide administration.....	8
3.4 Flow cytometric analysis and cell sorting (FACS).....	8
3.5 B cell receptor sequencing.....	8
3.6 BCR repertoire analysis.....	9
3.7 Histology.....	10
3.8 Single cell suspension of bone marrow.....	11
3.9 Single cell RNA-sequencing.....	11
<b>4 Results</b> .....	<b>12</b>
4.1 Isotype-switched B <sub>mem</sub> are abundant in spleen and BM.....	12
4.2 Exclusive antigen-receptor clonotypes identify distinct B <sub>mem</sub> repertoire of BM and spleen.....	13
4.3 B <sub>mem</sub> of BM and spleen differ in their expression of CD21 and CD62L.....	16
4.4 Memory B cells are quiescent and resting in G <sub>0</sub> of cell cycle.....	17
4.5 B <sub>mem</sub> co-localize with VCAM-1 <sup>+</sup> cells in the bone marrow.....	18
4.6 B <sub>mem</sub> - stromal co-localization is deterministic.....	20
4.7 BM stromal cells exhibit enormous heterogeneity.....	20
4.8 Distinct subpopulations of BM stromal cells for the maintenance of immune and hematopoietic cell subsets.....	22
<b>5 Discussion</b> .....	<b>24</b>
5.1 Tissue distribution of memory B cells.....	25
5.2 Lifestyle of memory B cells.....	25
5.3 Bone marrow niches for memory cells.....	25
<b>6 Literature</b> .....	<b>26</b>
<b>7 Statutory Declaration</b> .....	<b>31</b>
<b>8 Declaration of your own contribution to any publications</b> .....	<b>32</b>
<b>Copy of publications</b> .....	<b>II</b>
<b>Curriculum Vitae (CV)</b> .....	<b>III</b>
<b>List of Publications</b> .....	<b>IV</b>
<b>Acknowledgement</b> .....	<b>V</b>

# 1 Abstract

The adaptive immune system has the unique ability to remember and rapidly mount protective response against previously encountered pathogen. This feature of the immune system is termed immunological memory and the functional duty is carried out by differentiated T and B cells. The maintenance of memory cells is important to confer long-lasting protection for the organism. Also, strategic positioning of these memory cells throughout the organism is crucial to ensure timely response against recurrent antigenic stimulation. While the tissue distribution and maintenance of memory T and plasma cells has been described, the lifestyle of memory B cells ( $B_{mem}$ ) has not been well studied so far. In my doctoral thesis I investigated the tissue organization and lifestyle of memory B cells in mice, which would serve as the starting point for further translational studies in humans. To determine the tissue distribution, isotype-switched  $B_{mem}$  of spleen, bone marrow (BM), peripheral blood, and lymph nodes were enumerated under different immunization and infection protocols. The majority of isotype-switched  $B_{mem}$  were localized in the spleen, but a significant population was also contained within the BM. Comparison of the repertoire of B cell receptor (BCR), a unique identifier of each individual B cell, the repertoires of isotype-switched  $B_{mem}$  of spleen and BM revealed limited overlap of B cells with same BCR (clonotypes) generated during a specific immune response. The majority of  $B_{mem}$  clonotypes are expressed exclusively in either organ, demonstrating that isotype-switched  $B_{mem}$  of the two organs represent distinct resident populations with minimal exchange between them via blood circulation. Phenotypically, isotype-switched  $B_{mem}$  of the two organs differ in surface protein expression of CD21 (complement receptor) and CD62L (L-selectin) with subsets of  $CD21^{low}$  and  $CD21^{high}$  populations in the BM but not in spleen, also, isotype-switched  $B_{mem}$  of BM express higher levels of CD62L compared to those in spleen. Isotype-switched  $B_{mem}$  of BM and spleen are resting in the  $G_0$  of cell cycle as determined by the expression of the proliferative marker Ki67, and are refractory to *in vivo* treatment with cyclophosphamide (a DNA alkylating agent which kills proliferating cells). In the BM, isotype-switched  $B_{mem}$  are located in close proximity to reticular stromal cells expressing VCAM-1. To further understand the role of BM stromal cells in organization of survival niches for memory cells, the biology and functional properties of VCAM-1+ stromal cells were analyzed. Next generation sequencing single cell mRNA transcriptomes profiling of directly *ex vivo* isolated BM VCAM-1+ stromal cells revealed distinct subpopulation of stromal cells defined by the expression of cytokines and chemokines which have been described to be important for the maintenance and survival of subsets of hematopoietic and immune cells subsets. Altogether, the findings of this thesis demonstrate that murine  $B_{mem}$  are residing in the BM as distinct population of B cell memory and that

distinct subsets of BM stromal cells organize survival niches for different hematopoietic cells, including memory cells.

## Abstract (German)

Das adaptive Immunsystem hat die einzigartige Fähigkeit sich an zuvor vorgefundene Krankheitserreger zu erinnern und schnell gegen diese schützend zu reagieren. Diese Fähigkeit des Immunsystems heißt immunologisches Gedächtnis und wird von differenzierten T- und B-Zellen ausgeübt. Die Aufrechterhaltung der Gedächtniszellen ist wichtig um dem Organismus einen dauerhaften Schutz zu verleihen. Weiterhin ist eine strategische Positionierung dieser Gedächtniszellen im gesamten Organismus entscheidend um eine zeitnahe Reaktion gegen wiederkehrende antigenische Stimulierungen sicherzustellen. Während die Gewebeverteilung und -erhaltung von Gedächtnis T-Zellen und Plasma Zellen bereits gut beschrieben wurde, wurde der Lebensstil von Gedächtnis-B-Zellen ( $B_{\text{mem}}$ ) bislang nicht weiter untersucht. In meiner Doktorarbeit habe ich die Gewebeorganisation und den Lebensstil von Gedächtnis B-Zellen in Mäusen untersucht, welche als Ausgangspunkt für weitere translationale Studien am Menschen dient. Um die Gewebeverteilung zu untersuchen, wurden Isotyp-veränderte  $B_{\text{mem}}$  der Milz, des Knochenmarks, von peripherem Blut und von Lymphknoten unter verschiedenen Immunisierungs- und Infektionsprotokollen ausgezählt. Die Mehrheit der Isotyp-veränderten  $B_{\text{mem}}$  wurden in der Milz lokalisiert, es ist aber auch eine signifikante Population im Knochenmark enthalten. Der Vergleich des Repertoires des B-Zell-Rezeptors (BCR), einer einzigartigen Bezeichnung jeder individuellen B-Zelle, des Repertoires der Isotyp-veränderten  $B_{\text{mem}}$  der Milz und des Knochenmarks hat gezeigt, dass B-Zellen mit derselben BCR (Klonotypen), welche während einer spezifischen Immunreaktion generiert wurden, sich kaum überlappen. Die Mehrheit der  $B_{\text{mem}}$  Klonotypen wird ausschließlich in einem der beiden Organe exprimiert, was beweist, dass Isotyp-veränderte  $B_{\text{mem}}$  zweier Organe verschiedene Populationen mit nur minimalen Austausch über den Blutkreislauf repräsentieren. Phänotypisch, Isotyp-veränderte  $B_{\text{mem}}$  der beiden Organe unterscheiden sich in der Oberflächenproteinexpression von CD21 (Komplementrezeptor) und CD62L (L-Selektin) mit Untergruppen von  $CD21^{\text{low}}$  und  $CD21^{\text{high}}$  Populationen im Knochenmark, aber nicht in der Milz. Weiterhin beinhalten Isotyp-veränderte  $B_{\text{mem}}$  des Knochenmarks einen höheren Spiegel von CD62L im Vergleich zur Milz. Isotyp-veränderte  $B_{\text{mem}}$  des Knochenmarks und der Milz ruhen im  $G_0$  des Zellzyklus, wie durch die Expression des proliferativen Markers Ki67 bestimmt wurde, und sind widerstandsfähig gegen *in vivo* Behandlungen mit Cyclophosphamid (einem DNA alkylierenden Wirkstoff, der

wuchernde Zellen tötet). Im Knochenmark befinden sich Isotyp-veränderte B<sub>mem</sub> in unmittelbarer Nähe zu retikulären Stromazellen, die VCAM-1 exprimieren. Um die Rolle der Knochenmark Stromazellen bei der Organisation von Überlebensnischen für Gedächtniszellen genauer zu verstehen, wurden die Biologie und die funktionellen Eigenschaften von VCAM-1+ Stromazellen analysiert. Die Sequenzierung von Einzelzell-mRNA-Transkriptomen von direkt *ex vivo* isolierten Knochenmark VCAM-1+ Stromazellen ergab eindeutige Subpopulationen von Stromazellen, die durch die Expression von Cytokinen und Chemokinen definiert wurden, welche als wichtig für die Aufrechterhaltung und das Überleben von Subpopulationen von hämatopoetischen Zellen und Immunzellen beschrieben wurden.

Zusammenfassend beschreiben die Ergebnisse der Dissertation, dass murine B<sub>mem</sub> im Knochenmark als ausgeprägte ansässige Population des B-Zell-Gedächtnisses vorkommen und dass Subpopulationen von Knochenmark Stromazellen Überlebensnischen für verschiedene hämatopoetische Zellen, inklusive den Gedächtniszellen des Immunsystems, organisieren.

## 2 Introduction

### 2.1 Immunological memory

The adaptive immune system has the unique ability to remember and mount protective response against previously encountered pathogen in a more rapid and efficient manner. This ability of the immune system to confer protection against a previously encountered pathogen was already described in 430 BC by the ancient Greek historian Thucydides [1]. This feature of the immune system is termed immunological memory and the functional duty is carried out by well differentiated T and B cells [2]. The generation of protective immunological memory is also the underlying principle of immune protection acquired from immunization or vaccination.

### 2.2 Memory B cells

Antigen-experienced memory B cells ( $B_{\text{mem}}$ ) are an essential component of immunological memory. They are functionally superior compared to naïve cells and have a lower activation threshold when re-encountering pathogens [3]. Isotype-switched  $B_{\text{mem}}$  (IgG or IgA) produce antibodies with higher affinity and specificity needed to clear foreign antigen or pathogen during immune response [3]. The organization of B cell memory remains however unclear in the scientific community. Both non-switched  $\text{IgM}^+$  and isotype-switched  $B_{\text{mem}}$  have been described to be present in spleen, blood and bone marrow (BM) [4–6]. In humans, the spleen has been described as a major reservoir for *Vaccinia*-specific  $B_{\text{mem}}$  [7] and splenectomy leads to gradual loss of circulating  $B_{\text{mem}}$  [7,8]. This is however not the situation for tetanus toxoid (TT) infection as splenectomy does not lead to a loss of TT-specific  $B_{\text{mem}}$  [4], indicating that TT-specific memory B cells do not require the spleen for maintenance. These contrasting observations suggest that memory B cells which confer protective immunity against specific pathogens are also located in organs other than blood and spleen [9].

### 2.3 Tissue maintenance of memory lymphocytes

Subsets of long-lived memory lymphocytes ( $\text{CD4}^+$ ,  $\text{CD8}^+$  and plasma cells) have been shown to be maintained in different tissues including the BM. In the BM, dedicated niches provide the needed molecular signals to ensure the long term survival of these cells [10–14]. In contrast, knowledge about the role of BM in the maintenance of

memory B cells remains scarce. As with most hematopoietic and immune cells, the maintenance of B<sub>mem</sub> is likely to be dependent on both intrinsic factors and external signals from their immediate microenvironment.

## 2.4 BM stromal niches in maintenance of memory lymphocytes

BM stromal cells are integral component of survival niches for different immune cells like memory CD4+, CD8+ and plasma cells [10–14]. *In vivo*, BM stromal cells express vascular cell-adhesion molecule 1 (VCAM1; CD106) [15], CXCL12 and IL7, collagen II and XI [10–14] among other factors necessary for the survival, maintenance and development of various cells of the hematopoietic and immune system [10–14]. Although eosinophils were initially reported as integral component of survival niches for plasma cells [12,16], recent research findings published in 2018 showed that eosinophils are redundant for maintenance of long-lived plasma cells [17,18]. Long-lived CD4+ and CD8+ memory cells contact IL-7 expressing BM stromal cells [10,19]. The functional organization of BM stromal cells is however not well addressed. For example, it is not known if distinct subpopulations of BM stromal cells are specialized for organization of niches for particular subsets of memory cells. Also, knowledge about other factors expressed by stromal cells which might play a role in the maintenance of memory cells is lacking.

## 3 Materials and Methods

### 3.1 Mice

All mice were housed under specific pathogen-free conditions at the Deutsches Rheuma-Forschungszentrum Berlin, a Leibniz Institute (DRFZ). C57BL/6J mice were purchased from Charles River (Sulzfeld, Germany). Mice expressing GFP under the control of the *Prdm1* promoter (Blimp1-GFP)[20] were bred at the DRFZ animal facility. All animal experiments were performed according to institutional guidelines and licensed under German animal protection regulations.

### 3.2 Immunizations and infections

- 100µg NP-KLH (4-Hydroxy-3-nitrophenylacetyl (NP)) hapten conjugated to KLH (Keyhole Limpet Hemocyanin) with 10 µg LPS (*E. coli*, InvivoGen), subcutaneous (SC). For boost immunizations 10 µg NP-KLH without adjuvant was used.
- 100µg NP-CGG (NP hapten conjugated to Chicken Gamma Globulin (CGG)) in Incomplete Freund's adjuvant (IFA), three times (3X) at 21 days interval, intraperitoneal (IP) or subcutaneous.

- $2 \times 10^5$  plaque-forming units of the Armstrong strain of lymphocytic choriomeningitis virus (LCMV), intraperitoneal.
- $10^6$  colony-forming units of attenuated *Salmonella enterica* serovar typhimurium strain SL7207, intravenous.

### 3.3 Cyclophosphamide administration

C57BL/6J mice immunized three times (3x) IP with NP-CGG/IFA-immunized (at 21 days interval) to establish long-lived  $B_{mem}$  were treated twice (2X) with 50mg/kg cyclophosphamide (CyP), intravenous at 2 days interval and sacrificed on day 3 after the last treatment. Control mice were injected with Phosphate Buffered Saline (PBS) instead of cyclophosphamide.

### 3.4 Flow cytometric analysis and cell sorting (FACS)

Flow cytometric measurements and cell sorting were done according to standards defined in the guidelines to flow cytometry and cell sorting in immunological studies [21]. Antibodies were purchased from Miltenyi Biotec, Biolegend, eBioscience, or produced in DRFZ. All FACS data were acquired on MACSQuant (Miltenyi Biotec), BD FACSCanto II or BD FACSFortessa (BD Bioscience). BD Influx cell sorter (BD Bioscience) was used for cell sorting. Flow cytometric data were analyzed with FlowJo v10(Tree Star, Inc.). Total BM cell numbers were calculated based on cell numbers in a single femur of a mouse which is estimated to harbor 6.3% of total BM leading to a conversion factor of 7.9 for two femurs for total mouse BM [11].

#### 3.4.1 Memory B cells

Antibodies directed against the following murine antigens were used for analysis of memory B cells: Ki-67 (B56, BD Biosciences), CD11c (N418), CD19 (1D3), CD38 (90), CD138 (281-2), GL7 (GL7), IgA (C10-3), IgD (11.26c), IgG1 (A85-1), IgG2a/b (R2-40), IgG2b (A95-1 and MRG2b-85), IgM (M41), CD93 (AA4.1), CD5 (19-3), B220 (RA3.6B2), CD21/35 (7G6), CD29 (HM $\beta$ 1-1), CD39 (Duha59), CD62L (MEL-14).

#### 3.4.2 Bone marrow stromal cells

The following antibodies were used in analysis of BM stromal cells: anti-CD45 (30F11), anti-VCAM-1 (429), anti-CD31 (390) and anti-Ter119 (Ter119).

### 3.5 B cell receptor sequencing

$B_{mem}$  from BM (tibiae, femurs, pelvis) and spleen of immunized mice (3x NP-CGG) were magnetically enriched using the Memory B cell Isolation Kit (130-095-838 Miltenyi).  $B_{mem}$  cells were FACSsorted by gating on CD19<sup>+</sup>CD38<sup>+</sup>CD138<sup>-</sup>CD11c<sup>-</sup>GL7<sup>-</sup>IgM<sup>-</sup>IgD<sup>-</sup> small lymphocytes. Sorted cells per organ per mouse were split into equal halves to



give biological (cellular) replicates [22]. Biological replicates were processed independently from this point on. Total RNA was extracted from samples using the ZR RNA Miniprep Kit (Zymo Research) according to the manufacturer's protocol (Catalog nos. R1064 & R1065). Isolated RNA was splitted into equal halves and library preparation was performed to give technical duplicates. First-strand cDNA was synthesized with SMARTScribe Reverse Transcriptase (Clontech) using total RNA, a cDNA synthesis primer mix (mIgG12ab\_r1(KKACAGTCACTGAGCTGCT), mIgG3\_r (GTACAGTCACCAAGCTGCT), mIgA\_r (CCAGGTCACATTCATCGTG) by metabion international AG) and a 5' – template-switch adaptor with unique molecular identifiers (UMI) (SmartNNA (AAGCAGUGGTAUCAACGCAGAGUNNNNUNNNNUNNNNUCTT(rG)4)) according to the protocol “high-quality full length immunoglobulin profiling with unique molecular barcoding” by the Chudakov lab [23]. cDNA was purified with MinElute PCR purification Kit (Qiagen) and eluted in 10 µL 70°C nuclease-free H<sub>2</sub>O (Qiagen). The first and second PCR were performed according to the protocol by the Chudakov lab [23]. PCR 1 products were purified with MinElute PCR purification Kit (Qiagen) and eluted in 25 µL 70°C nuclease-free H<sub>2</sub>O (Qiagen). The products were also gel-purified from 2% agarose gels (extraction with MinElute gel extraction Kit (Qiagen); elution in 15 µL 70°C nuclease-free H<sub>2</sub>O (Qiagen). Adapter ligation was performed using the TruSeq® DNA PCR-Free Library Prep protocol (Illumina). The products were gel-purified from 2% agarose gels instead of bead purification as mentioned in the protocol (extraction with MinElute gel extraction Kit (Qiagen); elution in 10 µL 70°C nuclease-free H<sub>2</sub>O (Qiagen)). The quality of amplified libraries was verified by using an Agilent 2100 Bioanalyzer (2100 expert High Sensitivity DNA Assay). According to the fragment size, the libraries were quantified by qPCR using the KAPA Library Quantification Kit for Illumina platforms (KAPA Biosystems). Based on the result of the qPCR a final library pool with a concentration of 2 pM was used for sequencing with NextSeq 500 (Illumina) using the NextSeq 500/550 Mid Output Kit and 300 cycles (2x150bp).

### 3.6 BCR repertoire analysis

B Cell Receptor (BCR) repertoire analysis was performed using MIGEC-1.2.4a [24] in default parameter settings while adding a demultiplexing step for identification of IgG1/2, IgG3 and IgA heavy chains. After the MIGEC pipeline's “checkout” step isotypes were classified according to presence of mIgG12\_r2, mIgG3\_r2 and mIgA\_r2 primer sequences: AGTGGATAGACMGATG, AAGGGATAGACAGATG and TCAGTGGGTAGATGGTG, allowing for one mismatch against the primer sequence. Data were then processed independently for each isotype. The MIGEC segments file was adjusted to include only C57BL/6-specific V genes for mapping. MIGEC performs a UMI-guided correction to remove PCR as well as sequencing bias and errors. Each resulting consensus sequence was treated as one clone. Clones with identical V, D, and

J gene compositions and CDR3 nucleotide sequences were grouped together to define clonotypes. Solely clonotypes consistently found in both technical replicates of a given sample were considered in downstream analyses. Statistics on the overlap of repertoires between different samples were performed based on the presence of clonotypes. The degree of similarity between samples accounting for the abundance of clonotypes is represented by the cosine similarity [25].

## **3.7 Histology**

### **3.7.1 Preparation of histological sections**

Femoral bones were fixed in 4% PFA (Electron Microscopy Sciences) for 4 hours at 4°C, equilibrated in 30% sucrose/PBS, then frozen and stored at -80°C. 6µm cryosections of tissues were prepared. Tissue samples were first blocked with 1X PBS containing 10% FCS (Fetal Calf Serum) for 1h. Samples were then stained with antibodies in 0.1% Tween-20 (Sigma-Aldrich)/ 10% FCS/ 1XPBS for 1h. Antibodies towards following murine antigens were used: IgG2b (RMG2b-1), GFP (rabbit polyclonal), fibronectin (rabbit polyclonal), Ki67 (Sol-15), VCAM-1 (429), cadherin 17 (rabbit polyclonal), laminin (rabbit polyclonal, Sigma Aldrich), IgD (11.26c), Thy1 (T24, DRFZ), B220 (RA3.6B4), CD11c (N418), donkey anti-rabbit polyclonal IgG-AF488/647, streptavidin-AF594/647, donkey anti-goat polyclonal AF488. For nuclear staining, sections were stained with 1 µg/ml DAPI in PBS. Sections were mounted in Fluorescent Mounting Medium (DAKO).

### **3.7.2 Confocal microscopy**

For confocal microscopy, a Zeiss LSM710 with a 20x/0.8 numerical aperture objective lens was used. Images were generated by tile-scans and maximum intensity projection of 3-5 Z-stacks each with 1µm thickness. Image acquisition was performed using Zen 2010 Version 6.0 and images were analyzed by Zen 2012 Light Edition software (Carl Zeiss MicroImaging).

### **3.7.3 Manual image analysis**

To determine the nearest neighbors of  $B_{mem}$ , cells in direct cell-cell contact or a position within a 10µm radius of cell boundaries of  $B_{mem}$  were enumerated manually using resolution images of immunofluorescence staining acquired by confocal microscopy.

### **3.7.4 Modelling random co-localization**

To determine the probability of co-localization of BM  $B_{mem}$  to reticular stromal cells, cell-cell neighboring was modelled by random cell positioning [12]. Images of isotype-switched  $B_{mem}$  were positioned on histological images of VCAM-1 stained BM at random (1000 times), and the frequencies of co-localizing  $B_{mem}$  and stromal cells were then

determined. The modelled frequencies were then compared to the frequencies of the original histological images.

### **3.8 Single cell suspension of bone marrow**

BM flush-out and the empty bones (tibia and femur) were digested using an optimized protocol with 0.5 mg/ml Collagenase IV (Sigma-Aldrich), 1mg/ml DNase I (Sigma-Aldrich), 0.25 mg/ml Dispase II (Roche), with or without 5µg/ml Latrunculin B (Sigma-Aldrich), for 30 min at 37°C.

### **3.9 Single cell RNA-sequencing**

#### **3.9.1 Single cell library preparation and RNA-sequencing**

*Ex vivo* FACSsorted VCAM-1+CD45-Ter119-CD31- BM stromal cells (IL-7-GFP knock-in mice) were applied to the 10x Genomics platform using the Single Cell 3' Reagent Kit V2 (10x Genomics) and following the manufacturer's instructions. Upon adapter ligation and index PCR the quality of the obtained cDNA library was assessed by Qubit quantification, Bioanalyzer fragment analysis (HS DNA Kit, Agilent) and KAPA library quantification qPCR (Roche). The sequencing was performed on a NextSeq500 device (Illumina) using a High Output v2 Kit (150 cycles) with the recommended sequencing conditions (read1: 26nt, read2: 98nt, index1: 8 nt, index2: n.a.).

#### **3.9.2 BM stromal cells single cell RNA-seq analysis**

Illumina output was demultiplex and mapped to the mm10 reference genome by cellranger-2.0.2 (10x Genomics Inc.) using refdata-cellranger-mm10-1.2.0 in default parameter setting and 3000 expected cells. Raw counts were further analyzed using R 3.5.1 with Seurat package (Seurat\_2.3.4,) [26]. Potential lymphocyte and erythrocyte contamination cells expressing *Ptprc* (CD45) or hemoglobin subunits (*Hba*) respectively were detected and excluded prior the analysis, resulting in 1035 stromal cells. T-distributed Stochastic Neighbor Embedding (tSNE) and the underlying Principle Component Analysis was performed on 30 dimensions using variable genes as set by default (Fig. 4-15) or on a subset of 108 genes (Fig. 4-16), which are known for their role in mediating the communication between stromal cells and hematopoietic cells. Similarity of gene expression (co-expression) was estimated by the Jaccard similarity coefficient (Fig. 4-17). Heatmaps (Fig. 4-18) show the log<sub>2</sub>-transformed fold change of mean expression of positive and negative cells, displayed are the top 10 genes with the highest fold change. DiffExpTest-method was used for the statistical analysis of differential expressed genes [27].

## 4 Results

### 4.1 Isotype-switched B<sub>mem</sub> are abundant in spleen and BM

In order to investigate the tissue distribution of murine B<sub>mem</sub>, single cell suspension of spleen, BM, peripheral lymph nodes (pLN), mesenteric lymph nodes (mLN), and Peyer's patches (PP) were analyzed by flow cytometry. Surface expression of immunoglobulin isotype (IgG<sub>1</sub>, IgG<sub>2b</sub>, or IgA) was used to identify isotype-switched B<sub>mem</sub> by gating on CD19<sup>+</sup>CD38<sup>+</sup>CD138<sup>-</sup>GL7<sup>-</sup>small lymphocytes (Fig. 4-1). Mice were immunized with different experimental antigens (LCMV, NP-KLH, NP-CGG, *S. typhimurium*) via different routes of administration (sub-cutaneous, intravenous and intraperitoneal) and B<sub>mem</sub> enumerated in the memory phase of immune response. Different routes of administration were used to investigate how the route of pathogen entry influences the distribution of B<sub>mem</sub>.

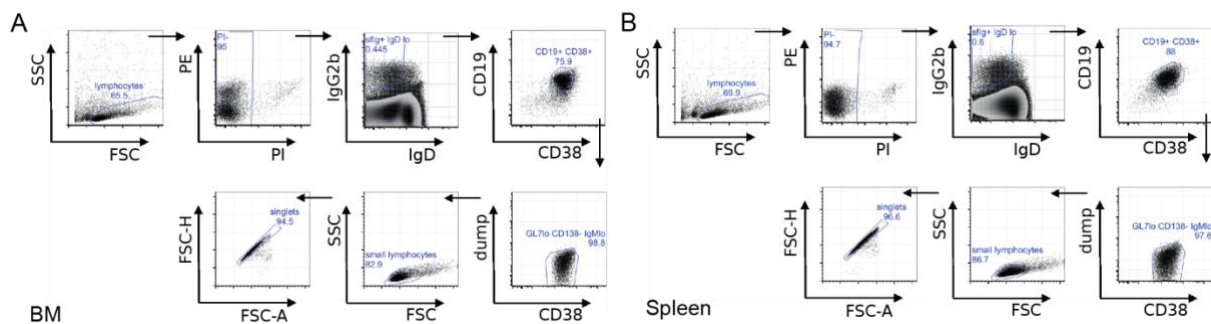


**Figure 4-1 Gating for isotype-switched B<sub>mem</sub> of BM and spleen.**

Switched B<sub>mem</sub> of BM (A) and spleen (B) were identified by expression of surface IgG<sub>2b</sub>, IgG<sub>1</sub>, or IgA and CD19, CD38 and lack of IgD, IgM, CD138, GL7 marker. Staining shown for IgG<sub>2b</sub> exemplarily.

The quantification analysis revealed that besides the spleen, the BM hosts significant proportion of B<sub>mem</sub>. Following the different immunization protocols, 32-60% of all isotype-switched B<sub>mem</sub> were detected in the spleen, 18-41% of isotype-switched B<sub>mem</sub> were located in the BM and 9-14% in peripheral lymph nodes (Fig. 4-2). The frequencies of memory B cells in peripheral lymph nodes (pLN) mesenteric lymph nodes (mLN), Peyer's Patches (PP) and blood were consistently lower compared to BM and spleen (Fig. 4-2). The observed distribution of memory B cells was independent of either the antigen used or the route of administration of the antigen.

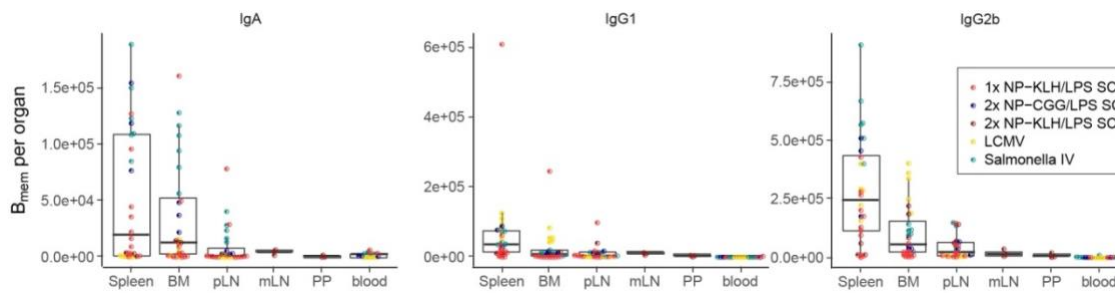


**Figure 4-2 Spleen and BM harbor major populations of isotype-switched  $B_{mem}$ .**

Cell numbers of isotype-switched  $B_{mem}$  per organ in C57BL/6 laboratory mice. Absolute cell numbers per organ calculated from flow cytometric counts (gated for  $IgG1^+$ ,  $IgG2b^+$ , or  $IgA^+$   $CD19^+CD38^+CD138^-GL7^-CD11c^-IgM^-IgD^-PI^-$  small lymphocytes);  $n=42$ , data pooled from 8 experiments with five different immunizations performed in mice aged 4-20 months and held under SPF conditions, colors indicate immunization. NP- 4-Hydroxy-3-nitrophenylacetyl; KHL- Keyhole Limpet Hemocyanin; CGG- Chicken Gamma Globulin; LPS-Lipopolysaccharide; LCMV- lymphocytic choriomeningitis virus

## 4.2 Exclusive antigen-receptor clonotypes identify distinct $B_{mem}$ repertoire of BM and spleen

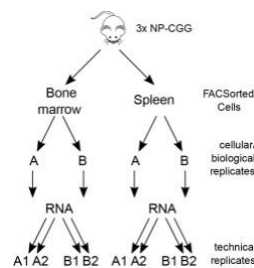


**Figure 4-3 Experimental setup for the comparison of BCR repertoire of switched  $B_{mem}$  of BM and spleen:**

After isolation, cells of the same organ were divided into equal proportions and processed as biological replicates. After RNA isolation, samples were split and processed as technical replicates.

Every B cell carries a unique membrane bound immunoglobulin (Ig) which is also known as the B Cell Receptor (BCR) [28]. BCRs are assembled during the B-cell development that involves random somatic recombination of V, D, J gene segments of the heavy chain locus and V, J gene segments of the light chain locus resulting in a huge diversity of BCRs [29]. Each single BCR (B cell clone) can be identified by its unique complementarity-determining region 3 (CDR3), part of the variable chain in BCR that bind to a specific antigen. The unique V, D, J gene segments rearrangement process makes it highly unlikely that any two naïve B cells express the same BCR although all progeny of a particular B cell keep the BCR with some additional mutations to the parent's BCR [28]. In this way B cell clones (progeny) of a particular initial B cell generated during an immune response can be traced and identified by their BCR. This unique property of BCR is valuable in the analysis of repertoire of  $B_{mem}$  generated in an immune response. BCR repertoire comparison of  $B_{mem}$  of different organs helps to

determine tissue exclusive (resident) populations and also to address the extent of exchange (via circulation) of  $B_{\text{mem}}$  populations between the different tissues.

High-throughput BCR RNA sequencing of  $IgG_1^+$  and  $IgG_2^+$  ( $IgG_{1/2}^+$ ),  $IgG_3^+$ , and  $IgA^+$  isotype-switched  $B_{\text{mem}}$  was performed using cells isolated from spleen and BM of three individual C57BL/6J mice, which had been immunized three times with NP-CGG minimum 73 days prior to analysis (Fig. 4-3). For all repertoire analyses, unique B cell clones were defined by 100% amino acid sequence identity of CDR3 regions. All clones with single counts were excluded to minimize confounding effects of sequencing errors and sequencing depth. Clonotypes (clonally related B cells generated from same single same naive B cell) were defined as clones with a common unique CDR3 sequence and, shared V, D, and J gene segment usage.

Determination of  $V_H$  gene family usage showed that  $IgG_{1/2}^+$ ,  $IgG_3^+$ , and  $IgA^+$  isotype-switched  $B_{\text{mem}}$  of BM and spleen per mouse are highly divergent in the distribution of  $V_H$  gene family usage (Fig. 4-4).

To determine repertoire overlap, the distribution of clonotypes between  $B_{\text{mem}}$  of BM and spleen was also analyzed. To minimize confounding effects of sequencing errors and sequencing depth, only those clonotypes consistently found in technical replicates were considered for repertoire comparison [30,31]. Isotype-switched  $B_{\text{mem}}$  of spleen and BM expressing  $IgG_{1/2}$ ,  $IgG_3$ , and  $IgA$ , respectively, showed a considerable fraction of exclusive organ clonotypes:  $IgG_{1/2}$ =46.1%-89.8%,  $IgG_3$ =43.7%-93.7%,  $IgA$ =49.9%-90.8% (Fig. 4-5). The proportion of clonotypes shared between  $IgG_{1/2}^+$ ,  $IgG_3^+$ , and  $IgA^+$   $B_{\text{mem}}$  of spleen and BM of individual mice was consistently significantly lower= $IgG_{1/2}^+$ =9.8%-29.4%,  $IgG_3^+$ =6.5%-29.8%,  $IgA^+$ =6.3%-34.5% (Fig. 4-5).



spleen  $B_{mem}$ ), the cosine similarity which measures the correlation of frequency of clonotypes in the samples was consistently higher: mean cosine similarity of 0.83-0.92 for  $IgG_{1/2}$ , 0.83-0.96 for  $IgG_3$ , 0.78-0.99 for  $IgA$ . This means that sampling half of spleen  $B_{mem}$  is enough to identify true clonotype and confirms that the size of the spleen and BM  $B_{mem}$  samples was enough to make meaningful conclusion of the BCR repertoire comparison. This high correlation of biological replicates is comparable to that of the RNA-technical replicates. On the contrary, the cosine similarity analysis of shared clonotypes between BM and spleen ( $IgG_{1/2}$ = 0.5-0.54,  $IgG_3$ = 0.54-0.55,  $IgA$ = 0.26-0.55) was significantly lower compared to that of organ replicates (biological and technical) (Fig. 4-6). The cosine similarity between BM and spleen  $B_{mem}$  is significantly minimal and suggests distinct subpopulations.

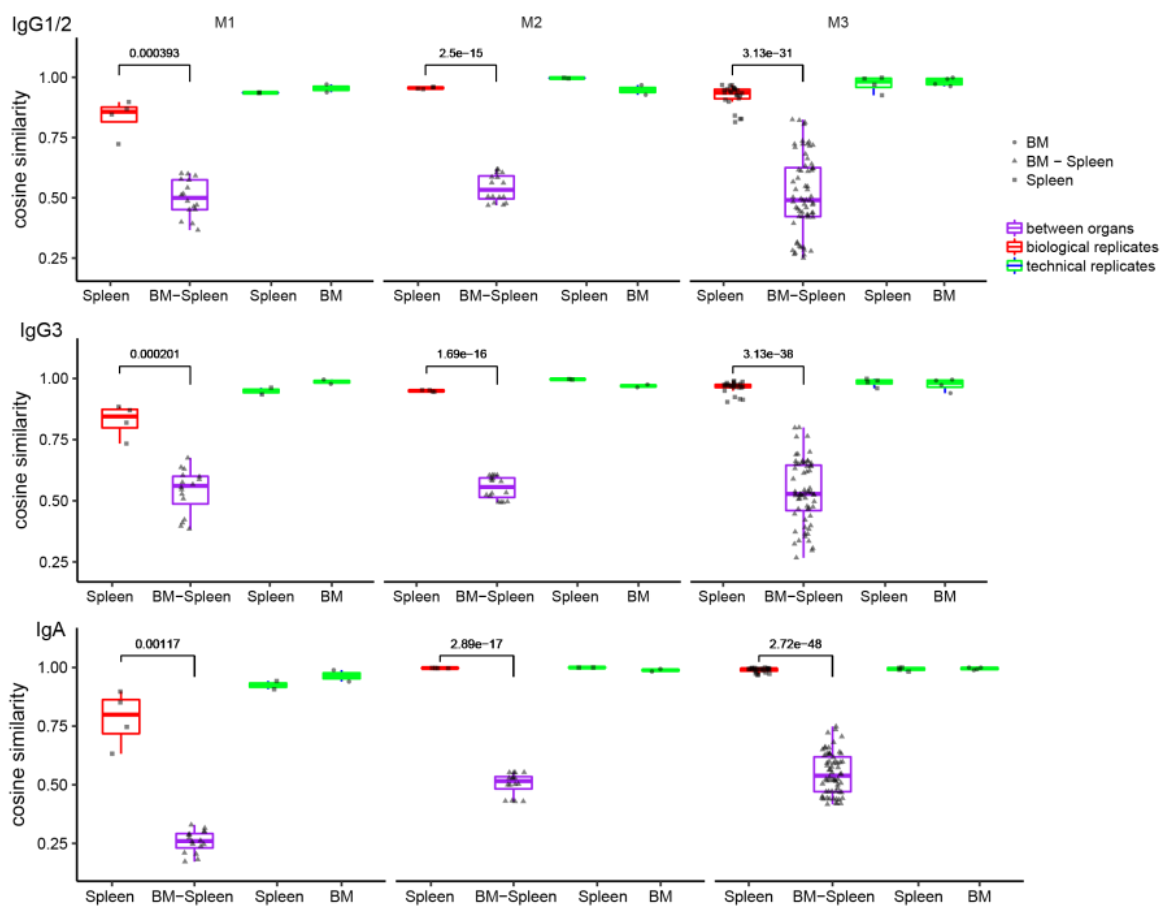


**Figure 4-6 Cosine similarity comparison of BCR (heavy chain CDR3) repertoires of switched  $B_{mem}$**

Cosine similarity comparison (accounting for clonotype frequencies) within technical replicates of  $IgG_{1/2}$ ,  $IgG_3$  and  $IgA$   $B_{mem}$  of spleen and BM (blue), within cellular replicates from spleens (red), and between spleen and BM (BM-Spleen, purple) of three individual mice. p values (Welch's test for difference of means of cosine similarity within shared  $IgH$  repertoire (spleen cellular replicates) and between spleen and BM replicates) are indicated.

### 4.3 $B_{mem}$ of BM and spleen differ in their expression of CD21 and CD62L



To determine whether  $B_{mem}$  of BM and spleen differed in their surface protein expression, the expression of more than 200 different surface markers comprising CDs and other cell surface markers (LegendScreen Mouse Cell Screen (PE) (# 700005 Biolegend) on  $CD19^+CD138^-CD38^+CD11c^-GL7^-IgM^-IgD^-IgG_{2b}^+$   $B_{mem}$  of BM and spleen was analyzed using flow cytometry. Gating was performed analogously to the strategy displayed in Fig. 4-1.

The surface markers screen analysis showed that  $IgG_{2b}^+$   $B_{mem}$  of BM and spleen differ in their expression pattern for CD21/35 and CD62L (Fig. 4-7). Expression levels of several surface molecules, such as CD20, TACI (CD267), and MHC class II was similar for  $IgG_{2b}^+$   $B_{mem}$  of BM and spleen. The expression of CD62L (L-selectin) was higher on  $IgG_{2b}^+$   $B_{mem}$  of BM compared to spleen. Expression of CD21/35 (CR2/1), the complement receptor [32,33] was reduced in BM  $IgG_{2b}^+$   $B_{mem}$  with about half of the cells expressing lower levels compared to those of spleen. The differences in expression of CD21/CD35 and CD62L identified from the high throughput screen were confirmed in independent experiments. The functional implication of these differences in protein expression is currently not clear and remains to be investigated.

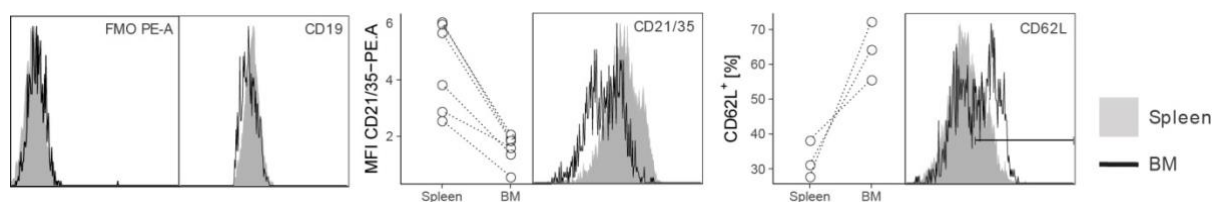


**Figure 4-7 Differential marker expression between spleen and BM  $IgG_{2b}^+$   $B_{mem}$**

Mean fluorescence intensity (MFI) or frequency of cells positive for a marker for paired bone marrow and spleen  $IgG_{2b}^+$   $B_{mem}$  is shown next to corresponding representative histogram. Gated for  $IgG_{2b}^+CD19^+CD38^+CD138^-GL7^-CD11c^-IgM^-IgD^-PI^-$  small lymphocytes, histogram plots are representative for five or more biological replicates from 3 independent experiments FMO PE: PE-channel fluorescence minus one control, FSC-A: forward-scatter area. (15 aged and immunized C57BL/6J mice)

#### 4.4 Memory B cells are quiescent and resting in $G_0$ of cell cycle

Long-lived memory lymphocytes ( $CD4^+$ ,  $CD8^+$  and plasma cells) have been described to be maintained in tissues in a state of quiescence (in terms of activation and proliferation) [10,34,35]. To investigate whether this is also the case for  $B_{mem}$ , the proliferative state of isotype-switched  $B_{mem}$  of BM and spleen was determined by intranuclear expression of the proliferative marker Ki67 using flow cytometry. Ki67 is expressed in all phases of the cell cycle, except  $G_0$  [36]. Ki-67 was expressed by as many as 9.3% (median: 8.0%) of switched  $IgG_{2b}^+$   $B_{mem}$  cells in spleen, and by no more than 4% (median: 2.6%) of isotype-switched  $B_{mem}$  of BM, showing that more than 90% of cells in the spleen and more than 95% in the BM were in the  $G_0$  phase of cell cycle, i.e. resting in terms of proliferation (Fig. 4-8).

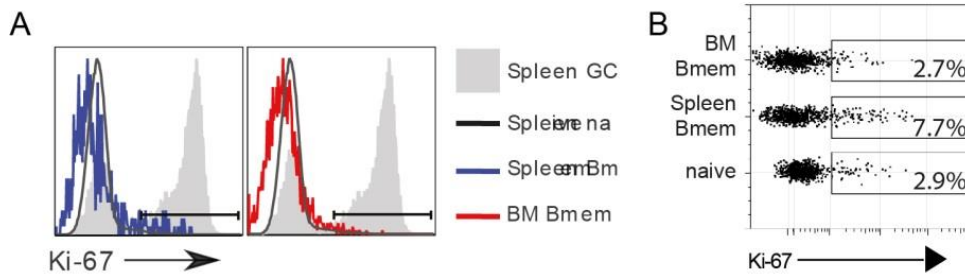


**Figure 4-8 IgG<sub>2b</sub><sup>+</sup> B<sub>mem</sub> of BM and spleen rest in G<sub>0</sub> of cell cycle**

(A) Flow-cytometric quantification of Ki-67 expression in IgG<sub>2b</sub><sup>+</sup> B<sub>mem</sub>, (IgG<sub>2b</sub><sup>+</sup>CD19<sup>+</sup>CD38<sup>+</sup>CD138<sup>-</sup>GL7<sup>-</sup>CD11c<sup>-</sup>IgM<sup>-</sup>IgD<sup>-</sup>PI<sup>-</sup> small) splenic naïve (IgM<sup>+</sup>IgD<sup>+</sup>IgG<sub>2b</sub><sup>-</sup>CD19<sup>+</sup>CD38<sup>+</sup>CD138<sup>-</sup>GL7<sup>-</sup>CD11c<sup>-</sup>PI<sup>-</sup> small lymphocytes) and germinal center (GC) (CD19<sup>+</sup>CD38<sup>lo</sup>GL7<sup>+</sup>CD11c<sup>-</sup>PI<sup>-</sup> lymphocytes) B cells. (B) frequencies of Ki-67<sup>+</sup> cells within the population indicated. Data is representative of 2 independent experiments.

To confirm *in vivo* quiescence (non-proliferative) of B<sub>mem</sub> as observed with the Ki67 staining, we treated immunized mice (in the memory phase) with cyclophosphamide. Cyclophosphamide is a DNA alkylating agent which kills proliferating cells [37]. B<sub>mem</sub> of both spleen and BM were refractory to treatment with cyclophosphamide. The number of isotype-switched B<sub>mem</sub> (IgG<sub>2b</sub>, IgG<sub>1</sub>, IgA) was not affected by the cyclophosphamide compared to the control treatment with PBS, whereas, overall CD19<sup>+</sup> B cell populations of both organs were significantly reduced (Fig. 4-9).

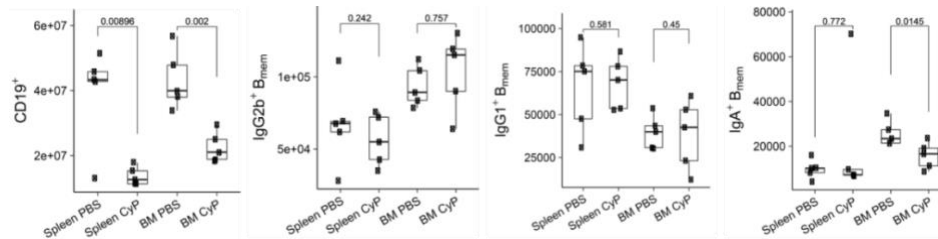


**Figure 4-9 Switched B<sub>mem</sub> are refractory to cyclophosphamide treatment**

Flow-cytometric quantification of CD19<sup>+</sup> B cells and IgG<sub>2b</sub><sup>+</sup> B<sub>mem</sub> in mice treated with Cyclophosphamide (CyP) or untreated controls (PBS) after immunization with 3x NP-CGG/IFA. Analysis was performed after 7 days of CyP. p value (Welch's test indicated). Representative data shown for one out of two independent experiments.

#### 4.5 B<sub>mem</sub> co-localize with VCAM-1<sup>+</sup> cells in the bone marrow

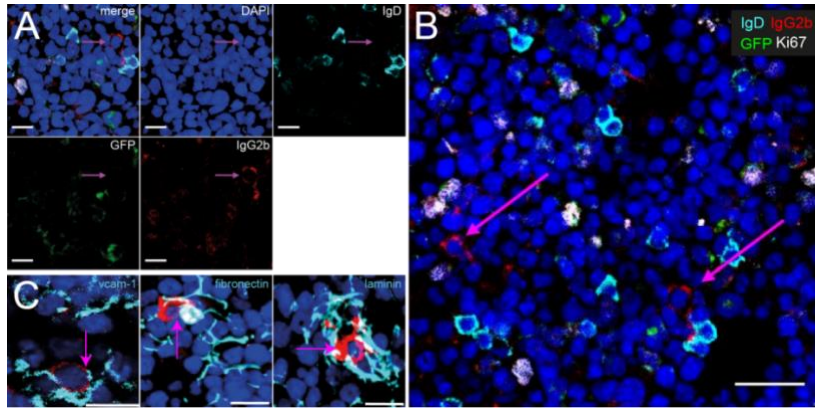


**Figure 4-10 IgG<sub>2b</sub><sup>+</sup> B<sub>mem</sub> of BM localize next to cells expressing VCAM-1, laminin and fibronectin**

A) Identification of BM IgG<sub>2b</sub><sup>+</sup> B<sub>mem</sub>. naive B cells and plasma cells were excluded by IgD and Blimp1-GFP, respectively. Cell nucleus was identified with DAPI (blue). Scale bar: 10µm. B) IgG<sub>2b</sub><sup>+</sup> B<sub>mem</sub> (Ki-67<sup>-</sup> IgD<sup>-</sup> Blimp1-GFP<sup>-</sup>) are dispersed as single cells throughout the BM. Arrows indicate IgG<sub>2b</sub><sup>+</sup>-staining DAPI<sup>+</sup> cells. Scale bar: 20µm. C) Co-localization of IgG<sub>2b</sub><sup>+</sup>GFP<sup>-</sup>IgD<sup>-</sup> IgG<sub>2b</sub><sup>+</sup> cells (arrows) with mesenchymal stromal cells (VCAM-1, fibronectin, laminin). Arrows indicate IgG<sub>2b</sub><sup>+</sup> staining DAPI<sup>+</sup> cells. Representative micrograph. Scale bars: 10µm.

The BM is an important organ in the tissue maintenance of long-lived memory lymphocytes (CD4<sup>+</sup>, CD8<sup>+</sup>, plasma cells). In the BM, plasma cells, memory CD4<sup>+</sup> and CD8<sup>+</sup> are localized in niches organized by reticular stromal cells [10,34,35]. BM niches for memory B cells have not been described. To investigate how the BM survival niches of B<sub>mem</sub> is organized; histology sections of BM (Blimp1-GFP mice) were analyzed by immunofluorescence. Switched IgG<sub>2b</sub><sup>+</sup> B<sub>mem</sub> were identified as IgG<sub>2b</sub><sup>+</sup>IgD<sup>-</sup>Ki-67<sup>-</sup> nucleated cells. GFP<sup>+</sup>IgG<sub>2b</sub><sup>+</sup> plasma cells [20] were excluded from analysis (Fig. 4-10A). Switched IgG<sub>2b</sub><sup>+</sup> memory B cells were dispersed as single cells throughout the BM (Fig. 4-10B). 75% of IgG<sub>2b</sub><sup>+</sup> memory B cells were in direct contact with reticular cells expressing VCAM-1 and fibronectin, and another 15 to 20% within 10µm vicinity of such cells (Fig. 4-10C, Fig. 4-11A). 53% of IgG<sub>2b</sub><sup>+</sup> B<sub>mem</sub> were directly contacting laminin-expressing stromal cells, and another 26% were in the 10µm vicinity of such cells (Fig. 4-10C, Fig. 4-11A).

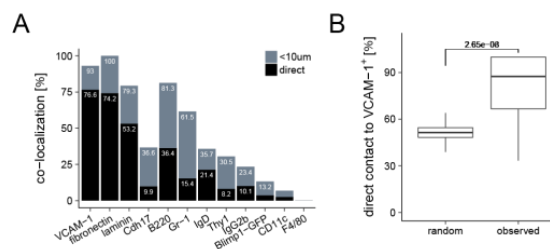


**Figure 4-11 Colocalization of B<sub>mem</sub> with stromal cells is deterministic**

(A) Co-localization of with mesenchymal stromal cells. Graph shows frequency of IgG<sub>2b</sub><sup>+</sup> cells in direct contact (black) or within 10µm (grey) of a cell stained for the molecule indicated. (C) Graphs represent direct co-localization of than 12000 simulated (random) cells (images from 7 BM slides) versus co-localization observed per slide for 28 slides from 4 mice with two or more analyzed B<sub>mem</sub> per slide (mean=5.66 cells per slide), p-value (Welch's test) indicated on graph.

## 4.6 B<sub>mem</sub> - stromal co-localization is deterministic

The analysis of BM sections showed that the majority of B<sub>mem</sub> co-localize with VCAM-1+ reticular stromal cells. To determine whether the contact of B<sub>mem</sub> to VCAM-1 expressing stromal cells is not a mere random association between the two cell types, co-localization of these cells types was simulated by randomization modelling [12]. The randomization modelling confirmed that the co-localization between B<sub>mem</sub> and reticular stromal cells was deterministic and cannot be attributed to mere randomness. The observed frequencies of co-localization (recorded at microscope) were significantly higher than in the randomly simulated co-localization (Fig. 4-11B). The co-localization of BM B<sub>mem</sub> and stromal cells is in line with expression of VLA4 (CD49d/CD29), a receptor for fibronectin and VCAM-1, and VLA6 (CD49f/CD29), a receptor for laminin [38], by IgG<sub>2b</sub><sup>+</sup> B<sub>mem</sub> (Fig. 4-12).

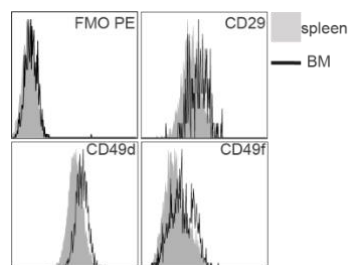


**Figure 4-12 B<sub>mem</sub> express receptors to VCAM-1, laminin and fibronectin** surface expression of VLA-4 and VLA-6 components CD29, CD49d, CD49f in spleen and bone marrow IgG<sub>2b</sub><sup>+</sup> B<sub>mem</sub>. Gated for IgG<sub>2b</sub><sup>+</sup>CD19<sup>+</sup>CD38<sup>+</sup>CD138<sup>-</sup>GL7<sup>-</sup>CD11c<sup>-</sup>IgM<sup>-</sup>IgD<sup>-</sup>PI<sup>-</sup> small lymphocytes; histogram plots are representative for three biological replicates.

## 4.7 BM stromal cells exhibit enormous heterogeneity

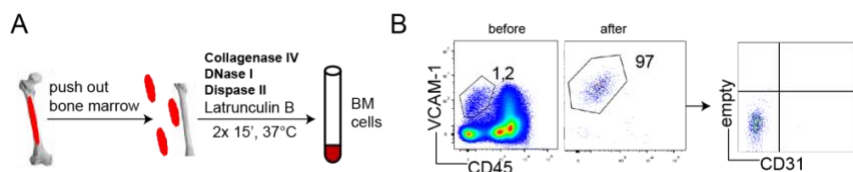


**Figure 4-13 Schematic overview of isolation of BM stromal cells.**

(A) Enzymatic digestion of BM.

(B) Cytometric isolation of VCAM-1<sup>+</sup>CD45<sup>-</sup>Ter119<sup>-</sup>CD31<sup>-</sup> BM stromal cells.

BM VCAM-1<sup>+</sup> stromal cells express cytokines and chemokines which attract and help in the maintenance of different subsets of memory T and long-lived plasma cells [39]. Although much is known about the organization of memory lymphocytes, corresponding research on the organization of BM stromal cells is scarce. Taking advantage of the latest single cell RNA sequencing high throughput technology, the phenotype and functional organization of BM stromal cells was addressed at the single cell resolution. BM cells (tibia and femur) were isolated by enzymatic digestion to generate single cell suspension (Fig. 4-13A). *Ex vivo* VCAM-1<sup>+</sup>CD45<sup>-</sup>Ter119<sup>-</sup>CD31<sup>-</sup> BM cells were then

sorted by FACS to 97% purity (Fig. 4-13B) and transcriptomes of individual cells were determined using 10X genomics-based droplet sequencing (Fig. 4-14). Transcriptomes of 1,167 individual stromal cells were analyzed with a mean of 398,739 reads per cell (Fig. 4-14A) resulting in a saturation rate of 95.6%, i.e. more than 95% of the total transcriptome was captured (Fig. 4-14B). 16,142 genes were detected in total, with a median of 1,538 genes per cell (Fig. 4-14A, C). Transcriptomes of individual cells were projected on a t-distributed stochastic neighbor embedding (t-SNE) analysis [40] to visualize the basic heterogeneity of the stromal cells (Fig. 4-15).

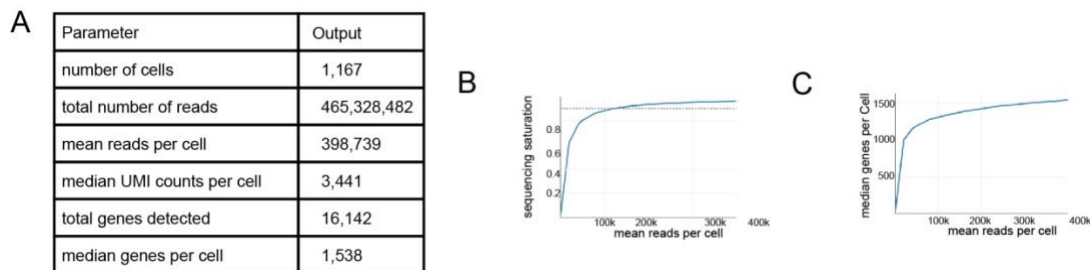


**Figure 4-14 Single cell RNA sequencing (sc RNA-seq) of BM stromal cells**

(A) Quality control (QC) summary of single cells sequencing output. (B) 10X genomics-based plot showing the mean read per cells, against the sequencing saturation. (C) Plot of the median number of genes detected per cell in relation to total reads per cell

Factors like *Vcam1*, *Cxcl12*, and *Kitl* important in the maintenance and development of different hematopoietic cells were expressed by more than 90% of the BM stromal cells. *Pdgfrb*, *Cadherin 11*(*Cdh11*), genes encoding for mesenchymal surface proteins were expressed by majority of cells, qualifying these genes as genuine stroma cells markers [41] (Fig. 4-15). On the level of single cell transcriptomes, cells expressing the various CD genes are dispersed within the t-SNE plots. Genes encoding cell surface molecules like *Lamp1* (CD107a), *Ox2* (CD200), *Cd1d1*, *Eng* (CD105), and *Cd44* were expressed individually by the stromal cells without defining unique subpopulations of stromal bone marrow (Fig. 4-15).

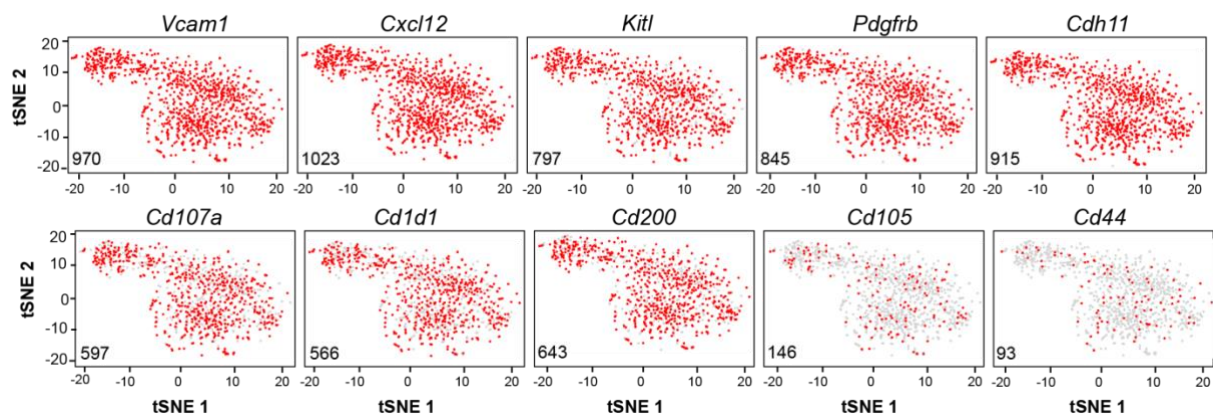


**Figure 4-15 t-SNE plots highlighting the expression (red) of individual genes**



## 4.8 Distinct subpopulations of BM stromal cells for the maintenance of immune and hematopoietic cell subsets

In the interaction between stromal cells and hematopoietic cells, the expression of chemokines and cytokines by stromal cells is essential for them to attract and control hematopoietic cells. The transcriptomes of individual BM stromal cells were analyzed for the expression of genes which encode for secreted proteins (cytokines and chemokines). A total of 108 genes were selected for further analysis, based on their established role in the communication of stromal cells with cells of the hematopoietic system.

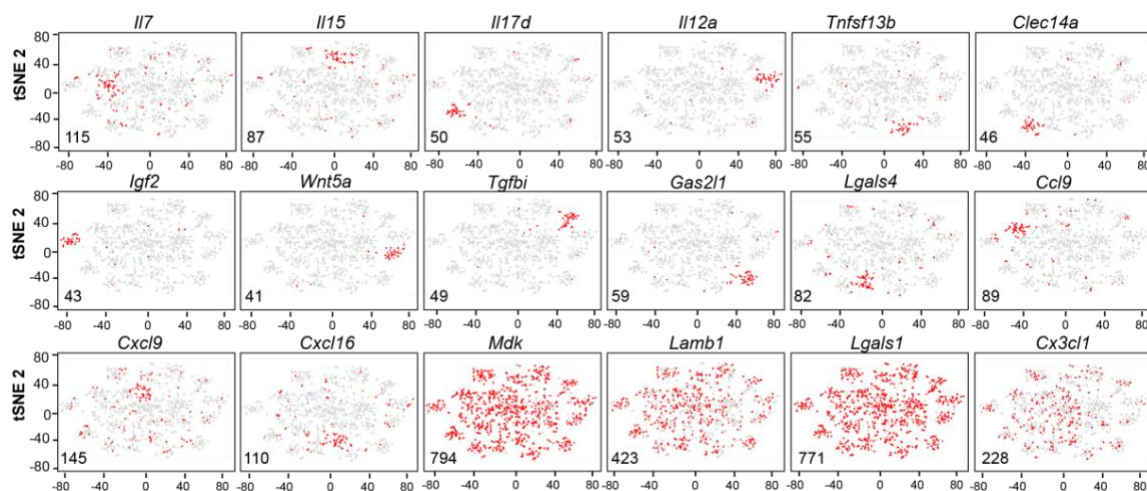


**Figure 4-16 t-SNE plots highlighting the expression (red) of individual genes**

Supervised clustering analysis of expression of these genes identified 14 non-overlapping subsets of stromal cells (Fig. 4-16). Genes like *Cxcl12*, *Kitl*, Colony Stimulating Factor 1 (*Csf1*) and Laminin B1 (*Lamb1*), were expressed by most stromal cells, hence they do not define distinct subpopulations of stromal cells (Fig. 4-16). Cells expressing the cytokines *Il7*, *Il15*, *Il12a*, *Il17d*, *Clec14a*, *Igf2*, *Lgals4*, *Tnfsf13b*, *Il4*, *Wnt5a* and *Tgfb1* formed unique subsets (Fig. 4-16). IL17D is a novel cytokine which inhibits the development of myeloid progenitor cells [42]. CLEC14A is a type I transmembrane involved in cell-to-cell adhesion, and thus shaping immune response [43]. IL12A has multiple effects on T and natural killer cells [44]. Expression of the chemokines *Ccl9*, *Cxcl9* and *Cxcl16* was restricted to distinct subsets, too. CXCL16 attracts memory T cells which express CXCR6 [45]. CCL9 and CCL7 attract subsets of dendritic [46] and T cells [47] respectively.

Expression of genes encoding for any of these chemokine/cytokines was exclusive to distinct subset of stromal cells, with less than 10% of cells co-expressing any two of these genes (Fig. 4-17). Stromal cells expressing these cytokines and chemokines expressed defined gene signatures, based on their entire transcriptomes, qualifying them as distinct subpopulations of stromal cells (Fig. 4-18).

The non-overlap expression of key cytokines and chemokines demonstrates that different subsets of BM stromal cells potentially attract and organize survival niches for the different memory lymphocytes. This demonstrates for the first time, existence of potential specialized stromal niches for the support and long-term maintenance of immune cells and other cells of the hematopoietic system

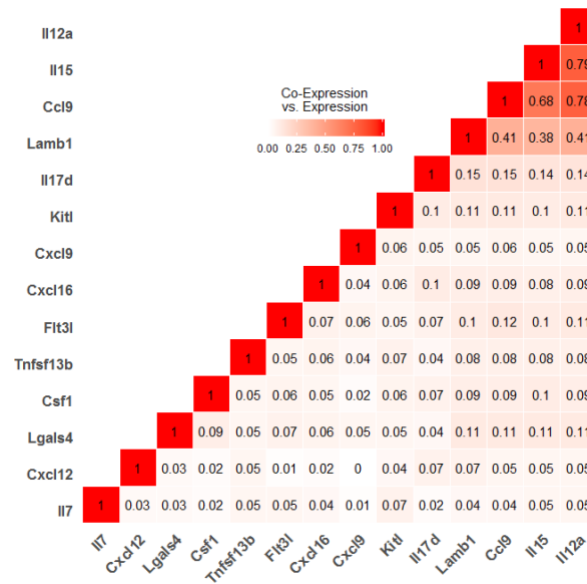


**Figure 4-17 Co-expression matrix showing the correlation of two genes.**

The similarity of gene expression (co-expression) of gene A and gene B was computed by Jaccard similarity coefficient  $((A \neq 0 \ \&\& \ B \neq 0) / (A \neq 0 \ || \ B \neq 0))$  where A and B refers to expression of genes A and B respectively)

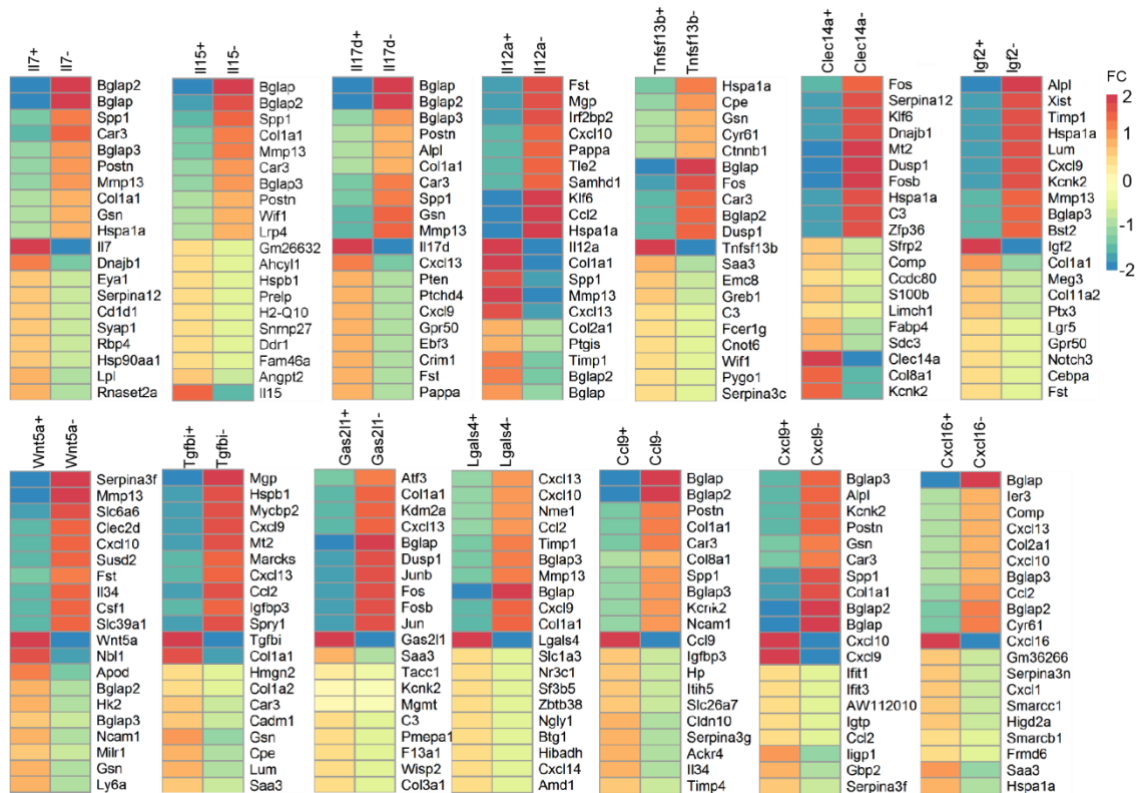


**Figure 4-18 Heatmap comparison of the gene expression profile of cells which express or do not express a single gene.**

Fold change (FC) shows the  $\log_2(\text{Average Expression positive cells}) - \log_2(\text{Average Expression negative cells})$ , displayed are the top 10 genes with the highest fold change. DiffExpTest-method was used for the statistical analysis of differential expressed genes

## 5 Discussion

The findings of this doctoral thesis demonstrate that B cell memory is compartmentalized similarly to T and plasma cells with significant populations of isotype-switched  $B_{\text{mem}}$  in BM and spleen. Isotype-switched  $B_{\text{mem}}$  of BM and spleen differ in BCR repertoires, suggesting that they might constitute separate compartments of B cell memory. It remains unclear whether (sub-) populations of these tissue resident isotype-switched  $B_{\text{mem}}$  contribute to the pool of circulating B cell memory. Also, memory B cells of the two organs show differences in their phenotype. The majority of  $B_{\text{mem}}$  of BM and spleen are quiescent and refractory to therapeutic targets which kill proliferative cells. In the BM,  $B_{\text{mem}}$  co-localize to reticular stromal cells in a deterministic manner guided by receptor-ligand interactions. BM stromal cells exhibit structural and functional organization with distinct sub-populations of BM stromal expressing factors important in the maintenance of subsets of memory lymphocytes. Subset of BM stromal cells (approximately 10%) express BAFF (B-cell Activating Factor) which is crucial for B and



plasma cells survival is also evident for the single cell RNA-sequencing transcriptome analysis.

## 5.1 Tissue distribution of memory B cells

These findings provide evidence for the existence of a resting population of  $B_{\text{mem}}$  in the murine BM. Overall, in mice the BM contains a significant number of isotype-switched  $B_{\text{mem}}$ . Isotype-switched  $B_{\text{mem}}$  in spleen and BM differ in presence and frequency of BCR repertoire. A significant proportion of 40% to 80% of the BCR clonotypes are expressed exclusively in either spleen or BM. Exclusive clonotypes indicate tissue residency and minimal exchange of the repertoire between the two organs. For those shared  $B_{\text{mem}}$  clonotypes (10-35%) between BM and spleen, the situation is less clear, they could be resident or constantly exchanged between the two organs. Although this doctoral thesis addressed the tissue distribution of isotype-switched memory B cells, it is likely that non-switched  $B_{\text{mem}}$  exhibit similar distribution pattern. Studies on tissue distribution of B cell memory in human has mostly being restricted to peripheral blood partly due to the difficult of access to tissues like BM and spleen. Human studies in this direction are needed to translate and better understand the tissue distribution of  $B_{\text{mem}}$  in humans. Strategic positioning and functional specialization of subsets of  $B_{\text{mem}}$  would ensure rapid, effective local and systemic protection during immune challenge.

## 5.2 Lifestyle of memory B cells

Switched memory B cells of BM and spleen are resting in terms of proliferation ( $G_0$  phase of the cell cycle) as shown by expression of the cell cycle marker Ki-67. *In vivo*,  $B_{\text{mem}}$  of BM and spleen are refractory to treatment with cyclophosphamide, a therapeutic agent which kills proliferating cells. This finding points to the longterm survival and resistance of memory B cells to therapeutic agents which eliminate other subsets of hematopoietic and immune cells. The finding on CD21 expression adds an additional level of complexity and heterogeneity of B cell memory. The functional implication of these phenotypic differences remains a matter of investigation.  $CD21_{\text{low}}$  B cells have been described as atypical, characterized by functional exhaustion and with a potential role in infection or autoimmunity [48,49].

## 5.3 Bone marrow niches for memory cells

In the BM, switched B<sub>mem</sub> localize individually to VCAM-1+ reticular stromal cells, similar to those maintaining memory T and plasma cells. The multiple receptor-ligand (survival factors) interactions between memory cells and stromal cells construe the importance of BM stromal cells in maintenance and organization of the immunological memory. The single cells transcriptome analysis shows for the first time that distinct subsets of BM stromal cells express the factors IL7, IL15, and Tnfsf13b (BAFF) which are important in the maintenance of memory CD4+, CD8+, B and plasma cells respectively via signaling through corresponding receptors expressed on the memory cells. It has long been shown that T cell support and antigenic stimulation of BCR are dispensable for the long-term maintenance of B<sub>mem</sub>. Stromal cells express several factors important for the survival of B<sub>mem</sub> in a receptor-ligand manner. Thus, stromal cells of the BM are also potentially autonomous in providing niches for the long-term maintenance of immune memory cells without the need for accessory cells in the niche. The findings of this thesis suggest the existence of specialized stromal niches for different subsets of immune memory cells. The exact survival signaling pathways induced in B<sub>mem</sub> by stromal cells should be investigated to help devise ways to boost protective immunological memory or deplete pathological memory cells in autoimmunity, chronic inflammation and cancer.

In conclusion, my doctoral thesis described the bone marrow as a major organ in the maintenance of long-lived quiescent memory B cells and that memory B cells of bone marrow differ from those in spleen in terms of BCR repertoire and surface protein expression. In the bone marrow, a subpopulation of reticular mesenchymal stromal cells organizes survival niches for the maintenance of memory B cells through the expression of important cytokines and chemokines.

## 6 Literature

1. Ahmed R, Gray D. Immunological Memory and Protective Immunity: Understanding Their Relation. *Science* (80- ) [Internet]. 1996;272(5258):54–60. Available from: <http://www.jstor.org/stable/2890771>
2. Tarlinton D. B-cell memory: are subsets necessary? *Nat Rev Immunol*. 2006;6(10):785–90.
3. Kurosaki T, Kometani K, Ise W. Memory B cells. *Nat Rev Immunol* [Internet]. 2015;15(3):149–59. Available from: <http://www.ncbi.nlm.nih.gov/pubmed/25677494>
4. Giesecke C, Frölich D, Reiter K, Mei HE, Wirries I, Kuhly R, Killig M, Glatzer T, Stölzel K, Perka C, Lipsky PE, Dörner T. Tissue distribution and dependence of responsiveness of human antigen-specific memory B cells. *J Immunol* [Internet]. 2014;192(7):3091–100. Available from: <http://www.ncbi.nlm.nih.gov/pubmed/24567530><http://www.jimmunol.org/content/192/7/3091.full>
5. Funakoshi S, Shimizu T, Numata O, Ato M, Melchers F, Ohnishi K. BILL-Cadherin/Cadherin-17 Contributes to the Survival of Memory B Cells. *PLoS One*

- [Internet]. 2015;10(1):e0117566. Available from: <http://dx.plos.org/10.1371/journal.pone.0117566>
6. Weill JC, Le Gallou S, Hao Y, Reynaud CA. Multiple players in mouse B cell memory. *Curr Opin Immunol*. 2013;25(3):334–8.
  7. Mamani-Matsuda M, Cosma A, Weller S, Faili A, Staib C, Garçon L, Hermine O, Beyne-Rauzy O, Fieschi C, Pers JO, Arakelyan N, Varet B, Sauvanet A, Berger A, Paye F, Andrieu JM, Michel M, Godeau B, Buffet P, Reynaud CA, Weill JC. The human spleen is a major reservoir for long-lived vaccinia virus-specific memory B cells. *Blood*. 2008;111(9):4653–9.
  8. Martinez-Gamboa L, Mei H, Loddenkemper C, Ballmer B, Hansen A, Lipsky PE, Emmerich F, Radbruch A, Salama A, Dörner T. Role of the spleen in peripheral memory B-cell homeostasis in patients with autoimmune thrombocytopenia purpura. *Clin Immunol* [Internet]. 2009;130(2):199–212. Available from: <http://dx.doi.org/10.1016/j.clim.2008.09.009>
  9. Gowans JL, Uhr JW. The carriage of immunological memory by small lymphocytes in the rat. *J Exp Med*. 1966 Nov;124(5):1017–30.
  10. Sercan Alp Ö, Durlanik S, Schulz D, McGrath M, Grün JR, Bardua M, Ikuta K, Sgouroudis E, Riedel R, Zehentmeier S, Hauser AE, Tsuneto M, Melchers F, Tokoyoda K, Chang H-D, Thiel A, Radbruch A. Memory CD8<sup>+</sup> T cells colocalize with IL-7<sup>+</sup> stromal cells in bone marrow and rest in terms of proliferation and transcription. *Eur J Immunol* [Internet]. 2015;45(4):975–87. Available from: <http://doi.wiley.com/10.1002/eji.201445295>
  11. Tokoyoda K, Zehentmeier S, Hegazy AN, Albrecht I, Grün JR, Löhning M, Radbruch A. Professional Memory CD4<sup>+</sup> T Lymphocytes Preferentially Reside and Rest in the Bone Marrow. *Immunity*. 2009;30(5):721–30.
  12. Zehentmeier S, Roth K, Cseresnyes Z, Sercan Ö, Horn K, Niesner RA, Chang H-D, Radbruch A, Hauser AE. Static and dynamic components synergize to form a stable survival niche for bone marrow plasma cells. *Eur J Immunol* [Internet]. 2014;44(8):2306–17. Available from: <http://doi.wiley.com/10.1002/eji.201344313>
  13. Hanazawa A, Hayashizaki K, Shinoda K, Yagita H, Okumura K, Löhning M, Hara T, Tani-ichi S, Ikuta K, Eckes B, Radbruch A, Tokoyoda K, Nakayama T. CD49b-dependent establishment of T helper cell memory. *Immunol Cell Biol* [Internet]. 2013;91(8):524–31. Available from: <http://www.nature.com/doi/10.1038/icb.2013.36>
  14. Hanazawa A, Löhning M, Radbruch A, Tokoyoda K. CD49b/CD69-Dependent Generation of Resting T Helper Cell Memory. *Front Immunol* [Internet]. 2013;4(July):5–8. Available from: <http://journal.frontiersin.org/article/10.3389/fimmu.2013.00183/abstract>
  15. Nilsson SK, Debatis ME, Dooner MS, Madri JA, Quesenberry PJ, Becker PS. Immunofluorescence characterization of key extracellular matrix proteins in murine bone marrow in situ. *J Histochem Cytochem*. 1998 Mar;46(3):371–7.
  16. Chu VT, Frohlich A, Steinhauser G, Scheel T, Roch T, Fillatreau S, Lee JJ, Löhning M, Berek C. Eosinophils are required for the maintenance of plasma cells in the bone marrow. *Nat Immunol*. 2011 Feb;12(2):151–9.
  17. Bortnick A, Chernova I, Spencer SP, Allman D. No strict requirement for eosinophils for bone marrow plasma cell survival. *Eur J Immunol*. 2018 May;48(5):815–21.
  18. Haberland K, Ackermann JA, Ipseiz N, Culemann S, Pracht K, Englbrecht M, Jack H-M, Schett G, Schuh W, Kronke G. Eosinophils are not essential for maintenance of murine plasma cells in the bone marrow. *Eur J Immunol*. 2018 May;48(5):822–8.
  19. Tokoyoda K, Zehentmeier S, Hegazy AN, Albrecht I, Grün JR, Löhning M, Radbruch A. Professional memory CD4<sup>+</sup> T lymphocytes preferentially reside and rest in the bone marrow. *Immunity*. 2009 May;30(5):721–30.
  20. Kallies A, Hasbold J, Tarlinton DM, Dietrich W, Corcoran LM, Hodgkin PD, Nutt SL. Plasma cell ontogeny defined by quantitative changes in blimp-1 expression. *J Exp Med* [Internet]. 2004;200(8):967–77. Available from: <http://www.pubmedcentral.nih.gov/articlerender.fcgi?artid=2211847&tool=pmcentrez&rendertype=abstract>
  21. Cossarizza A, Chang H-D, Radbruch A, Akdis M, Andra I, Annunziato F, Bacher

- P, Barnaba V, Battistini L, Bauer WM, Baumgart S, Becher B, Beisker W, Berek C, Blanco A, Borsellino G, Boulais PE, Brinkman RR, Buscher M, Busch DH, Bushnell TP, Cao X, Cavani A, Chattopadhyay PK, Cheng Q, Chow S, Clerici M, Cooke A, Cosma A, Cosmi L, Cumanò A, Dang VD, Davies D, De Biasi S, Del Zotto G, Della Bella S, Dellabona P, Deniz G, Dessing M, Diefenbach A, Di Santo J, Dieli F, Dolf A, Donnenberg VS, Dorner T, Ehrhardt GRA, Endl E, Engel P, Engelhardt B, Esser C, Everts B, Dreher A, Falk CS, Fehniger TA, Filby A, Fillatreau S, Follo M, Forster I, Foster J, Foulds GA, Frenette PS, Galbraith D, Garbi N, Garcia-Godoy MD, Geginat J, Ghoreschi K, Gibellini L, Goettlinger C, Goodyear CS, Gori A, Grogan J, Gross M, Grutzkau A, Grummitt D, Hahn J, Hammer Q, Hauser AE, Haviland DL, Hedley D, Herrera G, Herrmann M, Hiepe F, Holland T, Hombrink P, Houston JP, Hoyer BF, Huang B, Hunter CA, Iannone A, Jack H-M, Javega B, Jonjic S, Juelke K, Jung S, Kaiser T, Kalina T, Keller B, Khan S, Kienhofer D, Kroneis T, Kunkel D, Kurts C, Kvistborg P, Lannigan J, Lantz O, Larbi A, LeibundGut-Landmann S, Leipold MD, Levings MK, Litwin V, Liu Y, Lohoff M, Lombardi G, Lopez L, Lovett-Racke A, Lubberts E, Ludewig B, Lugli E, Maecker HT, Martrus G, Matarese G, Maueroeder C, McGrath M, McInnes I, Mei HE, Melchers F, Melzer S, Mielenz D, Mills K, Mirer D, Mjosberg J, Moore J, Moran B, Moretta A, Moretta L, Mosmann TR, Muller S, Muller W, Munz C, Multhoff G, Munoz LE, Murphy KM, Nakayama T, Nasi M, Neudorfl C, Nolan J, Nourshargh S, O'Connor J-E, Ouyang W, Oxenius A, Palankar R, Panse I, Peterson P, Peth C, Petriz J, Philips D, Pickl W, Piconese S, Pinti M, Pockley AG, Podolska MJ, Pucillo C, Quataert SA, Radstake TRDJ, Rajwa B, Rebhahn JA, Recktenwald D, Remmerswaal EBM, Rezvani K, Rico LG, Robinson JP, Romagnani C, Rubartelli A, Ruckert B, Ruland J, Sakaguchi S, Sala-de-Oyanguren F, Samstag Y, Sanderson S, Sawitzki B, Scheffold A, Schiemann M, Schildberg F, Schimisky E, Schmid SA, Schmitt S, Schober K, Schuler T, Schulz AR, Schumacher T, Scotta C, Shankey TV, Shemer A, Simon A-K, Spidlen J, Stall AM, Stark R, Stehle C, Stein M, Steinmetz T, Stockinger H, Takahama Y, Tarnok A, Tian Z, Toldi G, Tornack J, Traggiai E, Trotter J, Ulrich H, van der Braber M, van Lier RAW, Veldhoen M, Vento-Asturias S, Vieira P, Voehringer D, Volk H-D, von Volkman K, Waisman A, Walker R, Ward MD, Warnatz K, Warth S, Watson J V, Watzl C, Wegener L, Wiedemann A, Wienands J, Willmsky G, Wing J, Wurst P, Yu L, Yue A, Zhang Q, Zhao Y, Ziegler S, Zimmermann J. Guidelines for the use of flow cytometry and cell sorting in immunological studies. *Eur J Immunol*. 2017 Oct;47(10):1584–797.
22. Greiff V, Menzel U, Miho E, Weber C, Riedel R, Cook S, Valai A, Lopes T, Radbruch A, Winkler TH, Reddy ST. Systems Analysis Reveals High Genetic and Antigen-Driven Predetermination of Antibody Repertoires throughout B Cell Development. *Cell Rep [Internet]*. 2017 May 16 [cited 2018 Apr 26];19(7):1467–78. Available from: <https://www.sciencedirect.com/science/article/pii/S221112471730565X>
  23. Turchaninova MA, Davydov A, Britanova O V, Shugay M, Bikos V, Egorov ES, Kirgizova VI, Merzlyak EM, Staroverov DB, Bolotin DA, Mamedov IZ, Izraelson M, Logacheva MD, Kladova O, Plevova K, Pospisilova S, Chudakov DM. High-quality full-length immunoglobulin profiling with unique molecular barcoding. *Nat Protoc*. 2016 Sep;11(9):1599–616.
  24. Shugay M, Britanova O V, Merzlyak EM, Turchaninova MA, Mamedov IZ, Tuganbaev TR, Bolotin DA, Staroverov DB, Putintseva E V, Plevova K, Linnemann C, Shagin D, Pospisilova S, Lukyanov S, Schumacher TN, Chudakov DM. Towards error-free profiling of immune repertoires. *Nat Methods*. 2014 Jun;11(6):653–5.
  25. Meng W, Zhang B, Schwartz GW, Rosenfeld AM, Ren D, Thome JJC, Carpenter DJ, Matsuoka N, Lerner H, Friedman AL, Granot T, Farber DL, Shlomchik MJ, Hershberg U, Luning Prak ET. An atlas of B-cell clonal distribution in the human body. *Nat Biotechnol*. 2017 Sep;35(9):879–84.
  26. Satija R, Farrell JA, Gennert D, Schier AF, Regev A. Spatial reconstruction of single-cell gene expression data. *Nat Biotechnol*. 2015 May;33(5):495–502.
  27. McDavid A, Finak G, Chattopadhyay PK, Dominguez M, Lamoreaux L, Ma SS, Roederer M, Gottardo R. Data exploration, quality control and testing in single-

- cell qPCR-based gene expression experiments. *Bioinformatics*. 2013 Feb;29(4):461–7.
28. Corcoran AE. Immunoglobulin locus silencing and allelic exclusion. *Semin Immunol*. 2005 Apr;17(2):141–54.
  29. Croce CM, Shander M, Martinis J, Cicurel L, D’Ancona GG, Dolby TW, Koprowski H. Chromosomal location of the genes for human immunoglobulin heavy chains. *Proc Natl Acad Sci U S A*. 1979 Jul;76(7):3416–9.
  30. Greiff V, Menzel U, Haessler U, Cook SC, Friedensohn S, Khan TA, Pogson M, Hellmann I, Reddy ST. Quantitative assessment of the robustness of next-generation sequencing of antibody variable gene repertoires from immunized mice. *BMC Immunol* [Internet]. 2014;15:40. Available from: <http://www.pubmedcentral.nih.gov/articlerender.fcgi?artid=4233042&tool=pmcentrez&rendertype=abstract>
  31. Greiff V, Miho E, Menzel U, Reddy ST. Bioinformatic and Statistical Analysis of Adaptive Immune Repertoires. *Trends Immunol* [Internet]. 2015 Nov 1 [cited 2018 Apr 26];36(11):738–49. Available from: <https://www.sciencedirect.com/science/article/pii/S1471490615002239>
  32. Barrington RA, Schneider TJ, Pitcher LA, Mempel TR, Ma M, Barteneva NS, Carroll MC. Uncoupling CD21 and CD19 of the B-cell coreceptor. *Proc Natl Acad Sci U S A* [Internet]. 2009;106(34):14490–5. Available from: <http://www.pubmedcentral.nih.gov/articlerender.fcgi?artid=2732852&tool=pmcentrez&rendertype=abstract>
  33. Haas KM, Tedder TF. Role of the CD19 and CD21/35 receptor complex in innate immunity, host defense and autoimmunity. *Adv Exp Med Biol* [Internet]. 2005;560:125–39. Available from: <http://www.ncbi.nlm.nih.gov/pubmed/15934172>
  34. Okhrimenko A, Grün JR, Westendorf K, Fang Z, Reinke S, von Roth P, Wassilew G, Köhl AA, Kudernatsch R, Demski S, Scheibenbogen C, Tokoyoda K, McGrath MA, Raftery MJ, Schönrich G, Serra A, Chang H-D, Radbruch A, Dong J. Human memory T cells from the bone marrow are resting and maintain long-lasting systemic memory. *Proc Natl Acad Sci U S A* [Internet]. 2014;111(25):9229–34. Available from: <http://www.pubmedcentral.nih.gov/articlerender.fcgi?artid=4078840&tool=pmcentrez&rendertype=abstract>
  35. Siracusa F, Alp ÖS, Maschmeyer P, McGrath M, Mashreghi M-F, Hojyo S, Chang H-D, Tokoyoda K, Radbruch A. Maintenance of CD8<sup>+</sup> memory T lymphocytes in the spleen but not in the bone marrow is dependent on proliferation. *Eur J Immunol* [Internet]. 2017 Nov 1 [cited 2018 Apr 24];47(11):1900–5. Available from: <http://doi.wiley.com/10.1002/eji.201747063>
  36. Gerdes J, Lemke H, Baisch H, Wacker HH, Schwab U, Stein H. Cell cycle analysis of a cell proliferation-associated human nuclear antigen defined by the monoclonal antibody Ki-67. *J Immunol*. 1984 Oct;133(4):1710–5.
  37. Wheeler GP, Alexander JA. STUDIES WITH MUSTARDS. VI. EFFECTS OF ALKYLATING AGENTS UPON NUCLEIC ACID SYNTHESIS IN BILATERALLY GROWN SENSITIVE AND RESISTANT TUMORS. *Cancer Res* [Internet]. 1964 Sep 1 [cited 2018 Apr 26];24(8):1338–46. Available from: <http://www.ncbi.nlm.nih.gov/pubmed/14221792>
  38. Lisignoli G, Monaco MCG, Facchini A, Toneguzzi S, Cattini L, Hilbert DM, Lavaroni S, Belvedere O, Degrossi A. In vitro cultured stromal cells from human tonsils display a distinct phenotype and induce B cell adhesion and proliferation. *Eur J Immunol*. 1996;26(1):17–27.
  39. Tokoyoda K, Hauser AE, Nakayama T, Radbruch A. Organization of immunological memory by bone marrow stroma. *Nat Rev Immunol* [Internet]. 2010;10(3):193–200. Available from: <http://dx.doi.org/10.1038/nri2727>
  40. Laurens van der Maaten GH. Visualizing Data using t-SNE. 2008;9:2579–605.
  41. Morrison SJ, Scadden DT. The bone marrow niche for haematopoietic stem cells. *Nature* [Internet]. 2014;505:327–34. Available from: <http://www.ncbi.nlm.nih.gov/pubmed/24429631>
  42. Starnes T, Broxmeyer HE, Robertson MJ, Hromas R. Cutting edge: IL-17D, a novel member of the IL-17 family, stimulates cytokine production and inhibits hemopoiesis. *J Immunol*. 2002 Jul;169(2):642–6.

43. Geijtenbeek TBH, Gringhuis SI. Signalling through C-type lectin receptors: shaping immune responses. *Nat Rev Immunol*. 2009 Jul;9(7):465–79.
44. Wolf SF, Temple PA, Kobayashi M, Young D, Dicig M, Lowe L, Dzialo R, Fitz L, Ferez C, Hewick RM. Cloning of cDNA for natural killer cell stimulatory factor, a heterodimeric cytokine with multiple biologic effects on T and natural killer cells. *J Immunol*. 1991 May;146(9):3074–81.
45. van der Voort R, van Lieshout AWT, Toonen LWJ, Sloetjes AW, van den Berg WB, Figdor CG, Radstake TRDJ, Adema GJ. Elevated CXCL16 expression by synovial macrophages recruits memory T cells into rheumatoid joints. *Arthritis Rheum*. 2005 May;52(5):1381–91.
46. Zhao X, Sato A, Dela Cruz CS, Linehan M, Luegering A, Kucharzik T, Shirakawa A-K, Marquez G, Farber JM, Williams I, Iwasaki A. CCL9 is secreted by the follicle-associated epithelium and recruits dome region Peyer's patch CD11b+ dendritic cells. *J Immunol*. 2003 Sep;171(6):2797–803.
47. Weng Y, Siciliano SJ, Waldburger KE, Sirotina-Meisher A, Staruch MJ, Daugherty BL, Gould SL, Springer MS, DeMartino JA. Binding and functional properties of recombinant and endogenous CXCR3 chemokine receptors. *J Biol Chem*. 1998 Jul;273(29):18288–91.
48. Isnardi I, Ng Y-S, Menard L, Meyers G, Saadoun D, Srdanovic I, Samuels J, Berman J, Buckner JH, Cunningham-Rundles C, Meffre E. Complement receptor 2/CD21- human naive B cells contain mostly autoreactive unresponsive clones. *Blood*. 2010 Jun;115(24):5026–36.
49. Rakhmanov M, Keller B, Gutenberger S, Foerster C, Hoenig M, Driessen G, van der Burg M, van Dongen JJ, Wiech E, Visentini M, Quinti I, Prasse A, Voelxen N, Salzer U, Goldacker S, Fisch P, Eibel H, Schwarz K, Peter H-H, Warnatz K. Circulating CD21<sup>low</sup> B cells in common variable immunodeficiency resemble tissue homing, innate-like B cells. *Proc Natl Acad Sci U S A*. 2009 Aug;106(32):13451–6.

## 7 Statutory Declaration

“I, **Richard Kwasi Addo**, by personally signing this document in lieu of an oath, hereby affirm that I prepared the submitted dissertation on the topic: **BONE MARROW MAINTAINS ISOTYPE SWITCHED MEMORY B CELLS IN STROMAL NICHES**, independently and without the support of third parties, and that I used no other sources and aids than those stated.

All parts which are based on the publications or presentations of other authors, either in letter or in spirit, are specified as such in accordance with the citing guidelines. The sections on methodology (in particular regarding practical work, laboratory regulations, statistical processing) and results (in particular regarding figures, charts and tables) are exclusively my responsibility.

My contributions to any publications to this dissertation correspond to those stated in the below joint declaration made together with the supervisor. All publications created within the scope of the dissertation comply with the guidelines of the ICMJE (International Committee of Medical Journal Editors; [www.icmje.org](http://www.icmje.org)) on authorship. In addition, I declare that I am aware of the regulations of Charité – Universitätsmedizin Berlin on ensuring good scientific practice and that I commit to comply with these regulations.

The significance of this statutory declaration and the consequences of a false statutory declaration under criminal law (Sections 156, 161 of the German Criminal Code) are known to me.”

Date

Signature

## 8 Declaration of your own contribution to any publications

Publication 1:

### **Single-Cell transcriptomes of murine Bone Marrow Stromal Cells Reveal Niche-Associated Heterogeneity**

**Richard K. Addo**, Frederik Heinrich, Gitta Anne Heinz, Daniel Schulz, Özen Sercan-Alp, Katrin Lehmann, Cam Loan Tran, Markus Bardua, Mareen Matz<sup>3</sup>, Max Löhning, Anja E. Hauser, Andrey Kruglov, Hyun-Dong Chang, Pawel Durek, Andreas Radbruch, and Mir-Farzin Mashreghi.

European Journal of Immunology 2019

Contribution:

- First authorship
- Planning and preparation of the project together with Prof. Andreas Radbruch, Dr Hyun-Dong Chang and Dr. Mir-Farzin Mashreghi
- Conducting the animal experiment
- Enzymatic digestion and single cell isolation of bone marrow cells
- FACS sorting and analysis of data
- Independent graphical representation of the results in all Figures
- Essential contribution to the critical appraisal of the results with identification of the relevant findings of the study including their limitations
- Significant contribution to the processing and evaluation single cells RNA sequencing data
- Development of the manuscript leading to publication together with Prof. Dr. Andreas Radbruch, Dr. Hyun-Dong Chang and Dr. Mir-Farzin Mashreghi
- Collaboration with Prof. Dr. Andreas Radbruch, Dr. Hyun-Dong Chang and Dr. Mir-Farzin Mashreghi on the revision and implementation of the reviewers' comments

Publication 2:

### **MicroRNA-31 reduces the motility of proinflammatory T helper 1 lymphocytes**

Bardua M, Haftmann C, Durek P, Westendorf K, Buttgereit A, Tran CL, McGrath M, Weber M1, Lehmann K, **Addo RK**, Heinz GA, Stittrich AB, Maschmeyer P, Radbruch H, Lohoff M, Chang HD, Radbruch A, Mashreghi MF.

*Frontiers in Immunology, 2018*

Contribution:

- Co-authorship
- Essential contribution to the critical appraisal of the results with identification of the relevant findings of the study including their limitations.



- Significant contribution to the processing and evaluation of qRT-PCR data measuring miR-31, Foxo1, Sell, Klf2 and Cd69 expression in Figure 5
- FACS data analysis of Tbet (Figure 5D, 5F), Foxp3 (Figure 5G)
- collaboration on the revision and implementation of the reviewers' comments

Publication 3:

**The Regulation of IFN Type I Pathway Related Genes RSAD2 and ETV7 Specifically Indicate Antibody-Mediated Rejection After Kidney Transplantation**

Matz M, Heinrich F, Zhang Q, Lorkowski C, Seelow E, Wu K, Lachmann N, **Addo RK**, Durek P, Mashreghi MF, Budde K.

*Clinical Transplantation, 2018*

Contribution:

- Co-authorship
- Essential contribution to the critical appraisal of the results with identification of the relevant findings of the study including their limitations Figure 2 and Figure 3.
- Significant contribution to the processing and evaluation high throughput RNA sequencing data including selection of candidate genes Figure 2 and Figure 3



---

Signature, date and stamp of supervising university professor / lecturer

---

Signature of doctoral candidate

**Short Communication****Single-cell transcriptomes of murine bone marrow stromal cells reveal niche-associated heterogeneity**

*Richard K. Addo<sup>1</sup>, Frederik Heinrich<sup>1</sup>, Gitta Anne Heinz<sup>1</sup>, Daniel Schulz<sup>1</sup>, Özen Sercan-Alp<sup>1,2</sup>, Katrin Lehmann<sup>1</sup>, Cam Loan Tran<sup>1</sup>, Markus Bardua<sup>1</sup>, Mareen Matz<sup>3</sup>, Max Löhning<sup>4</sup>, Anja E. Hauser<sup>1,4</sup>, Andrey Kruglov<sup>1</sup>, Hyun-Dong Chang<sup>1</sup>, Pawel Durek<sup>1</sup>, Andreas Radbruch<sup>1</sup>  and Mir-Farzin Mashreghi<sup>1</sup> *

<sup>1</sup> Deutsches Rheuma-Forschungszentrum (DRFZ), an Institute of the Leibniz Association, Berlin, Germany

<sup>2</sup> Sanofi-Aventis Germany, Frankfurt am Main, Germany

<sup>3</sup> Division of Nephrology and Internal Intensive Care Medicine, Charité-Universitätsmedizin Berlin, Germany

<sup>4</sup> Department of Rheumatology and Clinical Immunology, Charité-Universitätsmedizin, Berlin, Germany

Bone marrow (BM) stromal cells are important in the development and maintenance of cells of the immune system. Using single cell RNA sequencing, we here explore the functional and phenotypic heterogeneity of individual transcriptomes of 1167 murine BM mesenchymal stromal cells. These cells exhibit a tremendous heterogeneity of gene expression, which precludes the identification of defined subpopulations. However, according to the expression of 108 genes involved in the communication of stromal cells with hematopoietic cells, we have identified 14 non-overlapping subpopulations, with distinct cytokine or chemokine gene expression signatures. With respect to the maintenance of subsets of immune memory cells by stromal cells, we identified distinct subpopulations expressing *Il7*, *Il15* and *Tnfsf13b*. Together, this study provides a comprehensive dissection of the BM stromal heterogeneity at the single cell transcriptome level and provides a basis to understand their lifestyle and their role as organizers of niches for the long-term maintenance of immune cells.

**Keywords:** bone marrow · cytokines · hematopoietic cells · single cell sequencing · stromal cells



Additional supporting information may be found online in the Supporting Information section at the end of the article.

**Introduction**

Bone marrow (BM) stromal cells provide distinct niches for the maintenance and development of hematopoietic cells, including

various cells of the immune system [1–5], but how the diversity of hematopoietic cells is matched by the diversity of mesenchymal stromal cells organizing their niches is poorly understood [6, 7]. In vivo, BM stromal cells have been shown to express vascular cell-adhesion molecule 1 (VCAM1; CD106) [8], CXCL12 and IL7, collagen II and XI [1–5], PDGFRB (platelet-derived growth factor receptor B), CDH11 (Cadherin 11), LepR (Leptin receptor), Nestin

**Correspondence:** Dr. Mir-Farzin Mashreghi and Dr. Pawel Durek  
e-mail: mashregi@drfz.de; pawel.durek@drfz.de

and other genes [9, 10], but a comprehensive analysis of their individual gene expression profiles has been missing.

In the present study, we describe a novel protocol for the isolation of BM stromal cells *ex vivo* by fluorescence-activated cell sorting, yielding more than 95% purity and more than 60% recovery. We have determined and describe here the individual, complete transcriptomes of more than 1000 individual BM stromal cells by single cell RNA sequencing (scRNA-seq). These cells show a remarkable heterogeneity, in particular with respect to the expression of genes encoding cell-bound and secreted molecules involved in the communication of stromal cells with cells of the hematopoietic system. We have identified distinct stromal subpopulations, which qualify to organize specific niches for distinct immune memory as well as hematopoietic cells.

## Results and discussion

### Isolation of individual BM stromal cells

In order to estimate the size of the stromal compartment in the BM, we have determined the frequency of radiation-resistant reticular cells in Ubiquitin:GFP chimeric mice [1], by fluorescence microscopy. The GFP+VCAM-1+CD31- reticular cell compartment constituted about 2% ( $1.945\% \pm 0.1007$  SEM) or  $\sim 5 \times 10^6$  of all BM cells *in situ* (Fig. 1A) [2]. Since BM stromal cells form a tight reticular network, their isolation as individual cells provides a challenge. Conventional single cell preparation methods use mechanical disruption and enzymes targeting adhesive extracellular matrix (collagenase, DNase and dispase) [11]. To break and prevent re-adhesion of stromal cells, we here describe the usage of Latrunculin B, a drug interfering with the polymerization of actin [12]. Addition of Latrunculin B to the digestion cocktail significantly doubled, as compared to isolation without Latrunculin B (Fig. 1B and 1C), the recovery of *ex vivo* isolated BM stroma cells. This cell recovery is about 60% of the cell numbers estimated *in situ* (Fig. 1C and 1D). More important, the addition of Latrunculin B did not affect the viability of the cells (Fig. 1E). Consequently, isolation of stromal cells was always performed with the addition to Latrunculin B to the digestion cocktail.

### Single cell transcriptomes of BM stromal cells

*Ex vivo* VCAM-1+CD45-Ter119-CD31- BM cells were sorted by FACS to 97% purity (Fig. 1F) and transcriptomes of individual cells were determined using 10X genomics-based droplet sequencing. Transcriptomes of 1167 individual stromal cells were analyzed with a mean of 398,739 reads per cell resulting in a saturation rate of 95.6% (Fig. 1G), i.e., more than 95% of each transcriptome was captured. A total of 16,142 genes were detected in total, with a median of 1,538 genes per cell (Fig. 1H and 1I). We used the entire transcriptomes of each cell to perform a t-distributed stochastic neighbor embedding (t-SNE) analysis [13] and visualize the basic

heterogeneity of the cells. Within the t-SNE plots, genes of interest expressed by cells are highlighted in red.

More than 90% of the BM stromal cells expressed the genes *Vcam1*, *Pdgfrb*, *LepR*, *Cadherin 11* (*Cdh11*), qualifying these genes as genuine stroma cells markers, but also confirming the quality of the cells [14] (Fig. 1J). The stromal cells did not express the pericyte marker *nestin* (*Nes*), [15] (Fig. 1J).

Most of the cells were resting in terms of proliferation, since they did not express the proliferation marker *Mki67* [16] (Fig. 1K), confirming earlier results obtained with EdU pulse chase labelling [3]. Nearly all cells expressed at least one of the Isocitrate dehydrogenases isoforms (*Igh1*, *Idh2* or *Idh3*), the rate limiting enzyme of the TCA [17] (Fig. 1K). With respect to the energy source of metabolism, stromal cells were heterogeneous, some expressing rate limiting enzymes *Pfkm* and *Pfkl* of the glycolytic pathway [18], or *Crat* for fatty acid oxidation [19] or *Hmgcs1* for ketogenesis [20].

Genes encoding cell surface molecules were often expressed individually by the stromal cells, as exemplified here for *Lamp1* (*Cd107a*), *Lamp2* (*Cd107b*), *Ox2* (*Cd200*), *Bst2* (*Cd317*), *Cd1d1*, *Cd63*, *Cd105*, *Cd24a*, *Cd44* and *Cd47* (Fig. 2A). At the level of single cell transcriptomes, cells expressing the various cluster of differentiation (CD) genes (Fig. 2A) are dispersed over the t-SNE plots. This observation suggests that stromal cells expressing or not a respective CD marker are closely related and do not necessarily represent distinct subpopulation. However, subpopulations expressing distinct combinations of CD markers can readily be identified by contrasting their expression as found by sequencing (Fig. 2B) and the proportion of cells expressing two or at least one of the genes encoding for surface proteins (Fig. 2C).

### Cytokine and chemokine expression is restricted to distinct subsets of stromal cells

In the interaction between stromal cells and hematopoietic cells, the expression of chemokines and cytokines by stromal cells is essential for them to attract and control hematopoietic cells. Thus, we analyzed the stromal cell transcriptomes for the expression of genes which encode for secreted proteins. We selected 108 genes (Supporting Information 1A) for further analysis, based on their established role in the communication of stromal cells with cells of the hematopoietic system. 37 of 108 selected genes were differentially regulated and were used for a supervised clustering analysis (Materials & methods section for detailed description). 14 non-overlapping cytokine/chemokine subsets of stromal cells were identified by the clustering analysis (Fig. 3A). In contrast, genes like *Cxcl12*, *Kitl*, colony stimulating factor 1 (*Csf1*) and Laminin B1 (*Lamb1*), were expressed by most stromal cells, hence they do not define distinct subpopulations of stromal cells based on positive and negative expression (Fig. 3A). Although *Cxcl12* is expressed in almost all stromal cells, we identified three subpopulations of stromal cells according to the expression level. 126 cells ( $\sim 12\%$ ) expressed low amounts (*Cxcl12lo*;  $< 4$  ln normalized unique molecular identifier (lnUMI) counts per cell; average

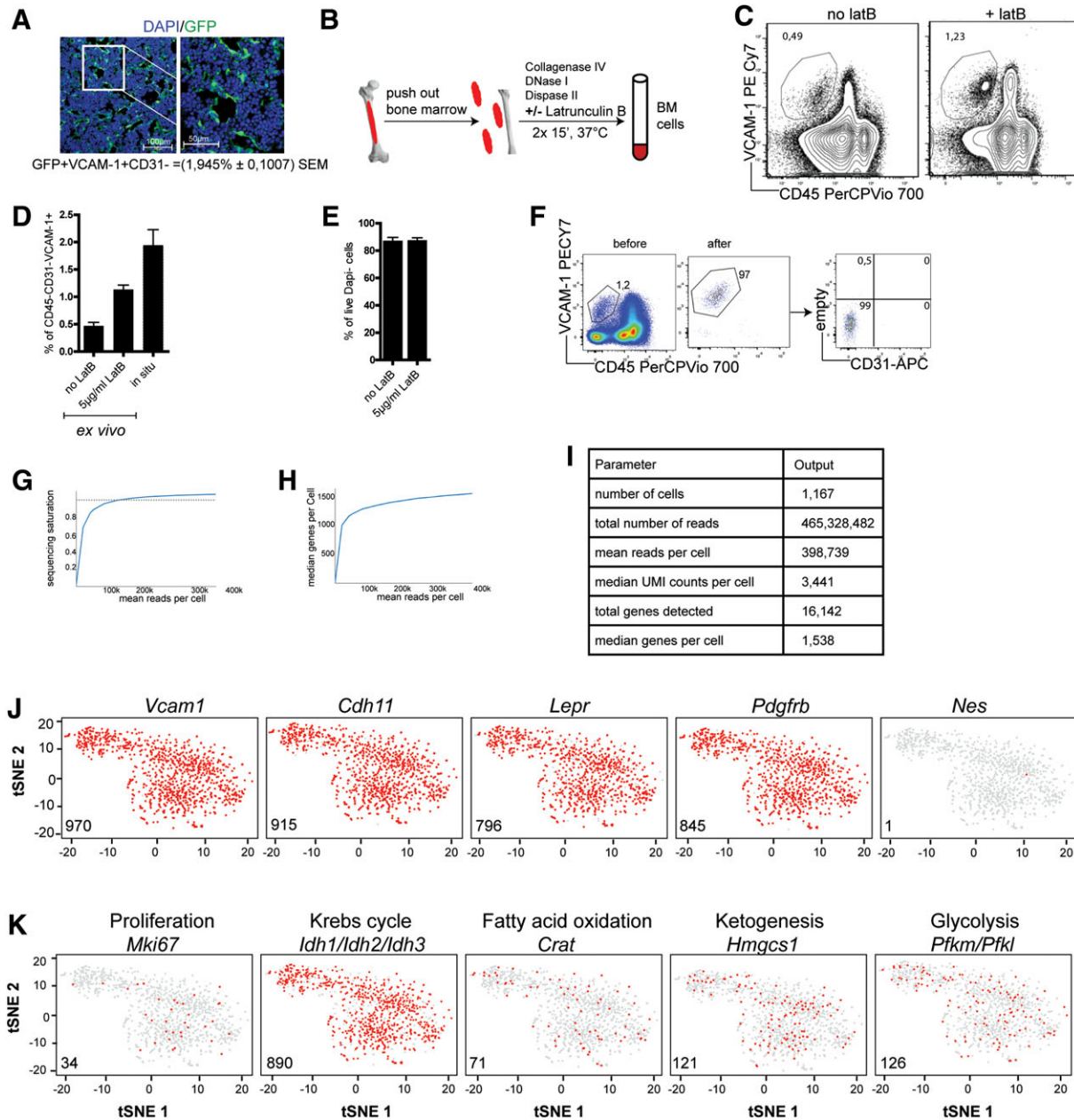


**Figure 1.** Isolation and single cell sequencing of ex vivo VCAM+CD45-CD31-Ter119- BM stromal cells. (A) In situ quantification of BM reticular stromal cells: DAPI+GFP+(VCAM-1+CD31-) reticular cells constituted  $1.945\% \pm 0.1007$  SEM of BM cells. Representative image of analysis of 30 histology sections from 5 different mice in 3 independent experiments. Scale bars: 100 and 50  $\mu\text{m}$ , 20x magnification (B) Schematic overview of isolation of BM stromal cells. (C) Representative dot plots of VCAM-1 against CD45 gated on CD31-Ter119-Dapi- comparing isolation with or without Latrunculin B. (D) Frequencies of ex vivo BM VCAM-1+ stromal cells isolated with or without addition of Latrunculin B compared to those determined in situ. (E) Frequencies of DAPI- (live) BM cells isolated with or without addition of Latrunculin B. (F) Representative plot of cytometric sorting of ex-vivo BM VCAM-1+CD45-CD31-Ter119- cells (G-I) Quality assessment of the 10x genomic sequencing, showing sequencing saturation (G) and median genes per cell (H) against the mean reads per cell and the summary of the sequencing (I). (J) t-SNE plots highlighting the expression (red) of individual BM stromal markers. (K) t-SNE plots showing the expression (red) of genes associated with cellular function of proliferation (cell cycle) and metabolism in individual cells. Data from (C and E) represent pooled results from 4 independent experiments each with 3–5 mice per group. Data from E is extracted from results of experiments described in (A and C). The t-SNE analyses shown in Fig. 1J and 1K are based on  $n = 1035$  individual stromal cells.

of 3.06 lnUMI counts), 80 cells (~8%) with intermediate expression level (*Cxcl12int*;  $\geq 4$  and  $\leq 5$  lnUMIs; average of 4.59 lnUMIs per cell) and 829 cells (80%) expressing high levels of *Cxcl12* (*Cxcl12high*;  $>5$  lnUMIs; average of 5.74 lnUMIs per cell) (Sup-

porting Information Fig. 2A). The three *Cxcl12* subpopulations differ in their molecular signatures and could potentially have different functions within the bone marrow (Supporting Information Fig. 2B).

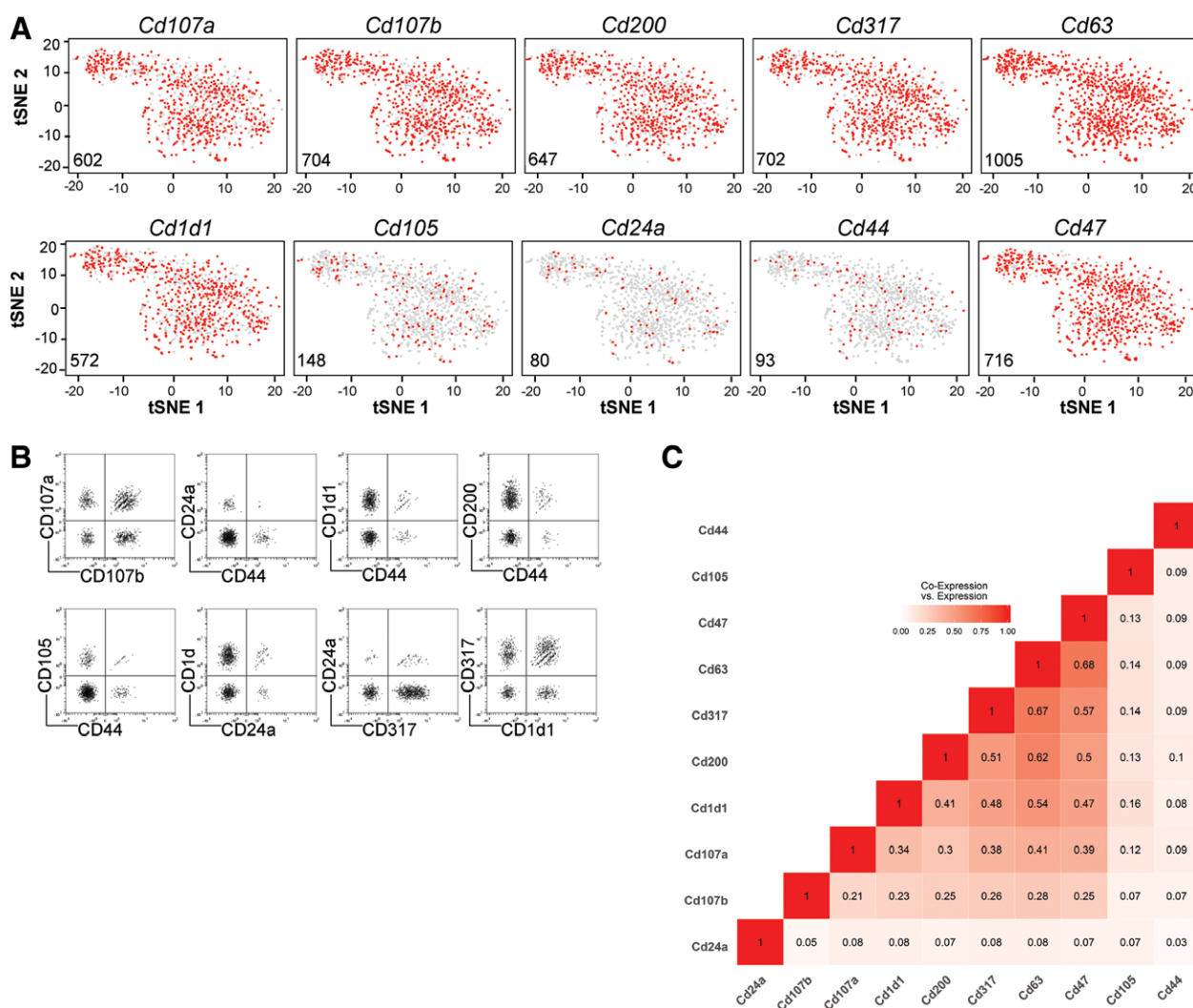


**Figure 2.** Expression of genes encoding CD markers. The experimental procedure is the same as described in the legend of Fig. 1. (A) t-SNE plots highlighting the distribution and expression (red) of genes encoding for surface markers. (B) Scatterplots; Co-expression of CD genes as found by normalized unique molecular identifier-counts (UMI-counts) from sequencing. Co-expression of genes were arcsinh-transformed for flow cytometric-like visualization, an artificial noise was subtracted to 0 counts. (C) Co-expression of selected CD-marker genes as defined by Jaccard similarity coefficient (Proportion of cells expressing two or at least one marker). The t-SNE analysis shown in Fig. 2 is based on  $n = 1035$  individual stromal cells.

In order to test the stability of the identified clusters, we applied Consensus Clustering based on random t-SNEs as well as Consensus Clustering as described by Kiselev et al. [21]. Both methods verified the stability of most of the identified clusters except the cluster for *Cxcl9*. The clusters for *Cxcl16* and *Il15* expressing stromal cells could be verified by the random t-SNE approach but not by the Consensus Clustering method from Kiselev et al. In addition, we identified clusters of stromal cells expressing *Il4ra* and *Tgfb1* by random t-SNE approach as well as clusters for *Il17rd*, *Ccl7*, *Cxcl1* and *Cxcl10* by using both stability algorithms (Supporting Information Figs. 2 and 3). Thus, cells expressing the cytokines *Il7*, *Il15*, *Il12a*, *Il17d*, *Clec14a*, *Igf2*, *Lgals4*, *Tnfsf13b*, *Il4*, *Wnt5a* and *Tgfb1*, or the chemokines *Ccl9*, *Cxcl16* form unique subsets of bone marrow stromal cells (Fig. 3A).

IL17D is a novel cytokine which inhibits the development of myeloid progenitor cells [22]. CLEC14A is a type I transmembrane involved in cell-to-cell adhesion, and thus shaping immune response [23]. IL12A has multiple effects on T and natural killer cells [24]. CXCL16 attracts memory T cells which express CXCR6 [25]. CCL9 and CCL7 attract subsets of dendritic [26] and monocytes, respectively [27]. Expression of any of these chemokine/cytokine genes was indeed exclusive to distinct stromal cells, with less than 10% of cells co-expressing any two of these genes as estimated by the Jaccard similarity coefficient (Fig. 3B). Furthermore, stromal cells expressing these cytokine and chemokine genes express defined gene signatures, based on their entire transcriptomes, qualifying them as distinct subpopulations of stromal cells (Fig. 3C).



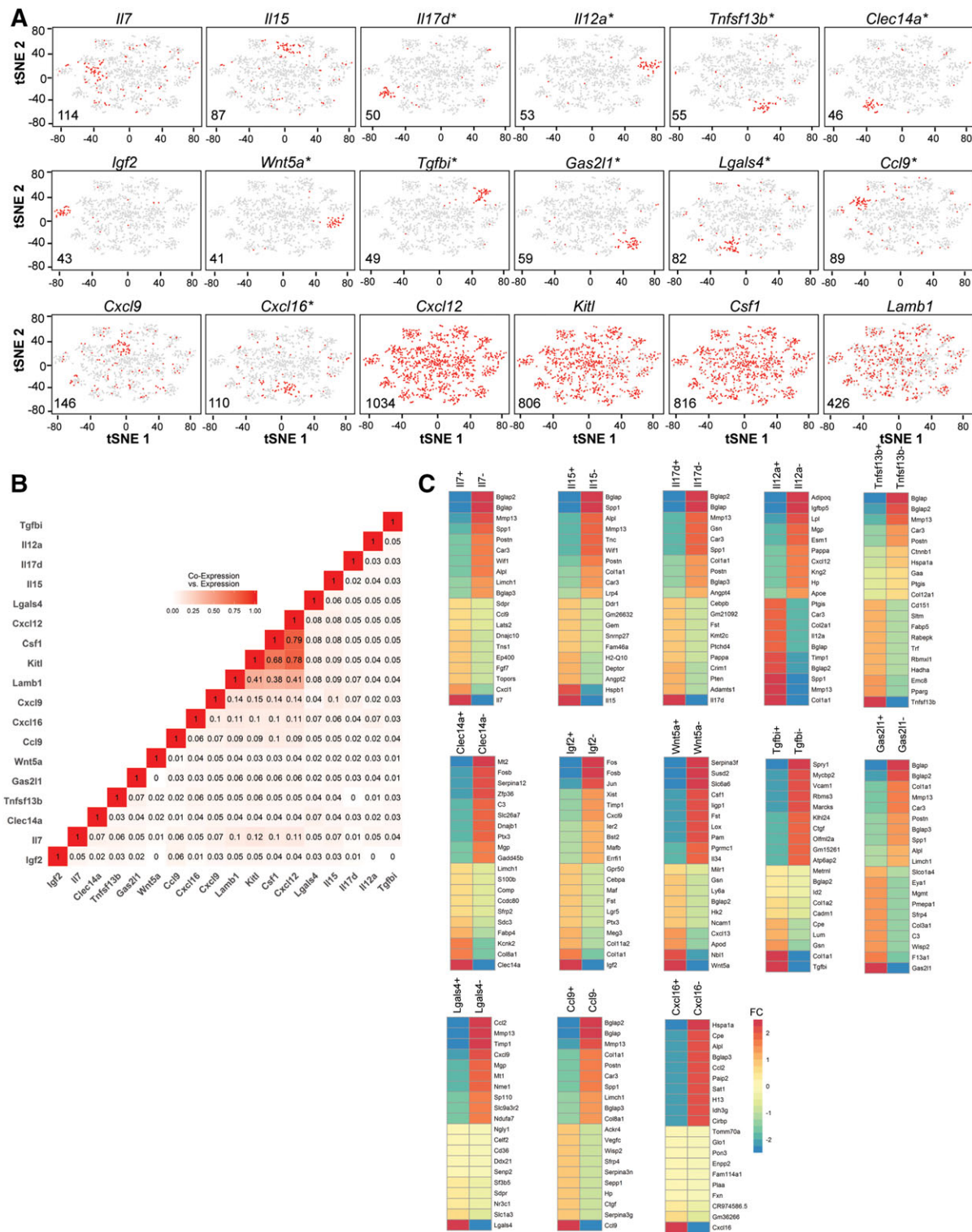


**Figure 3.** Cytokine and chemokine expression is restricted to distinct subsets of stromal cells. The experimental procedure is the same as described in the legend of Fig. 1. (A) t-SNE plots of supervised clustering of cells using 108 genes encoding secreted factors with known role in communication of stromal cells with cells of the hematopoietic system. Cells expressing a particular gene are highlighted in red (\* Defines stable clusters as defined by Consensus Clustering based on random t-SNEs and/or Consensus Clustering as proposed by Kiselev and colleagues [21]). (B) Co-expression of selected communication genes as defined by Jaccard similarity coefficient (Proportion of cells expressing two or at least one marker). (C) Comparisons of gene expression profiles expressing selected marker genes forming stable clusters. Fold change (FC) shows the log<sub>2</sub> (Average Expression of positive cells) - log<sub>2</sub> (Average Expression of negative cells), displayed are the top 10 genes with the highest fold change. DiffExpTest-method was used for the statistical analysis of differential expressed genes. The t-SNE analysis shown in Fig. 3 is based on *n* = 1035 individual stromal cells.

## Concluding remarks

BM has been identified as the residency of immune memory cells providing long-term protection against systemic pathogens. BM stromal cells have been postulated to organize the survival niches for these memory cells [1–5]. Analyzing the individual transcriptomes of more than 1000 murine BM stromal cells, we find a tremendous heterogeneity, with essentially no two cells expressing the same transcriptome. Nearly all stromal cells express CXCL12, a critical signal to attract immune memory cells or their precursors. Distinct subsets of stromal cells express IL-7 or IL-15, cytokines which have been invoked in the maintenance of CD4 and CD8 memory lymphocytes [28, 29]. More than 5% of the stromal cells express *Tnfrsf13b*, the gene encoding for the protein BAFF (B-cell activating factor), a cytokine critical for the maintenance of memory plasma cells [30]. Thus, BM stromal cells are potentially autonomous in providing niches for the long-term maintenance of immune memory cells. With regards to the maintenance of hematopoietic stem cells and early progenitors; *Cxcl12* is expressed by all stromal cells while *Kitl* and *Csf1* are expressed by about 80% of cells (Fig. 3A). *Flt3l* and *Il7* are expressed by small fraction of BM stromal cells. In perspective, this data set provides a considerably fundus towards an understanding of the interaction of stromal cells and hematopoietic cells on the single cell level.

## Materials and methods

### Mice

IL-7-GFP knock-in mice were kindly provided by Koichi Ikuta (Kyoto University, Japan). C57BL/6J and mice expressing GFP under control of the ubiquitin promoter (Ubq:GFP) were obtained from Jackson Laboratories (Germany) and housed under specific pathogen-free conditions at the DRFZ, Berlin. All experiments were approved by the federal state institution “Landesamt für Gesundheit und Soziales” (T0192/10), Berlin, Germany.

### Single cell suspension of BM

BM flush-out and the empty bones (tibia and femur) were digested with 0.5 mg/ml collagenase IV (Sigma-Aldrich), 1 mg/ml DNase I (Sigma-Aldrich), 0.25 mg/mL Dispase II (Roche), with or without 5 µg/mL Latrunculin B (Sigma-Aldrich), for 30 min at 37°C.

### Flow cytometry

Flow cytometry and cell sorting were performed as described [31]. The following antibodies were used: anti-CD45(30F11), anti-VCAM-1(429), anti-CD31(390), anti-Ter119(Ter119), antibodies were purchased from Miltenyi Biotec, Biolegend, or produced in

DRFZ. Dead cells were excluded by DAPI. Flow cytometric data were acquired on MACSQuant (Miltenyi Biotec). BDInflux cell sorter (BD Bioscience) was used for cell sorting. Flow cytometric data were analyzed with FlowJo (Tree Star, Inc.).

### In-situ quantification of radiation resistant BM stromal cells

Chimeric mice were generated as previously described [1]. Briefly, mice that express GFP ubiquitously were irradiated and reconstituted with BM cells from C57BL/6J mice. Immunofluorescence staining of BM sections was performed according to established protocol [1] using the following antibodies: anti-VCAM-1(429) and anti-CD31(390). For the nuclear staining, sections were stained with 1 µg/mL DAPI in PBS. Images were acquired using a Zeiss LSM710 confocal microscope with a 20 × /0.8 numerical aperture objective and were analyzed with Zen 2009 Light Edition software (Carl Zeiss Micro Imaging).

### Single cell RNA-sequencing

For single cell library preparation, ex vivo FACS sorted VCAM-1+CD45-Ter119-CD31- BM cells were applied to the 10X Genomics platform using the Single Cell 3' Reagent Kit V2 (10x Genomics) following the manufacturer's instructions. Upon adapter ligation and index PCR, the quality of the obtained cDNA library was assessed by Qubit quantification, Bioanalyzer fragment analysis (HS DNA Kit, Agilent) and KAPA library quantification qPCR (Roche). The sequencing was performed on a NextSeq500 device (Illumina) using a High Output v2 Kit (150 cycles) with the recommended sequencing conditions (read1: 26nt, read2: 98nt, index1: 8 nt, index2: n.a.).

### Sc RNA-seq analysis

Illumina output was demultiplexed and mapped to the mm10 reference genome by cellranger-2.0.2 (10x Genomics Inc.) using refdata-cellranger-mm10-1.2.0 in default parameter setting and 3000 expected cells. Raw UMI-counts were further analyzed using R 3.5.2 with Seurat package [32], as proposed by Butler and colleagues [33], including log-normalization of UMI-counts, detection of variable genes and scaling. T-distributed Stochastic Neighbour Embedding and the underlying Principle Component Analysis was performed based on 30 components using variable genes and a perplexity of 30 as set by default. Potential lymphocyte and erythrocyte contamination cells expressing *Ptprc* (CD45) or hemoglobin subunits (Hba) respectively were detected and excluded. Data were reanalyzed after excluding the contaminants using the remaining 1035 stromal cells (Fig. 1 J-L and 2A). Scatterplots for co-expression of genes were based on normalized UMI-counts, with an artificial noise subtracted from 0 counts for visualization (Fig. 2B). Co-expression matrices were

based on the Jaccard similarity coefficient of cells expressing two or at least one gene (Fig. 2C and Fig. 3B). Heat maps (Fig. 3C) show the log-transformed fold change of mean expression of positive and negative cells, displayed are the top 10 genes with the highest fold change. DiffExpTest-method was used for the statistical analysis of differential expressed genes [34]. The single cell RNA sequencing data reported in this paper have been deposited in the Gene Expression Omnibus (GEO) database, <https://www.ncbi.nlm.nih.gov/geo> (accession no. GSE131365).

### Analysis of stromal communication genes

For the analysis of stromal communication genes, a set of 108 genes were derived from literature (Supporting Information 1A). Out of these, 37 were detected as variable and used for t-SNE (Fig. 3A). Cluster stability was analyzed using random t-SNEs as well as Consensus Clustering as described by Kiselev and colleagues [21]. 1000 random t-SNEs were generated based on 80% of cells, using random seeds for both t-SNE and cell sampling. Clusters within each t-SNE were determined by density-based clustering (DBSCAN) as implemented in the java Apache Commons Mathematics Library “common.math3-3.4.1”, using Euclidian-Distance, minimum number of 10 cells for a cluster and an average distance to the tenth neighbor as the Epsilon-neighborhood. The consensus was defined as the ratio of co-occurrence of two cells in the same cluster and same random t-SNEs. Hierarchical clustering of cells was performed based on complete linkage and Euclidian Distance. Main clusters were defined by cutting the tree at 95% of its height, leading to 24 Clusters with more than 10 cells (Supporting Information 3A). Cluster stability is visualized by Silhouette-Plot (Supporting Information 3B). Markers for clusters were determined by the area under the receiver operating curve (AUC) based on the expression of the respective gene. Markers were defined by a threshold of  $AUC \geq 0.95$  (Supporting Information Fig. 3C). All markers were statistically significant with  $p$ -values  $< 2 \cdot 10^{-8}$  as determined by the Mann–Whitney-U-Test. The Consensus Clustering was performed for 2 to 50 expected clusters in default settings but disabling gene-filtering [21]. The optimal number of clusters was defined by the highest mean average silhouette width discarding clustering 2, 3 and 4 after visual inspection of the consensus matrix (Supporting Information Fig. 4A–C). Markers for the Consensus-Clusters were defined by  $AUC \geq 0.95$ .

**Acknowledgements:** This work was supported by the state of Berlin and the “European Regional Development Fund” to F.H., M.B., G.A.H., C.L.T. and M.F.M (ERDF 2014–2020, EFRE 1.8/11, Deutsches Rheuma-Forschungszentrum), by the Deutsche Forschungsgemeinschaft through DFG priority program 1468 IMMUNOBONE and SFB TRR130 (to A.R. and H.D.C.) and by the European Research Council through the Advanced Grant

IMMEMO (ERC-2010-AdG.20100317 Grant 268978 to A.R.) and “Leibniz ScienceCampus Chronic Inflammation”. A.E.H. was funded by the DFG (TRR130, HA5354/6-2 and HA5354/8-1). D.S. and M.L. are members of Pitzer Laboratory of Osteoarthritis Research funded by Willy Robert Pitzer foundation. R.K.A. and D.S. are members of Berlin-Brandenburg School for Regenerative Therapies. G.A.H. was supported by GSC 203 Berlin-Brandenburg School for Regenerative Therapies. We would like to thank Fritz Melchers for wonderful discussions and Koichi Ikuta (Kyoto University, Japan) for kindly providing the IL-7-GFP knock-in mice. We thank Tula Geske, Heidi Hecker-Kia and Heidi Schliemann for expert technical help, Toralf Kaiser and Jenny Kirsch for support in cell sorting, and Manuela Ohde and Patrick Thiemann for animal care.

**Conflict of interest:** The authors declare no financial or commercial conflict of interest.

### References

- Sercan Alp, O., Durlanik, S., Schulz, D., McGrath, M., Grun, J. R., Bardua, M., Ikuta, K. et al., Memory CD8(+) T cells colocalize with IL-7(+) stromal cells in bone marrow and rest in terms of proliferation and transcription. *Eur. J. Immunol.* 2015. 45: 975–987.
- Tokoyoda, K., Zehentmeier, S., Hegazy, A. N., Albrecht, I., Grun, J. R., Lohning, M. and Radbruch, A., Professional memory CD4+ T lymphocytes preferentially reside and rest in the bone marrow. *Immunity* 2009. 30: 721–730.
- Zehentmeier, S., Roth, K., Cseresnyes, Z., Sercan, O., Horn, K., Niesner, R. A., Chang, H. D. et al., Static and dynamic components synergize to form a stable survival niche for bone marrow plasma cells. *Eur. J. Immunol.* 2014. 44: 2306–2317.
- Hanazawa, A., Hayashizaki, K., Shinoda, K., Yagita, H., Okumura, K., Lohning, M., Hara, T. et al., CD49b-dependent establishment of T helper cell memory. *Immunol. Cell Biol.* 2013. 91: 524–531.
- Hanazawa, A., Lohning, M., Radbruch, A. and Tokoyoda, K., CD49b/CD69-dependent generation of resting T helper cell memory. *Front. Immunol.* 2013. 4: 183.
- Tokoyoda, K., Zehentmeier, S., Chang, H. D. and Radbruch, A., Organization and maintenance of immunological memory by stroma niches. *Eur. J. Immunol.* 2009. 39: 2095–2099.
- Tokoyoda, K., Hauser, A. E., Nakayama, T. and Radbruch, A., Organization of immunological memory by bone marrow stroma. *Nat. Rev. Immunol.* 2010. 10: 193–200.
- Nilsson, S. K., Debatis, M. E., Dooner, M. S., Madri, J. A., Quesenberry, P. J. and Becker, P. S., Immunofluorescence characterization of key extracellular matrix proteins in murine bone marrow in situ. *J. Histochem. Cytochem.* 1998. 46: 371–377.
- Yu, V. W. and Scadden, D. T., Hematopoietic stem cell and its bone marrow niche. *Curr. Top. Dev. Biol.* 2016. 118: 21–44.
- Yu, V. W. and Scadden, D. T., Heterogeneity of the bone marrow niche. *Curr. Opin. Hematol.* 2016. 23: 331–338.
- Houlihan, D. D., Mabuchi, Y., Morikawa, S., Niibe, K., Araki, D., Suzuki, S., Okano, H. et al., Isolation of mouse mesenchymal stem cells on the basis of expression of Sca-1 and PDGFR-alpha. *Nat. Protoc.* 2012. 7: 2103–2111.



- 12 Wakatsuki, T., Schwab, B., Thompson, N. C. and Elson, E. L., Effects of cytochalasin D and latrunculin B on mechanical properties of cells. *J. Cell Sci.* 2001. **114**: 1025–1036.
- 13 Laurens van der Maaten and Hinton, G., Visualizing Data using t-SNE. *J. Machine Learning Res.* 2008. **9**: 2579–2605.
- 14 Morrison, S. J. and Scadden, D. T., The bone marrow niche for haematopoietic stem cells. *Nature* 2014. **505**: 327–334.
- 15 Mendez-Ferrer, S., Michurina, T. V., Ferraro, F., Mazloom, A. R., MacArthur, B. D., Lira, S. A., Scadden, D. T. et al., Mesenchymal and haematopoietic stem cells form a unique bone marrow niche. *Nature* 2010. **466**: 829–834.
- 16 Gerdes, J., Lemke, H., Baisch, H., Wacker, H. H., Schwab, U. and Stein, H., Cell cycle analysis of a cell proliferation-associated human nuclear antigen defined by the monoclonal antibody Ki-67. *J. Immunol.* 1984. **133**: 1710–1715.
- 17 Stueland, C. S., Gorden, K. and LaPorte, D. C., The isocitrate dehydrogenase phosphorylation cycle. Identification of the primary rate-limiting step. *J. Biol. Chem.* 1988. **263**: 19475–19479.
- 18 Rapoport, T. A., Heinrich, R., Jacobasch, G. and Rapoport, S., A linear steady-state treatment of enzymatic chains. A mathematical model of glycolysis of human erythrocytes. *Eur. J. Biochem.* 1974. **42**: 107–120.
- 19 Jogl, G., Hsiao, Y. S. and Tong, L., Structure and function of carnitine acyltransferases. *Ann. N. Y. Acad. Sci.* 2004. **1033**: 17–29.
- 20 Cotter, D. G., Schugar, R. C. and Crawford, P. A., Ketone body metabolism and cardiovascular disease. *Am. J. Physiol. Heart Circ. Physiol.* 2013. **304**: H1060–1076.
- 21 Kiselev, V. Y., Kirschner, K., Schaub, M. T., Andrews, T., Yiu, A., Chandra, T., Natarajan, K. N. et al., SC3: consensus clustering of single-cell RNA-seq data. *Nat. Methods* 2017. **14**: 483–486.
- 22 Starnes, T., Broxmeyer, H. E., Robertson, M. J. and Hromas, R., Cutting edge: IL-17D, a novel member of the IL-17 family, stimulates cytokine production and inhibits hemopoiesis. *J. Immunol.* 2002. **169**: 642–646.
- 23 Geijtenbeek, T. B. and Gringhuis, S. I., Signalling through C-type lectin receptors: shaping immune responses. *Nat. Rev. Immunol.* 2009. **9**: 465–479.
- 24 Wolf, S. F., Temple, P. A., Kobayashi, M., Young, D., Diczig, M., Lowe, L., Dzialo, R. et al., Cloning of cDNA for natural killer cell stimulatory factor, a heterodimeric cytokine with multiple biologic effects on T and natural killer cells. *J. Immunol.* 1991. **146**: 3074–3081.
- 25 van der Voort, R., van Lieshout, A. W., Toonen, L. W., Sloetjes, A. W., van den Berg, W. B., Figdor, C. G., Radstake, T. R. et al., Elevated CXCL16 expression by synovial macrophages recruits memory T cells into rheumatoid joints. *Arthritis. Rheum.* 2005. **52**: 1381–1391.
- 26 Zhao, X., Sato, A., Dela Cruz, C. S., Linehan, M., Luegering, A., Kucharzik, T., Shirakawa, A. K. et al., CCL9 is secreted by the follicle-associated epithelium and recruits dome region Peyer's patch CD11b+ dendritic cells. *J. Immunol.* 2003. **171**: 2797–2803.
- 27 Cheng, J. W., Sadeghi, Z., Levine, A. D., Penn, M. S., von Recum, H. A., Caplan, A. I. and Hijaz, A., The role of CXCL12 and CCL7 chemokines in immune regulation, embryonic development, and tissue regeneration. *Cytokine* 2014. **69**: 277–283.
- 28 Berard, M., Brandt, K., Bulfone-Paus, S. and Tough, D. F., IL-15 promotes the survival of naive and memory phenotype CD8+ T cells. *J. Immunol.* 2003. **170**: 5018–5026.
- 29 Chetoui, N., Boisvert, M., Gendron, S. and Aoudjit, F., Interleukin-7 promotes the survival of human CD4+ effector/memory T cells by up-regulating Bcl-2 proteins and activating the JAK/STAT signalling pathway. *Immunology* 2010. **130**: 418–426.
- 30 Benson, M. J., Dillon, S. R., Castigli, E., Geha, R. S., Xu, S., Lam, K. P. and Noelle, R. J., Cutting edge: the dependence of plasma cells and independence of memory B cells on BAFF and APRIL. *J. Immunol.* 2008. **180**: 3655–3659.
- 31 Cossarizza, A., Chang, H. D., Radbruch, A., Akdis, M., Andra, I., Annunziato, F., Bacher, P. et al., Guidelines for the use of flow cytometry and cell sorting in immunological studies. *Eur. J. Immunol.* 2017. **47**: 1584–1797.
- 32 Satija, R., Farrell, J. A., Gennert, D., Schier, A. F. and Regev, A., Spatial reconstruction of single-cell gene expression data. *Nat. Biotechnol.* 2015. **33**: 495–502.
- 33 Butler, A., Hoffman, P., Smibert, P., Papalexi, E. and Satija, R., Integrating single-cell transcriptomic data across different conditions, technologies, and species. *Nat. Biotechnol.* 2018. **36**: 411–420.
- 34 McDavid, A., Finak, G., Chattopadhyay, P. K., Dominguez, M., Lamoreaux, L., Ma, S. S., Roederer, M. et al., Data exploration, quality control and testing in single-cell qPCR-based gene expression experiments. *Bioinformatics* 2013. **29**: 461–467.

**Abbreviations:** BM: Bone marrow · CD: Cluster of differentiation

**Full correspondence:** Dr. Mir-Farzin Mashreghi, Deutsches Rheuma-Forschungszentrum Berlin, Charitéplatz 1, 10117 Berlin, Germany  
E-mail: mashregi@drfz.de

**Additional correspondence:** Dr. Pawel Durek  
E-mail: pawel.durek@drfz.de

The peer review history for this article is available at <https://publons.com/publon/10.1002/eji.201848053>

Received: 13/12/2018

Revised: 11/4/2019

Accepted: 29/5/2019

Accepted article online: 31/5/2019



# MicroRNA-31 Reduces the Motility of Proinflammatory T Helper 1 Lymphocytes

Markus Bardua<sup>1</sup>, Claudia Haftmann<sup>1</sup>, Pawel Durek<sup>1</sup>, Kerstin Westendorf<sup>1</sup>, Antje Buttgereit<sup>1</sup>, Cam Loan Tran<sup>1</sup>, Mairi McGrath<sup>1</sup>, Melanie Weber<sup>1</sup>, Katrin Lehmann<sup>1</sup>, Richard Kwasi Addo<sup>1</sup>, Gitta Anne Heinz<sup>1</sup>, Anna-Barbara Stittrich<sup>2</sup>, Patrick Maschmeyer<sup>1</sup>, Helena Radbruch<sup>3</sup>, Michael Lohoff<sup>4</sup>, Hyun-Dong Chang<sup>1</sup>, Andreas Radbruch<sup>1†</sup> and Mir-Farzin Mashreghi<sup>1\*†</sup>

<sup>1</sup> Deutsches Rheuma-Forschungszentrum (DRFZ), Berlin, Germany, <sup>2</sup> Institute for Medical Immunology, Charité-Universitätsmedizin, Berlin, Germany, <sup>3</sup> Department of Neuropathology, Charité-Universitätsmedizin, Berlin, Germany, <sup>4</sup> Institute for Medical Microbiology and Hospital Hygiene, University of Marburg, Marburg, Germany

## OPEN ACCESS

### Edited by:

Remy Bosselut,  
National Cancer Institute (NCI),  
United States

### Reviewed by:

Leonid A. Pobeziński,  
University of Massachusetts Amherst,  
United States  
Koji Yasutomo,  
Tokushima University, Japan

### \*Correspondence:

Mir-Farzin Mashreghi  
mashreghi@drfz.de

<sup>†</sup>These authors have contributed  
equally to this work

### Specialty section:

This article was submitted to  
T Cell Biology,  
a section of the journal  
Frontiers in Immunology

**Received:** 16 August 2018

**Accepted:** 14 November 2018

**Published:** 06 December 2018

### Citation:

Bardua M, Haftmann C, Durek P,  
Westendorf K, Buttgereit A, Tran CL,  
McGrath M, Weber M, Lehmann K,  
Addo RK, Heinz GA, Stittrich A-B,  
Maschmeyer P, Radbruch H,  
Lohoff M, Chang H-D, Radbruch A  
and Mashreghi M-F (2018)  
MicroRNA-31 Reduces the Motility of  
Proinflammatory T Helper 1  
Lymphocytes.  
Front. Immunol. 9:2813.  
doi: 10.3389/fimmu.2018.02813

Proinflammatory type 1 T helper (Th1) cells are enriched in inflamed tissues and contribute to the maintenance of chronic inflammation in rheumatic diseases. Here we show that the microRNA- (miR-) 31 is upregulated in murine Th1 cells with a history of repeated reactivation and in memory Th cells isolated from the synovial fluid of patients with rheumatic joint disease. Knock-down of miR-31 resulted in the upregulation of genes associated with cytoskeletal rearrangement and motility and induced the expression of target genes involved in T cell activation, chemokine receptor- and integrin-signaling. Accordingly, inhibition of miR-31 resulted in increased migratory activity of repeatedly activated Th1 cells. The transcription factors T-bet and FOXO1 act as positive and negative regulators of T cell receptor (TCR)-mediated miR-31 expression, respectively. Taken together, our data show that a gene regulatory network involving miR-31, T-bet, and FOXO1 controls the migratory behavior of proinflammatory Th1 cells.

**Keywords:** CD4, miR-31, miRNA, target identification, T cell migration, Th1 cells, regulatory networks, antagomirs

## INTRODUCTION

Chronic synovial inflammation in rheumatoid arthritis (RA) is dependent on the migration and retention of T cells (1). Proinflammatory type 1 Th (Th1) cells are particularly enriched in the inflamed joints of patients with RA (2, 3). These cells express the transcription factor TWIST1, a hallmark of Th1 cells which have undergone repeated rounds of reactivation (4). TWIST1 limits inflammation (4) and, at the same time, promotes the survival of Th1 cells in inflamed tissues by up-regulating the microRNA (miR)-148a which targets the pro-apoptotic protein Bim (5, 6). This is in accordance with the observation that T cells isolated from inflamed joints are resistant to apoptosis (7) and persist in inflamed tissues despite state-of-the-art immunosuppressive therapies (4).

While trafficking of proinflammatory Th1 cells to sites of inflammation is well-characterized [reviewed in Mellado et al. (1)], the molecular mechanisms mediating their retention within inflamed tissues remain unclear. For CD4<sup>+</sup> T cells, this retention has been associated with chemokine receptor-, integrin-, and T cell receptor (TCR)-signaling that affect cell adhesion and motility (8–10). Generally, cell motility depends on the rearrangement of the actin

cytoskeleton. In T cells, this is mediated by a crosstalk of several signal transduction cascades including the phosphoinositide 3-kinase- (PI3K) signaling pathway activated via TCR and G-protein-coupled receptors (GPCRs), integrin signaling and the Ras homolog gene family- (Rho-) GTPases (11). It has been shown, that microRNAs interfering with these pathways are able to modulate the motility of lymphocytes (12–14). Thus, microRNAs might contribute to the persistence of proinflammatory Th1 cells in the inflamed tissues, by moderately and coordinately suppressing several genes involved in these signal transduction pathways (15).

Here we have identified the microRNA-31 (miR-31) as a regulator of migration in Th1 cells *in vitro*. MiR-31 is selectively and highly expressed in repeatedly activated murine Th1 cells and effector memory Th cells isolated from the synovial fluid of patients suffering from RA. MiR-31 targets a set of genes interfering with PI3K-, Rho-GTPase-, and integrin-signaling. Repeatedly activated Th1 cells expressing high levels of miR-31 showed significantly reduced migration toward CXCL10 compared to Th1 cells activated only once and expressing low amounts of miR-31. Migration of repeatedly activated Th1 cells could be restored by miR-31 inhibition using antagomirs. Expression of miR-31 was dependent on TCR activation, interferon (IFN-)  $\gamma$  and the Th1 master transcription factor T-bet. In contrast, the transcription factor Forkhead box protein O1 (FOXO1) inhibited miR-31 expression directly or by repressing T-bet and IFN- $\gamma$ .

Thus, miR-31 controls the motility of proinflammatory Th1 cells *in vitro*. The same mechanism might also contribute to the retention of inflamed tissue resident Th cells expressing high levels of miR-31, as observed in RA.

## MATERIALS AND METHODS

### Mice

C57BL/6, BALB/c, OTII, and *Tbx21*<sup>-/-</sup> mice were purchased from Charles Rivers and/or bred and kept under specific pathogen-free conditions at the internal animal facility of the DRFZ. Mice were treated conformable to law and euthanized by cervical dislocation. All experiments were approved by the federal state institution “Landesamt für Gesundheit und Soziales” (T0192/10) in Berlin, Germany.

### Cell Culture

CD4<sup>+</sup>CD62L<sup>hi</sup> (naïve) or CD4<sup>+</sup> lymphocytes from spleens and lymph nodes of 6- to 10-weeks old mice were isolated and purified as described (16). In brief, CD4<sup>+</sup> cells were labeled with  $\alpha$ CD4-FITC (GK1.5, DRFZ) followed by Magnetic Cell Sorting (MACS) with  $\alpha$ FITC microbeads (Miltenyi Biotec). Subsequent purification of CD4<sup>+</sup>CD62L<sup>hi</sup> cells was achieved using  $\alpha$ CD62L microbeads (Miltenyi Biotec). Unless stated otherwise, cells were cultured in “RPMI complete medium” (supplemented with 10% fetal calf serum (FCS), 100 units/ml penicillin, 0.1 mg/ml streptomycin and 10  $\mu$ M  $\beta$ -mercaptoethanol). To generate Th1, Th2, and Th17 lineage, CD4<sup>+</sup>CD62L<sup>hi</sup> cells from OTII mice were cultured (1:5) with irradiated (30 Gy), CD90.2 depleted splenocytes (as antigen presenting cells; APCs) in the presence of

OVA<sub>323–339</sub> (0.5 mM) in one of the following polarization media: RPMI complete medium supplemented with IL-12 (5 ng/ml, R&D Systems) and  $\alpha$ IL-4 (10  $\mu$ g/ml, 11B11) for Th1, IL-4 (100 ng/ml, culture supernatant of HEK293 cells transfected with murine IL-4 cDNA),  $\alpha$ IFN- $\gamma$  (10  $\mu$ g/ml, XMG 1.2), and  $\alpha$ IL-12 (10  $\mu$ g/ml C17.8) for Th2 and TGF- $\beta$ 1 (1 ng/ml, R&D Systems), IL-6, IL-23 (20 ng/ml, R&D Systems),  $\alpha$ IL-4, and  $\alpha$ IFN- $\gamma$  for Th17 differentiation (5). For the generation of repeatedly activated Th (rep) cells, viable cells were separated by density gradient centrifugation using Histopaque 1083 (Sigma Aldrich) and reactivated in corresponding polarization medium with freshly isolated APCs every 6 days for three times consecutively (5). For Th1 culture, IL-2 (10 ng/ml, R&D Systems) was added from the second stimulation on. Cells from C57BL/6, BALB/c and *Tbx21* were cultured ( $1 \times 10^6$  cells/ml) in Th1 polarization medium with IL-2 and activated with plate-bound  $\alpha$ CD3 and  $\alpha$ CD28 (3  $\mu$ g/ml, BD). Unless stated otherwise, cells were removed from the stimulus 48 h post activation and transferred into new cell culture plates. TGF- $\beta$ 1 (5 ng/ml,) or IFN- $\gamma$  (10 ng/ml, R&D Systems) was added where needed.

### Patient Material

T helper cells were isolated from the synovial fluid of patients suffering from RA or peripheral blood of healthy donors (HC) as described (5, 17). In brief, cells from RA patients were depleted for CD15<sup>+</sup> cells using MACS. Afterwards, CD3<sup>+</sup>CD4<sup>+</sup>CD14<sup>-</sup>CD45RO<sup>+</sup> cells were labeled and purified by Fluorescence Activated Cell Sorting (FACS). All gating strategies were performed according to the guidelines for the use of flow cytometry and cell sorting (18). Cells from the blood of HC were separated by density gradient centrifugation using LSM 1077, and purified by FACS as described above. If needed, cells were restimulated with PMA/Ionomycin for 3 h and/or lysed in TRIzol (Invitrogen). All human studies were approved by the Charité ethical committee and the informed consent of all participating subjects was obtained.

### Retroviral Transfection and Transduction of T Cells

Viral supernatant was obtained by calcium phosphate cotransfection of HEK293 cells with plasmids for ectopic expression of a constitutive active form of FOXO1 (pMIT-FOXO1A3) or the empty control (pMIT) (19) together with the retroviral packaging plasmids pCGP and the envelope plasmid pECO. Medium was replaced after 4 h with DMEM complete medium supplemented with HEPES (20 mM). Viral supernatant was collected 24 h–72 h later and stored at  $-80^{\circ}\text{C}$ . For the transduction of CD4<sup>+</sup> T cells from C57BL/6 mice, Th1 polarization medium was removed 36–40 h post activation and the viral supernatant supplemented with polybrene (8  $\mu$ g/ml) was added followed by centrifugation for 1.5 h at  $32^{\circ}\text{C}$  and 1,800 rpm. After 1 h of incubation at  $37^{\circ}\text{C}$  and 5% CO<sub>2</sub>, viral supernatant was replaced with the former culture supernatant. Forty-eight hours post transduction, cells were labeled with  $\alpha$ Thy1.1-PE (OX-7, BioLegend) and enriched by MACS using  $\alpha$ PE microbeads (Miltenyi Biotec) according to the

manufacturer's recommendations. Enrichment efficiency was controlled by flow cytometry (**Supplementary Figure 5**).

## Inhibition of MiR-31 by Antagomir Treatment

Specific, highly modified, cholesterol-coupled antagomir oligonucleotides (custom synthesized by Dharmacon) (20) were purchased lyophilized and reconstituted as described (21). A miR-31 specific Antagomir-31 (5-mC(\*)mA(\*)mGmCmUmAmUmGmCmAmGmCmAmUmCmUmUmG(\*)mC(\*)mC(\*)mU(\*)-3-Chol) and an unspecific Antagomir-SCR control (5-mU(\*)mC(\*)mAmCmGmCmAmGmAmUmUmCmAmUmAmA(\*)mC(\*)mG(\*)mU(\*)-3-Chol) were used. Modifications: 2-O-methyl-ribonucleotides (mN), phosphorothioates in the backbone (\*) and a cholesterol molecule (Chol) at the 3' end.

Repeatedly activated Th1 (Th1 rep) cells were treated ( $5 \times 10^6$  cells/ml) in serum-free siRNA delivery medium (ACCELL, Dharmacon) containing Antagomir-31 or Antagomir-SCR (1  $\mu$ M) for 1.5 h at 37°C and 5% CO<sub>2</sub>. Cell suspension was diluted (1:5) with Th1 polarization medium and reactivated with plate-bound  $\alpha$ CD3 and  $\alpha$ CD28 (3  $\mu$ g/ml). Inhibition efficiency was assessed by qRT-PCR.

## Inhibition of FOXO1 and FOXO3 by siRNA Treatment

A pool of 8 ACCELL siRNAs specific for *Foxo1* and *Foxo3* (4 siRNAs each, Dharmacon) was used to decrease the expression of *Foxo1* and *Foxo3* mRNAs. Th1 rep cells (two rounds of restimulation) ( $1 \times 10^7$  cells/ml) were treated with a mixture of this particular 8 siRNAs (0.25  $\mu$ M each) or an unspecific siSCR control (2  $\mu$ M) in serum free siRNA delivery medium (ACCELL, Dharmacon). After 2 h of incubation at 37°C and 5% CO<sub>2</sub>, cell suspension was diluted (1:1) with RPMI medium (final concentrations: 2.5% FCS, 10  $\mu$ g/ml aIL-4, 5 ng/ml IL-12 and 10 ng/ml IL-2) and cells were activated with plate-bound  $\alpha$ CD3 and  $\alpha$ CD28 (3  $\mu$ g/ml).

## Adhesion Assay

A high binding 96-well plate (Corning) was coated with ICAM-1 (R&D Systems) or IgG1 FC (R&D Systems) (10  $\mu$ g/ml) for 2 h at 37°C. Non-specific binding was blocked with adhesion buffer (HBSS Ca<sup>2+</sup> Mg<sup>2+</sup> supplemented with 1% BSA) for 1 h at 37°C. Th1 rep cells were washed twice with PBS, resuspended in pre-warmed, equilibrated adhesion buffer ( $2 \times 10^6$  cells/ml) and starved for 1 h at 37°C and 5% CO<sub>2</sub>. PMA (10 ng/ml), Ionomycin (1  $\mu$ g/ml) and CXCL10 (100 ng/ml, Immunotools) were added 10 min before the cell suspension was transferred into the coated wells (50  $\mu$ l/well). Forty-five minutes after incubation and adhesion at 37°C and 5% CO<sub>2</sub>, the plate was washed 4 times with 250  $\mu$ l warm adhesion buffer using an ELX washer according to the manufacturers recommendations. Adherent cells were detached with ice cold PBS/BSA/EDTA and counted using a MACSQuant (Miltenyi Biotec).

## Transwell Migration Assay

T helper cells were starved in RPMI supplemented with 0.5% fatty acid free BSA (Sigma Aldrich) (migration medium,  $4-8 \times 10^6$  cells/ml) for 1 h at 37°C and 5% CO<sub>2</sub>. Fifty microliters of the cell suspension, containing  $2-4 \times 10^5$  cells were transferred onto an ICAM-1 (10  $\mu$ g/ml) coated membrane (5  $\mu$ m pore size) in the upper well of a transwell plate (Corning). For transmigration toward the lower well containing 200  $\mu$ l migration medium supplemented with CXCL10 (100 nM), cells were incubated for 2 h at 37°C and 5% CO<sub>2</sub>. The number of transmigrated cells was assessed by a MACSQuant.

## RNA Isolation and qRT-PCR

Unless stated otherwise, all kits were used according to the manufacturer's recommendations. Total RNA was isolated using ZR RNA MiniPrep™ kit (Zymo Research). Expression values of mature miR-31 (hsa-miR-31, ThermoFisher, assay ID 002279; mmu-miR-31, assay ID 000185) and U6 snRNAs (assay ID 001973) were assessed by qRT-PCR using TaqMan Assays following cDNA synthesis with MircoRNA Reverse Transcription kit. For analysis, expression values of miR-31 were normalized by the change-in-threshold method ( $2^{-\Delta CT}$ ) to values of obtained from snU6.

Expression values of mRNAs were assessed by SYBR Green based qRT-PCR (Roche) using the following primer pairs: hypoxanthine guanine phosphoribosyltransferase (HPRT) forward 5'-TCCTCCTCAGACCGCTTTT-3', HPRT reverse 5'-CATAACCTGGTTCATCATCGC-3', Tbx21 forward 5'-TCC TGCAGTCTCTCCACAAGT-3', Tbx21 reverse 5'-CAGCTG AGTGATCTCTGCGT-3', FOXO1 forward 5'-CGGGCTGGA AGAATTCAATTC-3', FOXO1 reverse, 5'-AGTTCCTTCATT CTGCACTCGAA-3'. Alternatively mRNA was quantified by qRT-PCR based TaqMan Assays (ThermoFisher) using the following assays: ABLIM1 Mm01254316\_m1, CD28 Mm01253994\_m1, CD69 Mm01183378\_m1, CDC42 Mm01194005\_g1, EIF4EBP2 Mm00515675\_m1, FOXO1 Mm00490671\_m1, FOXO3 Mm01185722\_m1, HPRT Mm03024075\_m1, INFG Mm01168134\_m1, KLF2 Mm01244979\_g1, LATS2 Mm00497217\_m1, LPP Mm00724478\_m1, PPP2R2A Mm01317426\_g1, PPP3CA Mm01317678\_m1, Pri-miR-31 Mm03306874, RAC1 Mm01201653\_mH, RHOA Mm00834507\_g1, SELL Mm00441291\_m1, STK40 Mm00512134\_m1, and YWHAE Mm00494242\_m1.

In both cases, reverse transcription was performed using the Reverse Transcription kit (Applied Biosystems). For analysis, expression values were normalized by the change-in-threshold method ( $2^{-\Delta CT}$ ) to values of obtained from *Hprt*.

## Intracellular Staining

Prior to intracellular transcription factor staining, dead cells were labeled with fixable viability dye aqua (ThermoFisher). Cells were fixed and stained at room temperature using the FoxP3/Transcription Factor Staining kit (eBioscience) according to the manufacturer's recommendations with fixing and staining times of 1 h each. The following antibodies were used: T-Bet-PE (4B10, BioLegend) and FoxP3-eF450 (FJK-16s, eBioscience).



## Next Generation Sequencing and Determination of mRNA/miR-31 Binding Sites

RNA of Th1 cells after four rounds of restimulation was isolated using the RNeasy Micro kit (Qiagen) and cDNA libraries from a maximum of 100 ng total RNA were prepared using the Tru-Seq Standard Total RNA Library kit (Illumina) according to the manufacturer's recommendations. Quality control was performed with a bioanalyzer using the RNA 600 Pico Kit and RNA with a RIN > 8 was used for library preparation. Paired-end sequencing ( $2 \times 75$  nt) was performed on a NextSeq500 Illumina device using the NextSeq500/550 Mid output kit v2 (150 cycles). Raw sequence reads were mapped to mouse GRCm38/mm10 genome using TopHat2 (22) in very-sensitive settings for Bowtie2 (23). The total RNA-sequencing data reported in this paper have been deposited in the Gene Expression Omnibus (GEO) database, <https://www.ncbi.nlm.nih.gov/geo> (accession no. GSE122218).

A set of 421 conserved putative miR-31 target genes (PTs) was determined using TargetScanMouse 7.1 (24) (413 genes) and augmented by genes found in literature (8 genes) (Supplementary Table 1). To further delimitate the putative targets in Th1 cells the maximal ratio between the coverage of miR-31 binding regions in the 3'-UTR and the median coverage in exons were computed (also see Figure 2A). If multiple miR-31 bs within the 3'-UTR of one gene were present, the bs with the highest ratio was included.

## Determination of the miR-31 TSS and Promoter Analysis

The putative transcription start site (TSS) was determined by visual inspection of the RNA-Seq coverage of the genomic region upstream of the mmu-miR-31 stem loop locus (mirBase: chr4:88910557-88910662) and compared to published RNA-Seq data from CD8<sup>+</sup> T cells (25) using IGV-Browser (26, 27). The respective promoter region was determined visually by the

analysis of p300 (28), H3K4me3, and H3K27me3 (29) ChIP-seq data of murine Th1 cells using the Cistrome database (30). Putative binding sites for the transcription factors T-Bet, STAT1, STAT4, and FOXO1 within the promoter region were predicted by ECR Browser (31) based on TRANSFAC professional library V10.2 (32) with a matrix similarity of 0.75. Predicted sites were validated by the respective ChIP-Seq data using Cistrome database (30) for p300 (28), H3K4me3 and H3K27me3 (29), STAT1 (28), STAT4 (33), T-bet (34), and FOXO1 (35).

## Microarray Analysis After miR-31 Antagonism

Microarray experiments were performed according to Niesner et al. (4). In brief, Th1 rep cells were treated with Antagomir-31 or Antagomir-SCR and RNA was extracted 36, 48, and 72h after antagomir treatment and the RNA quality were controlled as described above. Ten micrograms of the RNA were reverse transcribed and hybridized to Mouse 430\_2 (Affymetrix). Raw signals were processed by the affy R package using RMA for normalization to quantify gene expression and MAS5 to determine the present and absent genes (37). Genes present in at least 50% of the Antagomir-31 or Antagomir-SCR treated samples at different time points were defined to be expressed and these genes were used for the follow-up analysis. The Affymetrix microarray data reported in this paper have been deposited in the GEO database, <https://www.ncbi.nlm.nih.gov/geo> (accession no. GSE122223).

Subramanian et al. (38), Mootha et al. (39) with PT and PT<sub>50</sub> as gene sets were performed with parameters as shown in Supplementary Table 2d. The significance of higher enrichment of the PT<sub>50</sub> over the PT set was evaluated by the Welch's test of nominal enrichment scores (NES)s from 1,000 independent GSEA's each using a randomly chosen subset of PT with sizes equal to the size of the PT<sub>50</sub> set.

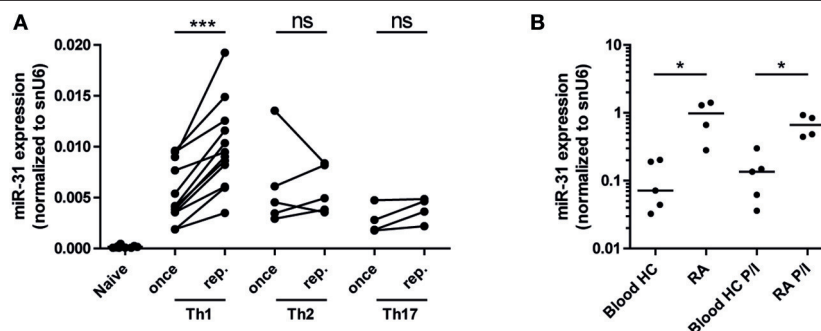


**FIGURE 1** | miR-31 is upregulated in murine Th1 rep cells, and in memory Th cells from the synovial fluid of RA patients. **(A)** miR-31 expression in once (day 6) and repeatedly (three rounds of restimulation with 6 day intervals) activated Th1, Th2, Th17, and *ex vivo* isolated naive CD4<sup>+</sup> cells normalized to snU6 determined by qRT-PCR. Each data point represents an independent experiment ( $n = 12$  [naive and Th1], 5 [Th2], 4 [Th17]) (Wilcoxon-Test for paired data, \*\*\*  $p \leq 0.001$ ). **(B)** miR-31 expression normalized to snU6 in CD3<sup>+</sup>CD4<sup>+</sup>CD14<sup>-</sup>CD45RO<sup>+</sup> T cells isolated from the synovial fluid of patients suffering from RA or blood from healthy control (HC) donors *ex vivo* or after 3 h of restimulation with PMA/ionomycin (P/I) ( $n = 5$  RA;  $n = 4$  HC) determined by qRT-PCR. Each data point represents an individual donor, horizontal bar: median (Mann-Whitney test for unpaired data, \*  $p \leq 0.05$ ).

For the evaluation of the biological function of miR-31 a GSEA was performed based on KEGG pathways with the same parameters as before. The interaction network was build based on STRING v10.5 using *mus musculus* as host organism. Only validated interactions were included using “low confidence” for experimentally and “high confidence” for database based interactions. The resulting network was arranged and modified manually for interpretation using the Cytoscape application (36). Genes were added to complete TCR- (*Cd3d*, *Cd3e*, *Cd3g*, *Lcp2*, *Zap70*, *Nck1*, and *Nck2*) and GPCR- (*Cxcr3*, *Gnai1*, *Gnai2*, and *Gnai3*) signaling. Genes without interactions were removed.

## Statistics

Unless stated otherwise, the Mann–Whitney test for unpaired data was used with  $*p \leq 0.05$ ,  $**p \leq 0.01$ , and  $***p \leq 0.001$ . Statistical analysis was performed with GraphPad Prism 5.02.

## RESULTS

### MiR-31 Is Upregulated in Repeatedly Activated Th1 Cells and in Synovial Fluid Th Cells From Patients With Rheumatoid Arthritis

As miR-31 has been shown to be expressed in CD4<sup>+</sup> (40) and CD8<sup>+</sup> T cells upon TCR stimulation (25), we aimed to investigate miR-31 expression after repeated antigenic TCR stimulation of murine Th1- cells and in memory Th cells isolated from the inflamed tissue of RA patients. With the rationale that Th cells involved in chronic inflammation have a history of repeated restimulation with persistent (auto-) antigens, we once (Th once) or repeatedly activated (Th rep) type 1 (Th1), type 2 (Th2), and type 17 (Th17) lymphocyte subsets (5) and analyzed the expression pattern of miR-31. MiR-31 was expressed in all investigated Th subsets, but was selectively upregulated (3.2-fold) in Th1 rep cells (Figure 1A). CD3<sup>+</sup>CD4<sup>+</sup>CD14<sup>-</sup>CD45RO<sup>+</sup> memory Th cells isolated from the synovial fluid of patients with RA expressed 8.4-fold (*ex vivo*) and 4.9-fold (after restimulation with PMA/ionomycin) higher levels of miR-31 when compared to their counterparts isolated from the peripheral blood (PB) of healthy subjects (HC) (Figure 1B). Thus, miR-31 was similarly upregulated in inflamed tissue derived Th cells of RA patients and in murine Th1 rep cells, suggesting a comparable function of miR-31 in these cell types.

### A Subset of Putative MiR-31 Target Genes Is Significantly Upregulated After MiR-31 Antagonism

Next, we aimed to identify putative miR-31 target genes in Th1 rep cells to investigate the regulatory impact of miR-31. We used TargetScanMouse7.1 (24) in combination with a literature screen to define a list of 421 putative targets (PTs) of miR-31, mainly based on phylogenetic conservation of miR-31 binding sites (bs) and on published targets (Supplementary Table 1). It has been described that activated and proliferating Th cells express mRNAs with shortened 3' untranslated regions (3'-UTRs) resulting in fewer microRNA target sites (41). To analyze

whether the defined PTs contain miR-31 bs within their 3'-UTR in the Th1 rep cells, we performed high throughput sequencing of total RNA (RNA-seq) from resting Th1 rep cells (Figure 2A) and determined the presence of the miR-31 bs in relation to the presence of the protein coding exons. A high ratio of miR-31 bs expression to the median exon expression of the respective transcript would indicate a high probability for miR-31 bs to be present. Of the 421 PTs, 282 were expressed in Th1 rep cells. One hundred thirty-four of them had a miR-31 bs to exon ratio > 0.9, 72 between 0.5 and 0.9, and 76 a ratio < 0.5. For 139 PTs no transcripts were detectable (Figure 2B). Hence, 206 PTs harbor at least one miR-31 bs in more than 50% of the expressed mRNA molecules (PT<sub>50</sub>) in Th1 rep cells (Figure 2B). To validate the predicted target genes of miR-31, we activated Th1 rep cells with anti-CD3- and anti-CD28-antibodies ( $\alpha$ CD3/28), concurrently inhibiting miR-31 with a specific antagomir (Antagomir-31) (21). The expression levels of the putative miR-31 targets were quantified by global transcriptome analysis 36, 48, and 72 h following T cell activation and antagomir treatment. MiR-31 expression was significantly reduced by 99% by Antagomir-31 treatment for a period of 72 h after reactivation when compared to Th1 rep cells treated with a control antagomir (Antagomir-SCR) (Figure 2C). No significant enrichment of PT or PT<sub>50</sub> was observed 36 and 48 h after miR-31 inhibition by gene set enrichment analysis (GSEA). However, after 72 h both PT and PT<sub>50</sub> gene sets were significantly enriched compared to Antagomir-SCR treated controls (NES 1.25;  $p \leq 0.017$  for PT and NES 1.34;  $p \leq 0.033$  for PT<sub>50</sub>) (Figure 2D), showing even higher enrichments for the PT<sub>50</sub> subset ( $p \leq 0.001$ ) (Figure 2E). Of note, 92 of 206 genes showed a positive correlation (rank metric score > 0) after miR-31 knock-down and thus were responsible for the higher enrichment score obtained for PT<sub>50</sub> (Supplementary Table 2a). By using our novel miRNA target identification approach, which includes the gene expression pattern of the putative targets and the presence of miRNA bs within the their 3'UTRs in a specific cell type, we could increase the identification rate of genes which were affected by miRNA inhibition. Thus, the identified genes are most likely direct target genes of the analyzed miRNA, here miR-31.

### MiR-31 Targets a Set of Motility Related Genes in Th1 Rep Cells

In order to elucidate the biological function of miR-31 in Th1 rep cells, we performed a GSEA after miR-31 antagonism based on the Kyoto Encyclopedia of Genes and Genomes (KEGG) pathways (42). Here, we focused on 72 h after antagomir treatment, since we observed an exclusive significant enrichment of putative miR-31 targets at this time (Figure 2D). We identified two gene sets as significantly enriched in Th1 rep cells treated with Antagomir-31 as compared to the Antagomir-SCR treated control: “Phosphatidylinositol 3-kinase signaling system” (40 genes,  $p = 0.01$ ; NES = 1.59) and “Regulation of actin cytoskeleton” (108 genes,  $p = 0.03$ ; NES = 1.36) (Figure 3A and Supplementary Tables 2b,c). Since PI3K signaling is part of the network that regulates the actin cytoskeleton (11), we focused on the gene set “Regulation of actin cytoskeleton”

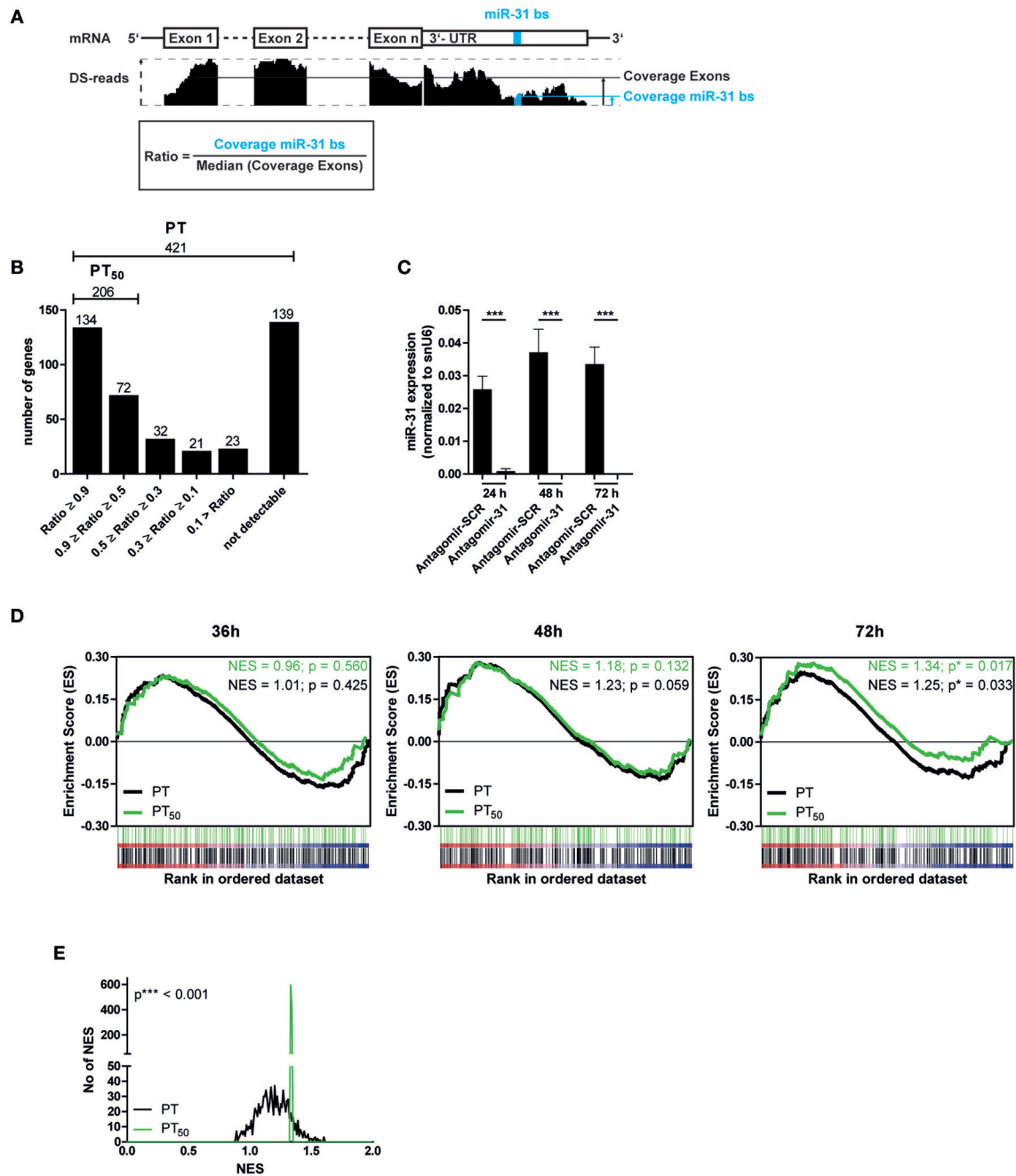


**FIGURE 2** | Significant upregulation of miR-31 targets after knock-down of miR-31. **(A)** Schematic overview of the method to determine the fraction of putative miR-31 target mRNA molecules that contain at least one miR-31 bs in their 3'-UTR. Depicted is the coverage (black bars, middle row) of  $n$  exons and the 3'-UTR (upper row) containing the miR-31 bs (indicated in blue). The ratio is calculated from the median coverage of the exons and the coverage of the miR-31 bs in the 3'-UTR (bottom row). **(B)** 421 putative miR-31 targets were grouped according to the ratio determined in **(A)**. **(C)** MiR-31 expression in Th1 rep cells 24, 48, and 72 h after activation with  $\alpha$ CD3/28 and treatment with Antagomir-31 or Antagomir-SCR normalized to snU6 determined by qRT-PCR. Data is shown as mean +SEM,  $n = 11$ , pooled from five independent experiments (Mann-Whitney test for unpaired data, \*\*\* $p \leq 0.001$ ). **(D)** GSEA with the PT- and PT<sub>50</sub>- gene-sets and the transcriptome data of Th1 rep cells 36, 48, and 72 h after activation with  $\alpha$ CD3/28 and treatment with Antagomir-31 or Antagomir-SCR. Data is shown as enrichment curves with each putative target gene (PT, black; PT<sub>50</sub>, green) in ranked order from most upregulated (left) to most downregulated (right). Nominal  $p$ -values are depicted in the figure. **(E)** Welch's test of nominal enrichment scores (NES) from 1,000 independent GSEA's each using a randomly chosen subset of PT with sizes equal to the size of the PT<sub>50</sub> set,  $p$ -value is depicted in the figure.

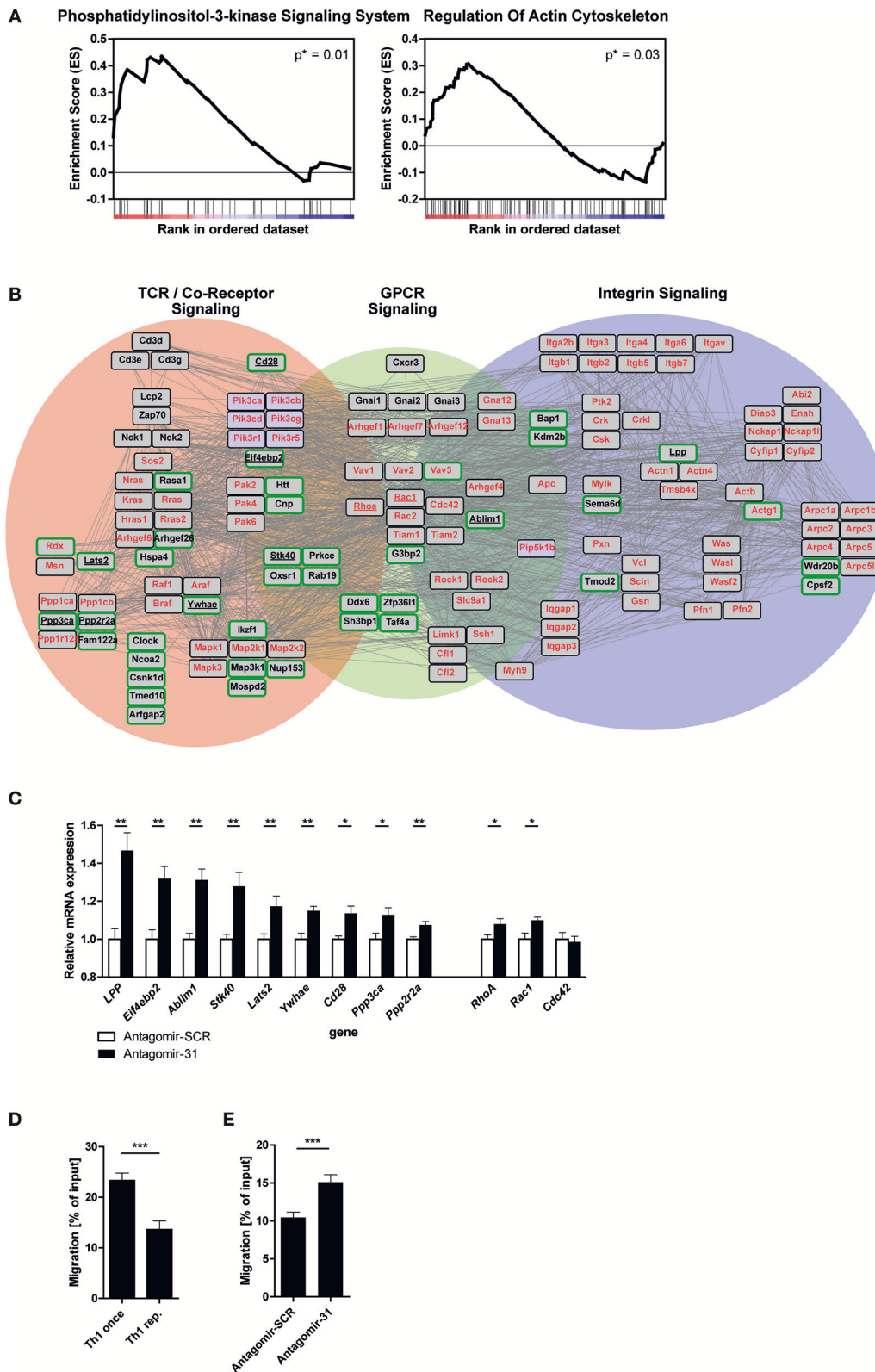


**FIGURE 3 |** miR-31 targets a set of genes involved in cytoskeletal rearrangement and miR-31 inhibition increases the motility of Th1 rep cells. **(A)** GSEA of the transcriptome data obtained from Th1 rep cells 72 h after activation with  $\alpha$ CD3/28 and treatment with Antagomir-31 or Antagomir-SCR with the KEGG-pathway database (v. 6.0) used as source for gene-sets. Data of two significantly enriched gene-sets is shown as enrichment curves with all genes in ranked order from most *(Continued)*



**FIGURE 3** | upregulated (left) to most downregulated (right). Nominal  $p$ -values are depicted in the figure. **(B)** Network of validated functional interactions among positively correlated miR-31 targets (green rimmed; **Figure 2D**) and the genes defining the gene set “regulation of actin cytoskeleton” (red). The resulting network was adapted to T cells (also see methods). Genes without interactions are not included. **(C)** QRT-PCR of target mRNA expression in reactivated Th1 rep cells 72 h after antagomir treatment relative to *Hprt* and normalized to Antagomir-SCR treated control. Data is shown as mean +SEM,  $n = 12$  (for *Lats2*, *RhoA*, *Stk40*, *Ywhae*) pooled from four independent experiments, or  $n = 6$  (for *Ablim1*, *Cd28*, *Cdc42*, *Eif4ebp2*, *LPP*, *Ppp2r2a*, *Ppp3ca*, *Rac1*) pooled from two independent experiments (Mann-Whitney test for unpaired data, \*\* $p \leq 0.01$ , \* $p \leq 0.05$ ). **(D,E)** Transwell migration assays with an ICAM-1 coated membrane (10  $\mu$ g/ml) and CXCL10 (100 ng/ml) in the lower compartment for once and repeatedly activated Th1 cells, 72 h after reactivation with  $\alpha$ CD3/28 **(D)** and Th1 rep cells, 72 h after antagomir treatment and reactivation with  $\alpha$ CD3/28 **(E)**, assessed by flow cytometry, normalized to inserted cell number. Data is shown as mean +SEM,  $n = 16$ –18 pooled from four independent experiments (Mann-Whitney test for unpaired data, \*\*\* $p \leq 0.001$ ).

in our follow-up analyses. We evaluated the connection of the 92 positively correlating, putative direct miR-31 targets with the 108 genes involved in the regulation of the actin cytoskeleton by creating a network of validated interactions using the Search Tool for the Retrieval of Interacting Genes/Proteins (STRING) (43) (**Figure 3B**). The resulting network shows the interactions between the PI3K-, Rho-GTPase- and integrin-signal transduction pathways and 41 of the 92 identified putative direct miR-31 targets. In Th1 cells the PI3K- pathway is addressed by TCR- and GPCR-signaling [here as an example CXC motif chemokine receptor (CXCR) 3], which is why we additionally integrated these factors into the network (for detailed description see methods). To validate some putative miR-31 targets from the identified network (**Figure 3B**) on mRNA level, we measured the expression of 9 candidates after miR-31 antagonism by qRT-PCR. All 9 putative target genes were significantly upregulated 72 h after Antagomir-31 treatment by 10 to 50% compared to Th1 rep cells treated with Antagomir-SCR (**Figure 3C**). The Rho-GTPases RHOA (Ras homolog gene family, member A), RAC1 (Ras-related C3 botulinum toxin substrate 1) and CDC42 (Cell division control protein 42 homolog) are key mediators of the cytoskeletal rearrangement and thus motility of T cells (11). Compared to Antagomir-SCR treated controls, Th1 rep cells treated with Antagomir-31, showed an upregulation of *RhoA* and *Rac1* by  $\sim 8$  and  $\sim 10\%$ , respectively. In contrast, *Cdc42* remained unchanged (**Figure 3C**). Thus, miR-31 indirectly regulates the expression of at least two of the central components for cytoskeletal rearrangement via its putative direct targets. Based on the network analysis we hypothesized that miR-31 might affect the adhesion and/or the motility of Th1 cells induced by the TCR-, chemokine receptor- and integrin-signaling.

### miR-31 Antagonism Increases the Motility of Repeatedly Activated Th1 Cells

To test the potential impact of miR-31 function on the rearrangement of the actin cytoskeleton, we assessed the adhesion of Th1 rep cells restimulated with PMA/ionomycin in the presence of CXC motif chemokine (CXCL) 10 and Intracellular Adhesion Molecule 1 (ICAM-1), i.e., the respective ligands for CXCR3 and Lymphocyte function-associated antigen 1 (LFA-1), both of which are expressed on Th1 rep cells (44, 45). We observed an increase of  $\sim 40\%$  in adherent Th1 rep cell number after inhibition of miR-31. Of note, this effect could only be observed in the presence of PMA/ionomycin, ICAM-1 and CXCL10 together (**Supplementary Figure 1**), which also mimics the milieu of inflamed tissues (46). To examine whether

miR-31 also regulates the motility of Th1 rep cells, we tested the migration of Th1 rep through an ICAM-1 coated membrane toward CXCL10 in an *in vitro* transwell migration assay, in which Th1 rep cells migrated  $\sim 50\%$  less than Th1 once cells (**Figure 3D**). This reduced migratory capacity of Th1 rep cells was partly rescued by Antagomir-31 treatment which significantly increased the migration of Th1 rep cells by  $\sim 30\%$  compared to Antagomir-SCR treatment (**Figure 3E**).

The PI3K-, Rho-GTPase- and integrin- signal transduction pathways which we identified to interact with target genes of miR-31 are also linked to T cell activation and thus T cell expansion and effector function. However, no differences in absolute cell numbers and the cytokine production of Th1 rep cells after antagomir treatment and reactivation with  $\alpha$ CD3/28 could be detected as compared to Antagomir-SCR treated cells (**Supplementary Figure 2**).

### miR-31 Is Induced by TCR Signaling in Th1 Cells

To investigate the induction of miR-31 during Th1 differentiation, we stimulated naive CD4<sup>+</sup> T cells with  $\alpha$ CD3/28 for 4 days in the presence of Th1 polarizing conditions, i.e., IL-12 and anti-IL-4 blocking antibodies. Compared to naive CD4<sup>+</sup> T cells, the expression of mature miR-31 was 5-fold upregulated 3 h post activation (p.a.) and further increased 15-fold at 24 h p.a (**Figure 4A**). Subsequently, miR-31 expression remained stable until day 3 and significantly decreased again by 30% until day 4 p.a. (**Figure 4A**). In contrast, resting Th1 rep cells already exhibited  $\sim 100$ -fold higher expression than naive Th cells, which did not increase until day 1 after  $\alpha$ CD3/28 activation (**Figure 4A**). Thereafter, Th1 rep cells maintained high levels of miR-31 throughout the remainder of the observation period until day 4 p.a. (**Figure 4A**). These results suggest that the induction of miR-31 during the initial phase of Th1 differentiation occurs via TCR signaling, whereas in Th1 rep cells additional mechanisms might be involved in the upregulation of miR-31.

### The Primary miR-31 Transcript in Th1 Cells Consists of 3 Exons and Its Genomic Locus Contains Th1 Specific Transcription Factor Binding Sites in the Putative Promoter Region

To understand the transcriptional regulation of miR-31 in Th1 cells, we first determined the transcriptional start site (TSS) for the primary miR-31 transcript using total RNA-seq data

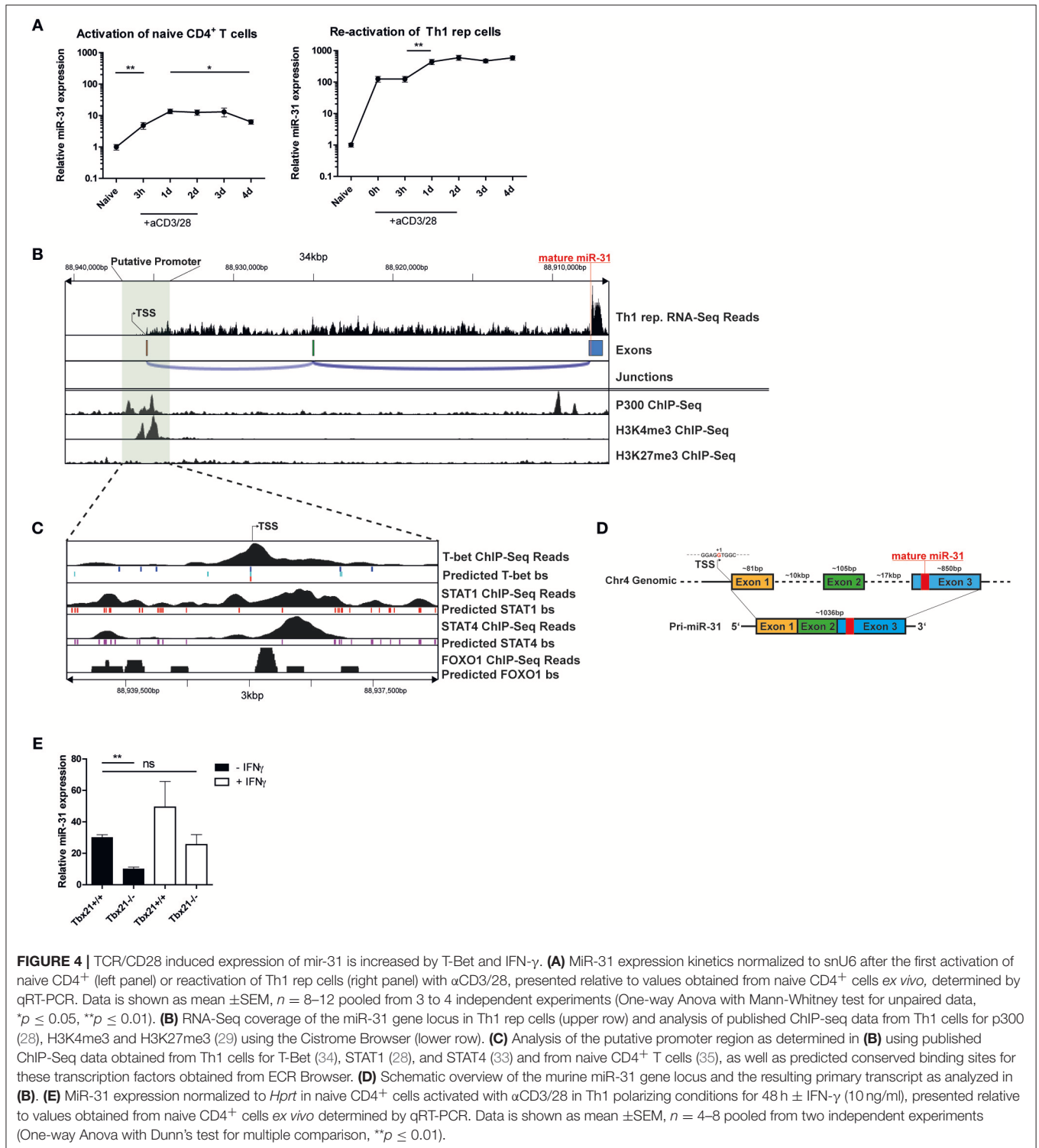


**FIGURE 4 |** TCR/CD28 induced expression of miR-31 is increased by T-Bet and IFN- $\gamma$ . **(A)** MiR-31 expression kinetics normalized to snU6 after the first activation of naive CD4<sup>+</sup> (left panel) or reactivation of Th1 rep cells (right panel) with  $\alpha$ CD3/28, presented relative to values obtained from naive CD4<sup>+</sup> cells *ex vivo*, determined by qRT-PCR. Data is shown as mean  $\pm$  SEM,  $n = 8-12$  pooled from 3 to 4 independent experiments (One-way Anova with Mann-Whitney test for unpaired data, \* $p \leq 0.05$ , \*\* $p \leq 0.01$ ). **(B)** RNA-Seq coverage of the miR-31 gene locus in Th1 rep cells (upper row) and analysis of published ChIP-seq data from Th1 cells for p300 (28), H3K4me3 and H3K27me3 (29) using the Cistrome Browser (lower row). **(C)** Analysis of the putative promoter region as determined in **(B)** using published ChIP-Seq data obtained from Th1 cells for T-Bet (34), STAT1 (28), and STAT4 (33) and from naive CD4<sup>+</sup> T cells (35), as well as predicted conserved binding sites for these transcription factors obtained from ECR Browser. **(D)** Schematic overview of the murine miR-31 gene locus and the resulting primary transcript as analyzed in **(B)**. **(E)** MiR-31 expression normalized to *Hprt* in naive CD4<sup>+</sup> cells activated with  $\alpha$ CD3/28 in Th1 polarizing conditions for 48 h  $\pm$  IFN- $\gamma$  (10 ng/ml), presented relative to values obtained from naive CD4<sup>+</sup> cells *ex vivo* determined by qRT-PCR. Data is shown as mean  $\pm$  SEM,  $n = 4-8$  pooled from two independent experiments (One-way Anova with Dunn's test for multiple comparison, \*\* $p \leq 0.01$ ).

from Th1 rep cells. The putative TSS of the murine primary miR-31 transcript is located approximately at chromosomal position mm10:chr4:88,938,478 and spans an intergenic region of  $\sim 28.6$  kb (Figures 4B,D), which confirms the TSS previously determined by homology analysis of mouse and man (25). The primary transcript expressed by Th1 rep cells consists of 3

exons and has a size of  $\sim 1,036$  bp (Figure 4D). By reanalyzing Th1 cell ChIP-seq (chromatin immunoprecipitation followed by sequencing) data of p300 (28) and H3K4me3 (29) occupancy using the Cistrome database (30), we observed enrichment of p300 and H3K4me3 binding in close proximity of the putative TSS (Figure 4B). Furthermore, we could identify a

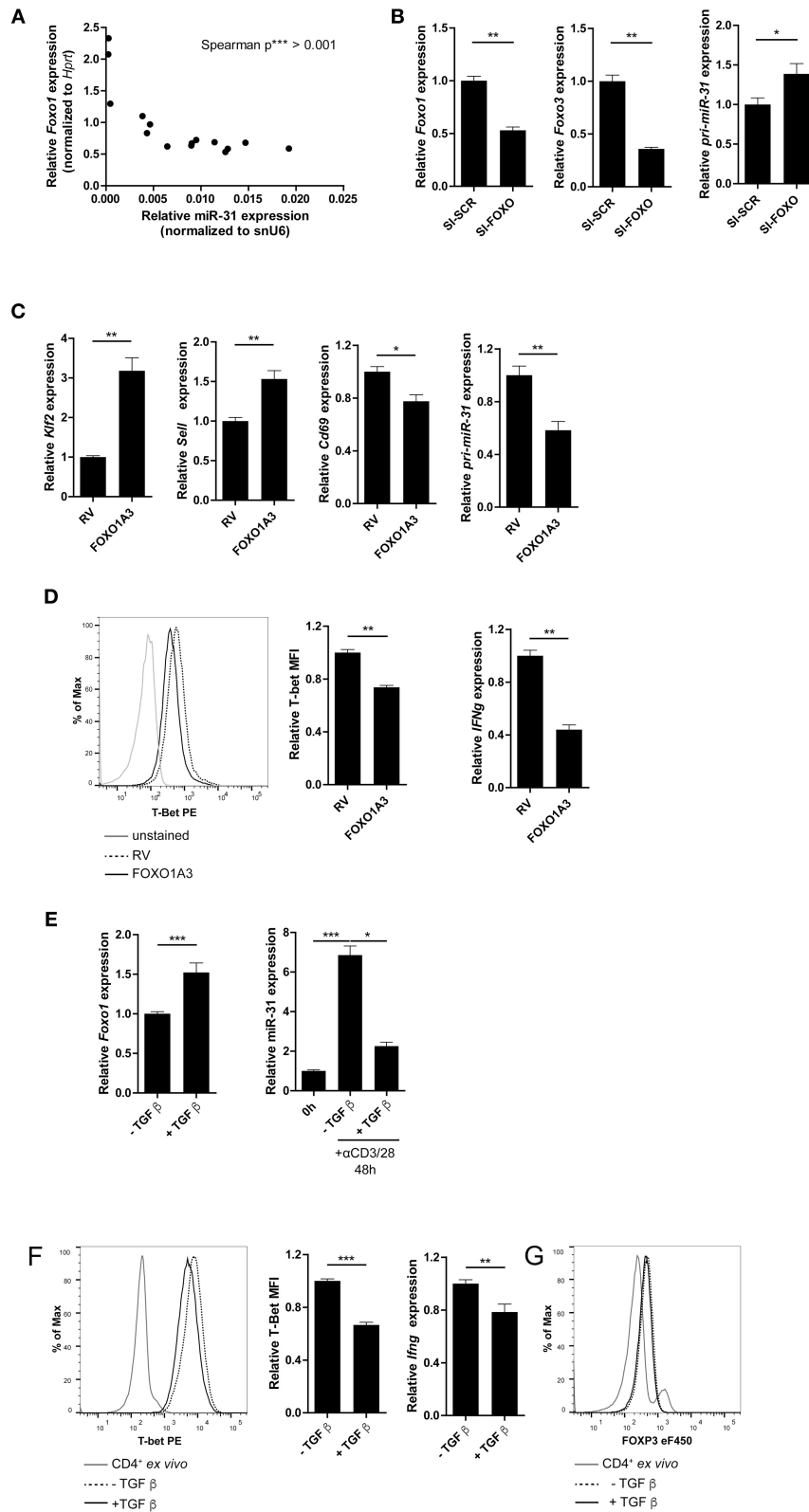


**FIGURE 5 | FOXO1 represses T-bet and miR-31 in Th1 cells. (A)** Correlation between miR-31 expression normalized to snU6 and *Foxo1* expression normalized to *Hprt* determined five times in 6 day intervals from naive to Th1 rep cells (qRT-PCR) ( $n = 15$  from one experiment,  $p$  value is depicted in the figure). **(B)** *Foxo1*, *Foxo3* and *pri-miR-31* expression normalized to *Hprt* in repeatedly (two rounds of stimulation) activated Th1 cells, treated with a pool of 8 siRNAs specific for

(Continued)

**FIGURE 5** | *Foxo1* and *Foxo3* or a SI-SCR control, analyzed 48 h after siRNA treatment by qRT-PCR, presented relative to the SI-SCR control. Data is shown as mean  $\pm$ SEM,  $n = 6$  pooled from two independent experiments (Mann-Whitney test for unpaired data,  $^*p \leq 0.05$ ,  $^{**}p \leq 0.01$ ) (C) *Klf2*, *Sell*, *Cd69* and *pri-miR-31* expression normalized to *Hprt* in activated  $CD4^+$  cells transduced 36–40 h post activation with a retroviral vector expressing a constitutive active FOXO1 (FOXO1A3) or an empty control vector (RV). Cells were cultured under Th1 polarizing conditions for additional 48 h. Expression was analyzed by qRT-PCR 48 h post transduction and is presented relative to RV. Data is shown as mean  $\pm$ SEM,  $n = 6$  pooled from two independent experiments (Mann-Whitney test for unpaired data,  $^{**}p \leq 0.01$ ) (D) Representative intracellular protein staining and T-Bet protein expression in the samples analyzed in (C), presented as MFI of T-Bet, normalized to RV assessed by flow cytometry. Data is shown as mean  $\pm$ SEM,  $n = 5$ –11 pooled from three independent experiments (Mann-Whitney test for unpaired data,  $^{**}p \leq 0.01$ ) (E) *Foxo1* expression normalized to *Hprt* in Th1 rep cells activated with  $\alpha$ CD3/28 under Th1 polarizing conditions for 48 h  $\pm$ TGF $\beta$ , presented relative to values obtained from untreated Th1 rep cells determined by qRT-PCR. Data is shown as mean  $\pm$ SEM,  $n = 9$  pooled from 3 independent experiments (Mann-Whitney test for unpaired data,  $^{**}p \leq 0.01$ ,  $^{***}p \leq 0.001$ ). MiR-31 expression normalized to snU6 in the same cells, presented relative to Th1 rep cells before reactivation assessed by qRT-PCR. Data is shown as mean  $\pm$ SEM,  $n = 9$  pooled from three independent experiments (One-way Anova with Dunn's test for multiple comparison,  $^*p \leq 0.05$ ,  $^{***}p \leq 0.001$ ) (F) Representative intracellular protein staining of Th1 rep cells activated with  $\alpha$ CD3/28 under Th1 polarizing conditions for 48 h  $\pm$ TGF $\beta$  and T-Bet protein expression, presented as MFI of T-Bet, normalized to untreated Th1 rep cells. Data is shown as mean  $\pm$ SEM,  $n = 2$ –3 pooled from four independent experiments (Mann-Whitney test for unpaired data,  $^{***}p \leq 0.001$ ). *Irfng* expression normalized to *Hprt* in the samples analyzed in (A), presented relative to RV. Data is shown as mean  $\pm$ SEM,  $n = 6$  pooled from two independent experiments (Mann-Whitney test for unpaired data,  $^*p \leq 0.05$ ,  $^{**}p \leq 0.01$ ) (G) Representative intracellular FOXP3 protein staining of Th1 rep cells activated with  $\alpha$ CD3/28 in Th1 polarizing conditions for 48 h  $\pm$ TGF- $\beta$ .

CpG island close to this site using UCSC Genome Browser (47) (Supplementary Figure 3). To identify transcription factors (TFs), which regulate the transcription of miR-31 in Th1 cells, we performed an *in silico* promoter analysis in a region  $\pm 1.5$  kb relative to the putative TSS (mm10:chr4:88937246-88940346) using the Evolutionary Conservation of Genomes (ECR) Browser (31). We identified a set of binding sites for TFs important for Th1 differentiation, including Signal Transducer And Activator Of Transcription (STAT) 1, STAT4, T-bet, and FOXO1 (Figure 4C). Reanalysis of additional ChIP-seq data sets showed STAT1 (28), STAT4 (33), and T-bet (34) in close vicinity to the putative TSS of the primary miR-31 transcript (Figure 4C). Since *Foxo1* expression decreased after repeated activation (Supplementary Figure 4), we also analyzed ChIP-Seq data from naive  $CD4^+$  cells (35) and detected FOXO1-dependent DNA enrichment in the putative miR-31 promoter region. Taken together, we suggest that the expression of miR-31 in Th1 rep cells might be upregulated by a positive feedback loop in a direct or indirect fashion by the activation and induction of STAT1, STAT4, and T-bet as well as the downregulation of FOXO TFs.

### TCR Mediated miR-31 Expression in Th1 Cells Is Increased by T-Bet and the Effector Cytokine IFN- $\gamma$

In order to validate that T-bet promotes the expression of miR-31, naive  $CD4^+$  T cells isolated from *Tbx21*<sup>-/-</sup> or wildtype (WT) mice were activated with  $\alpha$ CD3/28 for 48 h under Th1 polarizing conditions. The induction of miR-31 expression was diminished by  $\sim 50\%$  in activated *Tbx21* deficient Th cells compared to wild type cells (Figure 4E). MiR-31 induction after Th cell activation could be increased to WT levels by adding 10 ng/ml recombinant IFN- $\gamma$  (Figure 4E). In addition to the *in silico* ChIP-Seq analysis, these data suggest that STAT1, STAT4, and T-bet enforce the expression of miR-31 in differentiating Th1 cells.

### FOXO1 Represses T-Bet and miR-31 Expression in Th1 Cells

FOXO1 binds to the TSS of *pri-miR-31* in naive Th cells and most likely inhibits the expression of miR-31 in these cells. Therefore, we analyzed *Foxo1* expression in Th1 rep cells. *Foxo1* expression

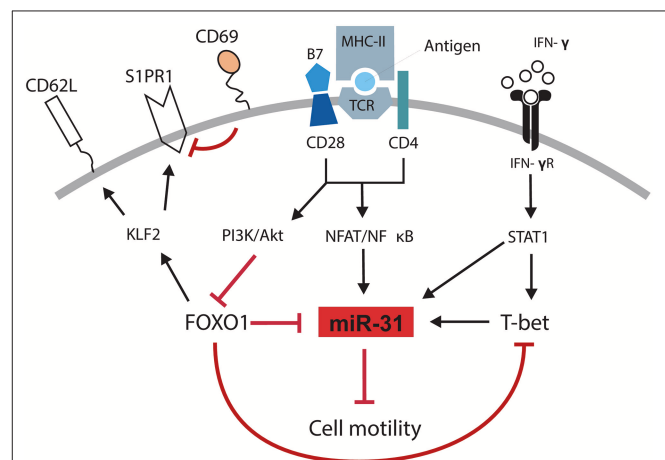


**FIGURE 6** | Schematic overview of mechanisms controlling the motility of Th1 rep cells. Antigenic stimulation of the TCR and CD28 leads to the activation of NFAT/NF $\kappa$ B and the PI3K/Akt pathway. IFN- $\gamma$  induces the activation and expression of STAT1 and T-Bet, respectively. NFAT/NF $\kappa$ B induces the expression of miR-31 which might be amplified by STAT1 and T-bet and reduces the cell motility. PI3K/Akt inactivates FOXO1 which supports the expression of miR-31 either in a direct fashion or by disabling the FOXO1 dependent inhibition of T-bet. Simultaneously, the inhibition of FOXO1 reduces the expression of KLF2, CD62L, and S1PR1 and induces the expression of CD69.

in these cells was reduced by  $\sim 20\%$  compared to Th1 once cells (Supplementary Figure 4). In addition, *Foxo1* expression negatively correlated with miR-31 expression upon repeated rounds of restimulation in Th1 cells (Figure 5A). To investigate whether FOXO transcription factors including FOXO1, and its functional redundant family member FOXO3, actively repress miR-31, we inhibited *Foxo1* and *Foxo3* mRNAs with a pool of 8 different siRNAs (SI-FOXO) in Th1 rep cells. *Foxo1* and *Foxo3* expression were reduced by  $\sim 50$  and  $\sim 65\%$ , respectively, when compared to control (SI-SCR) treated cells (Figure 5B). This reduction was associated with an increased expression of the primary miR-31 transcript (*pri-miR-31*) by  $\sim 40\%$  (Figure 5B, Supplementary Figure 6A shows data for mature miR-31).

The repressive function of FOXO1 on miR-31 expression in Th1 cells was further validated by the ectopic overexpression of a constitutively active form of FOXO1 (FOXO1A3) (19).



The FOXO1A3 transduced cells were magnetically enriched by the surface reporter marker Thy1.1 (**Supplementary Figure 5**) 48 h after transduction. Consistent with published results (48), the expression of the FOXO1 induced transcription factor *Klf2* (Krüppel-like Factor 2) and *Sell*, a gene which encodes for the protein CD62L (L-selectin), were upregulated by 3.2- and 1.5-fold, respectively. In contrast, *Cd69* was down regulated ~20% in cells ectopically overexpressing FOXO1A3 as compared to cells transduced with an empty retroviral vector (RV) (**Figure 5C**). As expected, the *pri-miR-31* was reduced by ~40% upon overexpression of FOXO1A3 (**Figure 5C**, **Supplementary Figure 6B** shows data for mature miR-31), which was associated with a reduced expression of *Ifng* mRNA by ~60% as well as T-bet protein by ~30% as determined by flow cytometry (**Figure 5D**).

It is known, that the Transforming growth factor (TGF)  $\beta$  stabilizes the expression of total FOXO1 protein (19). Therefore, we induced FOXO1 expression in Th1 rep cells by re-activating the cells in the presence of recombinant TGF $\beta$ . Forty-eight hours p.a., *Foxo1* mRNA expression increased by ~50% in the presence of TGF $\beta$  as compared to the untreated control, while miR-31 expression decreased by 70% (**Figure 5E**, **Supplementary Figure 6C** shows data for *pri-miR-31*). Furthermore, T-bet protein and *Ifng* mRNA were significantly reduced in TGF $\beta$  treated Th1 rep cells by ~30 and ~22%, respectively (**Figure 5F**). This TCR induced miR-31 expression can be blocked by *in vitro* addition of TGF $\beta$ , and is most likely due to the induction of FOXP3 (Forkhead-Box-Protein P3) that directly binds within the miR-31 promoter blocking its transcription (40). Notably, the treatment with TGF $\beta$  did not cause FOXP3 expression in fully differentiated Th1 rep cells, indicating different control mechanisms for miR-31 expression in different T-cell subsets (**Figure 5G**). Therefore, the inactivation of FOXO TFs seems to be necessary in order to provide high levels of miR-31 in Th1 rep cells.

## DISCUSSION

We and others have previously shown that T cells isolated from inflamed tissues of patients with chronic inflammatory diseases are enriched for a Th1 phenotype characterized by the expression of the transcription factor TWIST1 and the secretion of the Th1 signature cytokine IFN- $\gamma$  (2–4). Interestingly, these cells can be readily found in the inflamed tissues of patients undergoing state-of-the-art immunosuppressive therapies suggesting that they escape from conventional therapeutic interventions (4). This might be due to adaptation of the cells to the inflamed milieu, e.g., by the induction of the anti-apoptotic microRNA miR-148a (5). However, it has remained elusive how these cells are kept in the inflamed tissues, where they mediate and perpetuate chronic inflammation. Here we identified a molecular pathway which controls the motility of Th1 cells with a history of repeated restimulation (**Figure 6**). The periodic TCR-mediated activation of these cells resulted in an IFN- $\gamma$  and T-bet dependent upregulation of miR-31, which could be abrogated by FOXO1, a transcription factor expressed in resting Th1 cells. MiR-31 reduced the motility of proinflammatory Th1 cells by regulating the expression of genes which are involved in the rearrangement

of actin cytoskeleton downstream of TCR-, chemokine receptor- and integrin-signaling.

To decipher which biological functions are altered following the upregulation of miR-31 in Th1 rep cells we sought to identify its target mRNAs in this particular cell type. Usually, target identification is based on computational prediction of microRNA bs (24). This method delivers a vast number of potential targets including numerous false positive results (49) which have to be excluded experimentally (50). One reason for this could be that most prediction algorithms do not consider 3'-UTR length and, thus, physical presence of predicted miRNA bs. However, it is known that upon stimulation, Th cells in particular shorten their 3'-UTR in order to escape miRNA mediated control (41). By considering the presence of miRNA bs in the 3'UTR, we were able to account for this phenomenon and to increase the identification rate of genes which were affected by the inhibition of miR-31. Interestingly, we observed a significant induction of these genes only after 72 h of activation and Antagomir-31 treatment in restimulated Th1 rep cells. This might be due to the fact that restimulated T cells, in addition to shortening the 3'-UTR, also repress the function of the RNA induced silencing complex (RISC) by ubiquitination and degradation of Argonaute proteins (51) and so escape miRNA mediated control. Taken together, our novel approach for target identification takes kinetic aspects into account which appear to be of great importance for miRNA function in stimulated T cells. To experimentally prove that the identified putative targets are directly regulated by interaction of their 3'UTR with miR-31, reporter assays have to be performed. Indeed, some of the putative targets, e.g., *Stk40* and *Lats2*, were already verified elsewhere using a luciferase reporter assay (25).

Our analysis revealed a modest increase of putative direct or indirect miR-31 target gene expression ranging from 10 to 50% after miR-31 inhibition. These genes are functionally linked to signals downstream of the TCR, chemokine receptors and integrins, as we observed in our network analysis. It is widely accepted that the impact of a miRNA on a specific cellular function increases by targeting several factors that belong to the same biological pathway or protein complex (52, 53). For example, miR-181a targets multiple phosphatases downstream of the TCR and augments the sensitivity of T cells to cognate antigen stimulation (54). Accordingly, by reducing several components of the three pathways mentioned above, miR-31 repressed the motility of Th1 rep cells, most likely by affecting rearrangement of the actin cytoskeleton and cell adhesion. This repression could be attributed to the upregulation of miR-31, as knock-down of miR-31 rescued the motility of Th1 rep cells. Of note, we could not observe a difference in *Cxcr3* expression in these cells (data not shown), which excludes the possibility of disturbed chemokine sensing due to the expression of miR-31. Interestingly, Moffett et al. identified miR-31 as a mediator of CD8<sup>+</sup> T cell exhaustion by regulating some of the same genes that we also identified as being affected by miR-31 inhibition (25). We assume that these genes also have an impact on TCR-, chemokine receptor- and integrin-signaling in CD8<sup>+</sup> T cells and thus, miR-31 might also be able to suppress the motility of exhausted cytotoxic T cells. Our results in Th1 rep cells are further corroborated by Fuse et al. showing the KEGG-pathway

“rearrangement of actin cytoskeleton” to be enriched for miR-31 target genes and, that a reduced expression of miR-31 is associated with increased migration and invasion of prostate cancer cells (55). Furthermore, miR-31 could also be linked to the migratory behavior of glioma cells (56), ovarian- (57), breast- (58), and gastric cancer cells (59) and hepatocellular carcinoma cells (60). Since TCR mediated activation of the PI3K- and Rho-GTPase- signal transduction pathways also affects the expansion and effector functions of T cells (61), we investigated a possible impact of miR-31 on this. However, knockdown of miR-31 by 99% neither had an effect on the expansion of Th1 rep cells, nor on their cytokine production. This is in line with a study using CD4 specific conditional miR-31 knockout mice and demonstrating that miR-31 has no effect on the proliferation of T cells (40).

Why is miR-31 exclusively upregulated in Th1 rep cells resulting in their reduced motility? Interestingly, we observed a delayed induction of miR-31 in Th1 rep cells as compared to naive CD4<sup>+</sup> T cells activated under Th1 polarizing conditions. We speculate that the induction of miR-31 in Th1 rep cells is not only dependent on TCR signaling, but also on the master transcription factor T-bet, suggesting that the additional upregulation of miR-31 in Th1 rep cells is dependent on a network of transcription factors active only in Th1, and not in Th2 and Th17 cells. On account of this, we propose that the expression of miR-31 in Th1 rep cells might be sequentially orchestrated via a positive feed-back mechanism involving TCR signaling and the cytokines IFN- $\gamma$  and IL-12, which activate STAT1, STAT4 (62), and T-bet (5) either independently or synergistically. This is supported by the presence of functional binding sites for the Th1 specific transcription factors T-bet, STAT1, and STAT4 in the proximal promoter region of *pri-miR-31* in Th1 once cells and corroborated by our results obtained from studies with T-bet deficient T cells. With high probability a similar positive feed-back transcriptional mechanism might be active in Th1 rep cells, because these cells produce high amounts of IFN- $\gamma$  and upregulate T-bet (5). However, it remains to be shown, whether the three TFs, STAT1, STAT4, and T-bet, also bind to the proximal promoter of *pri-miR-31* and to what extent each individual TF contributes to the upregulation of miR-31.

Furthermore, we identified FOXO1 as a suppressor of miR-31 expression in Th1 cells. FOXO1 is highly expressed in resting naive Th cells (63), inhibits cell cycle progression (64, 65), represses T-bet in Th1 cells (66), and regulates T cell homing (67). Ectopic overexpression of a constitutively active form of FOXO1, or *in vitro* TGF $\beta$  treatment to induce *Foxo1* expression, led to miR-31 repression and reduced levels of T-bet and the effector cytokine *Ifng*. The repression of miR-31 can be either mediated directly by FOXO1 binding to the promoter of *pri-miR-31*, or indirectly by reducing T-bet and IFN- $\gamma$  expression. Moreover, we could show that enforced FOXO1A3 expression induced *Sell* (CD62L) and *Klf2* and reduced *Cd69* expression. Taken together, it is possible that the induction of KLF2, CD62L, and CCR7 (67) and a simultaneous repression of CD69 and miR-31 by FOXO1 might license T cells to recirculate to secondary lymphoid organs (48, 68) and to egress from the inflamed tissue (69).

In this study, we used *in vitro* generated Th1 cells, which were subjected to repeated rounds of activation as a model for Th cells derived from inflamed tissues of patients with chronic inflammation (4–6, 70). They mimic inflamed tissue resident Th cells expressing similar levels of the TF TWIST1 (4). In contrast to exhausted dysfunctional CD8<sup>+</sup> T cells (71), Th1 rep cells are very efficient in their effector function and induce inflammation in murine transfer colitis (6, 70) and Ovalbumin-induced arthritis (4). In humans, a markedly expanded CD4<sup>+</sup> T cell population expressing the exhaustion marker PD-1 can be found in the inflamed joints of RA patients. These cells are not anergic or exhausted but can readily provide help to B-cells (72). In line with this observation, we found that the expression of miR-31 was also strongly upregulated in memory Th cells isolated from the synovial fluid of RA patients as compared to their counterparts from the blood, suggesting a different role of this miRNA in CD4<sup>+</sup> cells in chronic inflammation as compared to exhausted CD8<sup>+</sup> cells from chronic viral infections (25). In addition, the cells within the inflamed joint receive signals which favor Th1 polarization and miR-31 induction. This is in line with our previous studies showing the upregulation of T-bet and the activity of the IL-12/STAT4 axis in memory T cells isolated from inflamed tissues of patients with autoimmune diseases including RA (4, 5). We hypothesize that the milieu within the inflamed synovium of RA patients favors the induction of miR-31, on the one hand by a repeated auto-antigenic stimulation inducing the expression of T-bet and IFN- $\gamma$ , and on the other, by IL-7 expression (73) which represses FOXO1 (48), thereby arresting proinflammatory Th cells in the inflamed tissue, where they receive survival signals that counteract immunosuppressive therapies and promote inflammation (4). Therefore, our observation that the miR-31 reduces the motility of Th1 rep cells *in vitro* might reflect the situation in a chronic inflammatory setting. We suggest evaluating the function of miR-31 on Th1 rep cell motility in a chronic inflammatory setting using conditional miR-31 knockout mice (25) or transferring miR-31 expressing or Antagomir-31 treated human Th cells in a humanized model of arthritic inflammation (74) in future studies. In conclusion, reducing miR-31 levels by Antagomir-31 treatment could be a novel approach to mobilize therapy resistant proinflammatory Th1 cells from the inflamed tissues and eventually to resolve chronic inflammation.

## AUTHOR CONTRIBUTIONS

MB designed the study and performed experiments, analyzed data and wrote the manuscript. CH, PD, KW, AB, MM, CLT, MW, RKA, KL, A-BS, PM, and HR did experiments and/or analyzed data. ML, H-DC, and GAH discussed the results, provided conceptual advice and commented on the manuscript. AR and M-FM designed the study, supervised research and wrote the manuscript.

## ACKNOWLEDGMENTS

This work was supported by the state of Berlin and the European Regional Development Fund to MB, GAH, PM,

CLT, and M-FM (ERDF 2014–2020, EFRE 1.8/11, Deutsches Rheuma-Forschungszentrum); M-FM was supported by the e:Bio Innovationswettbewerb Systembiologie program of the Federal Ministry of Education. Supported by the German Research Council (DFG, SFB 650, and GRK1121), IMI JU-funded project BTCure and the European Research Council advanced grant ERC-2010-AdG\_20100317 Grant 268987 to AR and PM was supported by EUTRAIN, a FP7 Marie Curie Initial Training Network for Early Stage Researchers funded by the European Union (FP7-PEOPLE-2011-ITN-289903). The DRFZ is a Leibniz Institute. GAH was supported by GSC 203 Berlin-Brandenburg School for Regenerative Therapies, Charité–Universitätsmedizin Berlin, Berlin 13353, Germany.

## REFERENCES

- Mellado M, Martinez-Munoz L, Cascio G, Lucas P, Pablos JL, Rodriguez-Frade JM. T Cell migration in rheumatoid arthritis. *Front Immunol.* (2015) 6:384. doi: 10.3389/fimmu.2015.00384
- Morita Y, Yamamura M, Kawashima M, Harada S, Tsuji K, Shibuya K, et al. Flow cytometric single-cell analysis of cytokine production by CD4+ T cells in synovial tissue and peripheral blood from patients with rheumatoid arthritis. *Arthr Rheum.* (1998) 41:1669–76. doi: 10.1002/1529-0131(199809)41:9<1669::AID-ART19>3.0.CO;2-G
- Yamada H, Nakashima Y, Okazaki K, Mawatari T, Fukushi JI, Kaibara N, et al. Th1 but not Th17 cells predominate in the joints of patients with rheumatoid arthritis. *Ann Rheum Dis.* (2008) 67:1299–304. doi: 10.1136/ard.2007.080341
- Niesner U, Albrecht I, Janke M, Doeblis C, Loddenkemper C, Laxberg MH, et al. Autoregulation of Th1-mediated inflammation by twist1. *J Exp Med.* (2008) 205:1889–901. doi: 10.1084/jem.20072468
- Haftmann C, Stittrich AB, Zimmermann J, Fang Z, Hradilkova K, Bardua M, et al. miR-148a is upregulated by Twist1 and T-bet and promotes Th1-cell survival by regulating the proapoptotic gene Bim. *Eur J Immunol.* (2015) 45:1192–205. doi: 10.1002/eji.201444633
- Maschmeyer P, Petkau G, Siracusa F, Zimmermann J, Zugel F, Kuhl AA, et al. Selective targeting of pro-inflammatory Th1 cells by microRNA-148a-specific antagomirs *in vivo*. *J Autoimmun.* (2018) 89:41–52. doi: 10.1016/j.jaut.2017.11.005
- Salmon M, Scheel-Toellner D, Huissoon AP, Pilling D, Shamsadeen N, Hyde H, et al. Inhibition of T cell apoptosis in the rheumatoid synovium. *J Clin Invest.* (1997) 99:439–46. doi: 10.1172/JCI119178
- Buckley CD, Amft N, Bradfield PF, Pilling D, Ross E, Arenzana-Seisdedos F, et al. Persistent induction of the chemokine receptor CXCR4 by TGF-beta 1 on synovial T cells contributes to their accumulation within the rheumatoid synovium. *J Immunol.* (2000) 165:3423–9. doi: 10.4049/jimmunol.165.6.3423
- Ledgerwood LG, Lal G, Zhang N, Garin A, Esses SJ, Ginhoux F, et al. The sphingosine 1-phosphate receptor 1 causes tissue retention by inhibiting the entry of peripheral tissue T lymphocytes into afferent lymphatics. *Nat Immunol.* (2008) 9:42–53. doi: 10.1038/ni1534
- McLachlan JB, Jenkins MK. Migration and accumulation of effector CD4+ T cells in nonlymphoid tissues. *Proc Am Thorac Soc.* (2007) 4:439–42. doi: 10.1513/pats.200606-137MS
- Dupre L, Houmadi R, Tang C, Rey-Barroso J. T Lymphocyte migration: an action movie starring the actin and associated actors. *Front Immunol.* (2015) 6:586. doi: 10.3389/fimmu.2015.00586
- Dagan LN, Jiang X, Bhatt S, Cubedo E, Rajewsky K, Lossos IS. miR-155 regulates HGAL expression and increases lymphoma cell motility. *Blood* (2012) 119:513–20. doi: 10.1182/blood-2011-08-370536
- Petkau G, Kawano Y, Wolf I, Knoll M, Melchers F. MiR221 promotes precursor B-cell retention in the bone marrow by amplifying the PI3K-signaling pathway in mice. *Eur J Immunol.* (2018) 18:975–89. doi: 10.1002/eji.201747354
- Liu J, Li W, Wang S, Wu Y, Li Z, Wang W, et al. MiR-142-3p attenuates the migration of CD4(+) T cells through regulating actin cytoskeleton via RAC1 and ROCK2 in arteriosclerosis obliterans. *PLoS ONE* (2014) 9:e95514. doi: 10.1371/journal.pone.0095514
- Baumjohann D, Ansel KM. MicroRNA-mediated regulation of T helper cell differentiation and plasticity. *Nat Rev Immunol.* (2013) 13:666–78. doi: 10.1038/nri3494
- Richter A, Lohning M, Radbruch A. Instruction for cytokine expression in T helper lymphocytes in relation to proliferation and cell cycle progression. *J Exp Med.* (1999) 190:1439–50.
- Westendorf K, Okhrimenko A, Grun JR, Schliemann H, Chang HD, Dong J, et al. Unbiased transcriptomes of resting human CD4(+) CD45RO(+) T lymphocytes. *Eur J Immunol.* (2014) 44:1866–9. doi: 10.1002/eji.201344323
- Cossarizza A, Chang HD, Radbruch A, Andra I, Annunziato F, Bacher P, et al. Guidelines for the use of flow cytometry and cell sorting in immunological studies. *Eur J Immunol.* (2017) 47:1584–797. doi: 10.1002/eji.201646632
- Bothur E, Raifer H, Haftmann C, Stittrich AB, Brustle A, Brenner D, et al. Antigen receptor-mediated depletion of FOXP3 in induced regulatory T-lymphocytes via PTPN2 and FOXO1. *Nat Commun.* (2015) 6:8576. doi: 10.1038/ncomms9576
- Krutzfeldt J, Rajewsky N, Braich R, Rajeev KG, Tuschl T, Manoharan M, et al. Silencing of microRNAs *in vivo* with 'antagomirs'. *Nature* (2005) 438:685–9. doi: 10.1038/nature04303
- Haftmann C, Riedel R, Porstner M, Wittmann J, Chang HD, Radbruch A, et al. Direct uptake of Antagomirs and efficient knockdown of miRNA in primary B and T lymphocytes. *J Immunol Methods* (2015) 426:128–33. doi: 10.1016/j.jim.2015.07.006
- Kim D, Pertea G, Trapnell C, Pimentel H, Kelley R, Salzberg SL. TopHat2: accurate alignment of transcriptomes in the presence of insertions, deletions and gene fusions. *Genome Biol.* (2013) 14:R36. doi: 10.1186/gb-2013-14-4-r36
- Langmead B, Salzberg SL. Fast gapped-read alignment with Bowtie 2. *Nat Methods.* (2012) 9:357–9. doi: 10.1038/nmeth.1923
- Agarwal V, Bell GW, Nam JW, Bartel DP. Predicting effective microRNA target sites in mammalian mRNAs. *Elife* (2015) 4:e05005. doi: 10.7554/eLife.05005
- Moffett HF, Cartwright ANR, Kim HJ, Godec J, Pyrdol J, Aijo T, et al. Wucherpfennig: the microRNA miR-31 inhibits CD8+ T cell function in chronic viral infection. *Nat Immunol.* (2017) 18:791–9. doi: 10.1038/ni.3755
- Robinson JT, Thorvaldsdóttir H, Winckler W, Guttman M, Lander ES, Getz G, et al. Integrative genomics viewer. *Nat Biotechnol.* (2011) 29:24–6. doi: 10.1038/nbt.1754
- Thorvaldsdóttir H, Robinson JT, Mesirov JP. Integrative Genomics Viewer (IGV): high-performance genomics data visualization and exploration. *Brief Bioinform.* (2013) 14:178–92. doi: 10.1093/bib/bbs017
- Vahedi G, Takahashi H, Nakayamada S, Sun HW, Sartorelli VY, Kanno J, et al. STATs shape the active enhancer landscape of T cell populations. *Cell* (2012) 151:981–93. doi: 10.1016/j.cell.2012.09.044
- Lu KT, Kanno Y, Cannons JL, Handon R, Bible P, Elkahloun AG, et al. Functional and epigenetic studies reveal multistep differentiation and plasticity of *in vitro*-generated and *in vivo*-derived follicular T helper cells. *Immunity* (2011) 35:622–32. doi: 10.1016/j.immuni.2011.07.015

## SUPPLEMENTARY MATERIAL

The Supplementary Material for this article can be found online at: <https://www.frontiersin.org/articles/10.3389/fimmu.2018.02813/full#supplementary-material>



30. Mei S, Qin Q, Wu Q, Sun H, Zheng R, Zang C, et al. Cistrome Data Browser: a data portal for ChIP-Seq and chromatin accessibility data in human and mouse. *Nucleic Acids Res.* (2017) 45:D658–62. doi: 10.1093/nar/gkw983
31. Ovcharenko I, Nobrega MA, Loots GG, Stubbs L. ECR Browser: a tool for visualizing and accessing data from comparisons of multiple vertebrate genomes. *Nucleic Acids Res.* (2004) 32:W280–6. doi: 10.1093/nar/gkh355
32. Matys V, Kel-Margoulis OV, Fricke E, Liebich I, Land S, Barre-Dirrie A, et al. TRANSFAC and its module TRANSCmpel: transcriptional gene regulation in eukaryotes. *Nucleic Acids Res.* (2006) 34:D108–10. doi: 10.1093/nar/gkj143
33. Wei L, Vahedi G, Sun HW, Watford WT, Takatori H, Ramos HL, et al. Discrete roles of STAT4 and STAT6 transcription factors in tuning epigenetic modifications and transcription during T helper cell differentiation. *Immunity* (2010) 32:840–51. doi: 10.1016/j.immuni.2010.06.003
34. Nakayama S, Kanno Y, Takahashi H, Jankovic D, Lu KT, Johnson TA, et al. Early Th1 cell differentiation is marked by a Tfh cell-like transition. *Immunity* (2011) 35:919–31. doi: 10.1016/j.immuni.2011.11.012
35. Stone EL, Pepper M, Katayama CD, Kerdiles YM, Lai CY, Emslie E, et al. ICOS coreceptor signaling inactivates the transcription factor FOXO1 to promote Tfh cell differentiation. *Immunity* (2015) 42:239–51. doi: 10.1016/j.immuni.2015.01.017
36. Shannon P, Markiel A, Ozier O, Baliga NS, Wang JT, Ramage D, et al. Cytoscape: a software environment for integrated models of biomolecular interaction networks. *Genome Res.* (2003) 13:2498–504. doi: 10.1101/gr.1239303
37. Gautier L, Cope L, Bolstad BM, Irizarry RA. Affy-analysis of Affymetrix GeneChip data at the probe level. *Bioinformatics.* (2004) 20:307–15. doi: 10.1093/bioinformatics/btg405
38. Subramanian A, Tamayo P, Mootha VK, Mukherjee S, Ebert BL, Gillette MA, et al. Gene set enrichment analysis: A knowledge-based approach for interpreting genome-wide expression profiles. *Proc Natl Acad Sci USA.* (2005) 102:15545–50. doi: 10.1073/pnas.0506580102
39. Mootha VK, Lindgren CM, Eriksson KF, Subramanian A, Sihag S, Lehar J, et al. PGC-1alpha-responsive genes involved in oxidative phosphorylation are coordinately downregulated in human diabetes. *Nat Genet.* (2003) 34:267–73. doi: 10.1038/ng1180
40. Zhang L, Ke F, Liu Z, Bai J, Liu J, Yan S, et al. MicroRNA-31 negatively regulates peripherally derived regulatory T-cell generation by repressing retinoic acid-inducible protein 3. *Nat Commun.* (2015) 6:7639. doi: 10.1038/ncomms8639
41. Sandberg R, Neilson JR, Sarma A, Sharp PA, Burge CB. Proliferating cells express mRNAs with shortened 3' untranslated regions and fewer microRNA target sites. *Science* (2008) 320:1643–7. doi: 10.1126/science.1155390
42. Kanehisa M, Goto S. KEGG: kyoto encyclopedia of genes and genomes. *Nucleic Acids Res.* (2000) 28:27–30.
43. Szklarczyk D, Morris JH, Cook H, Kuhn M, Wyder S, Simonovic M, et al. The STRING database in 2017: quality-controlled protein-protein association networks, made broadly accessible. *Nucleic Acids Res.* (2017) 45:D362–8. doi: 10.1093/nar/gkw937
44. Verma NK, Fazil MH, Ong ST, Chalasani ML, Low JH, Kottaiswamy AP, et al. Correction: LFA-1/ICAM-1 ligation in human T cells promotes Th1 polarization through a GSK3beta signaling-dependent notch pathway. *J Immunol.* (2016) 197:2039–40. doi: 10.4049/jimmunol.1601160
45. Bonecchi R, Bianchi G, Bordignon P, D'Ambrosio P, Lang D, Borsatti R, et al. Differential expression of chemokine receptors and chemotactic responsiveness of type 1 T helper cells (Th1s) and Th2s. *J Exp Med.* (1998) 187:129–34.
46. Lee E, Lee ZHY, Song YW. The interaction between CXCL10 and cytokines in chronic inflammatory arthritis. *Autoimmun Rev.* (2013) 12:554–7. doi: 10.1016/j.autrev.2012.10.001
47. Kent WJ, Sugnet CW, Furey TS, Roskin KM, Pringle TH, Zahler AM, et al. The Human Genome Browser at UCSC. *Genome Re.* (2002) 12:996–1006. doi: 10.1101/gr.229102
48. Kerdiles YM, Beisner DR, Tinoco R, Dejean AS, Castrillon DH, DePinho RA, et al. Foxo1 links homing and survival of naive T cells by regulating L-selectin, CCR7 and interleukin 7 receptor. *Nat Immunol.* (2009) 10:176–84. doi: 10.1038/ni.1689
49. Bartel DP. MicroRNAs: target recognition and regulatory functions. *Cell* (2009) 136:215–33. doi: 10.1016/j.cell.2009.01.002
50. Alexiou P, Maragkakis M, Papadopoulos G, Reczko L, Hatzigeorgiou AG. Lost in translation: an assessment and perspective for computational microRNA target identification. *Bioinformatics* (2009) 25:3049–55. doi: 10.1093/bioinformatics/btp565
51. Bronevetsky Y, Villarino AV, Easley CJ, Barbeau R, Barczak AJ, Heinz G, et al. T cell activation induces proteasomal degradation of Argonaute and rapid remodeling of the microRNA repertoire. *J Exp Med.* (2013) 210:417–32. doi: 10.1084/jem.20111717
52. Mehta A, Baltimore D. MicroRNAs as regulatory elements in immune system logic. *Nat Rev Immunol.* (2016) 16:279–94. doi: 10.1038/nri.2016.40
53. Linsley PS, Schelter J, Burchard J, Kibukawa M, Martin M, Bartz M, et al. Transcripts targeted by the microRNA-16 family cooperatively regulate cell cycle progression. *Mol Cell Biol.* (2007) 27:2240–52. doi: 10.1128/MCB.02005-06
54. Li QJ, Chau J, Ebert PJ, Sylvester G, Min H, Liu G, et al. miR-181a is an intrinsic modulator of T cell sensitivity and selection. *Cell* (2007) 129:147–61. doi: 10.1016/j.cell.2007.03.008
55. Fuse M, Kojima S, Enokida H, Chiyomaru T, Yoshino H, Nohata N, et al. Tumor suppressive microRNAs (miR-222 and miR-31) regulate molecular pathways based on microRNA expression signature in prostate cancer. *J Hum Genet.* (2012) 57:691–9. doi: 10.1038/jhg.2012.95
56. Hua D, Ding D, Han X, Zhang W, Zhao N, Foltz G, et al. Human miR-31 targets radixin and inhibits migration and invasion of glioma cells. *Oncol Rep.* (2012) 27:700–6. doi: 10.3892/or.2011.1555
57. Ibrahim FF, Jamal R, Syafruddin SE, Ab Mutalib NS, Saidin S, MdZin RR, et al. MicroRNA-200c and microRNA-31 regulate proliferation, colony formation, migration and invasion in serous ovarian cancer. *J Ovarian Res.* (2015) 8:56. doi: 10.1186/s13048-015-0186-7
58. Luo LJ, Yang F, Ding JJ, Yan DL, Wang DD, Yang SJ, et al. MiR-31 inhibits migration and invasion by targeting SATB2 in triple negative breast cancer. *Gene* (2016) 594:47–58. doi: 10.1016/j.gene.2016.08.057
59. Chen Z, Liu S, Xia Y, Wu K. MiR-31 Regulates Rho-associated kinase-myosin light chain (ROCK-MLC) pathway and inhibits gastric cancer invasion: roles of RhoA. *Med Sci Monit.* (2016) 22:4679–91. doi: 10.12659/MSM.898399
60. Zhao G, Han C, Zhang Z, Wang L, Xu J. Increased expression of microRNA-31-5p inhibits cell proliferation, migration, and invasion via regulating Sp1 transcription factor in HepG2 hepatocellular carcinoma cell line. *Biochem Biophys Res Commun.* (2017) 490:371–377. doi: 10.1016/j.bbrc.2017.06.050
61. Smith-Garvin JE, Koretzky GA, Jordan MS. T cell activation. *Annu Rev Immunol.* (2009) 27:591–619. doi: 10.1146/annurev.immunol.021908.132706
62. Schulz EG, Mariani L, Radbruch A, Hofer T. Sequential polarization and imprinting of type 1 T helper lymphocytes by interferon-gamma and interleukin-12. *Immunity* (2009) 30:673–83. doi: 10.1016/j.immuni.2009.03.013
63. Stittrich AB, Haftmann C, Sgouroudis E, Kuhl AA, Hegazy AN, Panse I, et al. The microRNA miR-182 is induced by IL-2 and promotes clonal expansion of activated helper T lymphocytes. *Nat Immunol.* (2010) 11:1057–62. doi: 10.1038/ni.1945
64. Stahl M, Dijkers PF, Kops GJ, Lens SM, Coffey PJ, Burgering BM, et al. The forkhead transcription factor FoxO regulates transcription of p27Kip1 and Bim in response to IL-2. *J Immunol.* (2002) 168:5024–31. doi: 10.4049/jimmunol.168.10.5024
65. Haftmann C, Stittrich AB, Sgouroudis E, Matz M, Chang H, Radbruch DAM, et al. Lymphocyte signaling: regulation of FoxO transcription factors by microRNAs. *Ann N Y Acad Sci.* (2012) 1247:46–55. doi: 10.1111/j.1749-6632.2011.06264.x
66. Kerdiles YM, Stone EL, Beisner DR, McGargill MA, Ch'en IL, Stockmann C, et al. Foxo transcription factors control regulatory T cell development and function. *Immunity* (2010) 33:890–904. doi: 10.1016/j.immuni.2010.12.002
67. Fabre S, Carrette F, Chen J, Lang V, Semichon M, Denoyelle C, et al. FOXO1 regulates L-Selectin and a network of human T cell homing molecules downstream of phosphatidylinositol 3-kinase. *J Immunol.* (2008) 181:2980–9. doi: 10.4049/jimmunol.181.5.2980
68. Gubbels Bupp MR, Edwards B, Guo C, Wei D, Chen G, Wong BE, et al. T cells require Foxo1 to populate the peripheral lymphoid organs. *Eur J Immunol.* (2009) 39:2991–9. doi: 10.1002/eji.200939427



69. Gomez D, Diehl MC, Crosby EJ, Weinkopff T, Debes GF. Effector T cell egress via afferent lymph modulates local tissue inflammation. *J Immunol.* (2015) 195:3531–6. doi: 10.4049/jimmunol.1500626
70. Albrecht I, Niesner U, Janke M, Menning A, Loddenkemper C, Kuhl AA, et al. Persistence of effector memory Th1 cells is regulated by Hopx. *Eur J Immunol.* (2010) 40:2993–3006. doi: 10.1002/eji.201040936
71. Zehn D, Wherry EJ. Immune memory and exhaustion: clinically relevant lessons from the LCMV model. *Adv Exp Med Biol.* (2015) 850:137–52. doi: 10.1007/978-3-319-15774-0\_10
72. Rao DA, Gurish MF, Marshall JL, Slowikowski K, Fonseka CY, Liu Y, et al. Pathologically expanded peripheral T helper cell subset drives B cells in rheumatoid arthritis. *Nature* (2017) 542:110–4. doi: 10.1038/nature20810
73. Hartgring SA, van Roon J, Wenting-van Wijk M, Jacobs KM, Jahangier ZN, Willis CR, et al. Elevated expression of interleukin-7 receptor in inflamed joints mediates interleukin-7-induced immune activation in rheumatoid arthritis. *Arthr Rheum.* (2009) 60:2595–605. doi: 10.1002/art.24754
74. O'Boyle G, Fox CR, Walden HR, Willet JD, Mavin ER, Hine DW, et al. Chemokine receptor CXCR3 agonist prevents human T-cell migration in a humanized model of arthritic inflammation. *Proc Natl Acad Sci USA.* (2012) 109:4598–603. doi: 10.1073/pnas.1118104109

**Conflict of Interest Statement:** The authors declare that the research was conducted in the absence of any commercial or financial relationships that could be construed as a potential conflict of interest.

Copyright © 2018 Bardua, Haftmann, Durek, Westendorf, Buttgereit, Tran, McGrath, Weber, Lehmann, Addo, Heinz, Stittrich, Maschmeyer, Radbruch, Lohoff, Chang, Radbruch and Mashreghi. This is an open-access article distributed under the terms of the Creative Commons Attribution License (CC BY). The use, distribution or reproduction in other forums is permitted, provided the original author(s) and the copyright owner(s) are credited and that the original publication in this journal is cited, in accordance with accepted academic practice. No use, distribution or reproduction is permitted which does not comply with these terms.

**The Regulation of IFN Type I Pathway Related Genes RSAD2 and ETV7 Specifically Indicate Antibody-Mediated Rejection After Kidney Transplantation**

Matz M, Heinrich F, Zhang Q, Lorkowski C, Seelow E, Wu K, Lachmann N, **Addo RK**, Durek P, Mashreghi MF, Budde K.

*Clinical Transplantation*, 2018

DOI: <https://doi.org/10.1111/ctr.13429>

## **Curriculum vitae (CV)**

My curriculum vitae does not appear in the electronic version of my paper for reasons of data protection."

## List of publications

### **Single-Cell transcriptomes of murine Bone Marrow Stromal Cells Reveal Niche-Associated Heterogeneity**

**Richard K. Addo**, Frederik Heinrich, Gitta Anne Heinz, Daniel Schulz, Özen Sercan-Alp, Katrin Lehmann, Cam Loan Tran, Markus Bardua, Mareen Matz, Max Löhning, Anja E. Hauser, Andrey Kruglov, Hyun-Dong Chang, Pawel Durek, Andreas Radbruch, and Mir-Farzin Mashreghi.

European Journal of Immunology 2019      Impact Factor :**4.248**

### **MicroRNA-31 reduces the motility of proinflammatory T helper 1 lymphocytes**

Bardua M, Haftmann C, Durek P, Westendorf K, Buttgerit A, Tran CL, McGrath M, Weber M, Lehmann K, **Addo RK**, Heinz GA, Stittrich AB, Maschmeyer P, Radbruch H, Lohoff M, Chang HD, Radbruch A, Mashreghi MF.

*Frontiers in Immunology*, 2018      Impact factor: **5.511**

### **The Regulation of IFN Type I Pathway Related Genes RSAD2 and ETV7 Specifically Indicate Antibody-Mediated Rejection After Kidney Transplantation**

Matz M, Heinrich F, Zhang Q, Lorkowski C, Seelow E, Wu K, Lachmann N, **Addo RK**, Durek P, Mashreghi MF, Budde K.

*Clinical Transplantation*, 2018      Impact Factor: **1.518**

### **Distinct subsets of isotype-switched memory B cells in murine bone marrow and spleen**

René Riedel, \***Richard Addo**, Pawel Durek, Jannis Kummer, Gitta Anne Heinz, Victor Greiff, Daniel Schulz, Cora Klaeden, Ulrike Menzel, Stefan Kröger, Ulrik Stervbo, Ralf Köhler, Claudia Haftmann, Frederik Heinrich, Silvia Kühnel, Katrin Lehmann, Patrick Maschmeyer, Mairi McGrath, Sandra Naundorf, Stefanie Hahne, Özen Sercan-Alp, Francesco Siracusa, Jonathan Stefanowski, Melanie Weber, Kerstin Westendorf, Jakob Zimmermann, Anja E. Hauser, Sai T. Reddy, Mir-Farzin Mashreghi, Hyun-Dong Chang and Andreas Radbruch

In preparation

\*Shared first authorship

## Acknowledgement

I would like to express my special appreciation to Prof. Dr. Andreas Radbruch for giving me the opportunity to learn and nurture my research skills while working on multiple interesting projects in his lab. His immense knowledge, guidance and mentorship in times of difficulties helped me to learn how to overcome challenges and setbacks in science. He has been a tremendous mentor for me. I could not have imagined having a better advisor and mentor for my Ph.D work. I would like to thank Dr. Hyun-Dong Chang and Dr Mir-Farzin Mashreghi at the DRFZ for their dedicated supervision and support. Their insightful inputs and guidance have been priceless. I also want to thank Prof. Roland Lauster for accepting to be a member of my Ph.D mentoring committee.

My sincere gratitude goes to the entire “AG-Radbruch-AG-Chang-AG-Mashreghi” group: Daniel Schulz, Katrin Lehmann, Gitta Heinz, Cam Loan Tran, Rene Riedel, Rebecca Cornelis, Alexander Beller, Jannis Kummer, Patrick Maschmeyer and all those I did not mention explicitly - for the collaborative scientific work, discussions and making my time at the DRFZ a memorable one.

I appreciate Dr. Pawel Durek and Dr. Frederik Heinreich for the enormous help and guidance in Bioinformatics. Thanks for always being available where-and-when-ever I needed your inputs. To Dr. Toralf Kaiser of the FCCF at DRFZ, a million thanks for the assistance during hours of cell sorting. To Dr. Andrey Kruglov “*spasibo*”, thanks for all the stimulating discussions and the refreshing Russian lessons.

I would also like to express my gratitude to the Berlin-Brandenburg School of Regenerative Therapies (BSRT) for the numerous educative courses, especially to Dr. Sabine Bartosch for the excellent coordination and guidance. In the same vain, a big thanks goes to the Integrated Research Training Group „B cells and beyond“ of TRR130.

To all my friends and family in Germany and faraway places across the world, I am thankful for the prayers and care and believing in me.

To my dear wife, Stefanie Addo, words cannot express how grateful I am for the sacrifices, encouragement, constant support during this Ph.D adventure.

Not by any chance the least, I thank the almighty God for how far he has brought me! I will forever be grateful.